NASA TECHNICAL NOTE

NASA TN D-1990

NASA TN D-1990

HEAT-TRANSFER AND WEIGHT ANALYSIS OF A MOVING-BELT RADIATOR SYSTEM FOR WASTE HEAT REJECTION IN SPACE

by Richard J. Flaherty

Lewis Research Center
Cleveland, Ohio

NATIONAL AERONAUTICS AND SPACE ADMINISTRATION • WASHINGTON, D. C. • AUGUST 1964

HEAT-TRANSFER AND WEIGHT ANALYSIS OF A MOVING-BELT RADIATOR SYSTEM FOR WASTE HEAT REJECTION IN SPACE

By Richard J. Flaherty

Lewis Research Center
Cleveland, Ohio

NATIONAL AERONAUTICS AND SPACE ADMINISTRATION

For sale by the Office of Technical Services, Department of Commerce,
Washington, D.C. 20230 -- Price $2.25

CONTENTS

HEAT-TRANSFER AND WEIGHT ANALYSIS OF A MOVING-BELT RADIATOR SYSTEM FOR WASTE HEAT REJECTION IN SPACE

by Richard J. Flaherty

Lewis Research Center

SUMMARY

A theoretical analysis has been conducted of the heat-transfer and weight characteristics of a moving-belt radiator system in which waste heat is transferred to the belt by contact with the outer surface of a rotating or stationary drum in which working-fluid vapor is condensing. An eigenvalue solution for the conductive heat transfer from the condensing vapor through the drum wall and drum-belt interface to the belt is derived. A simplified approximate relation for the heat transfer is also presented.

An analysis of the drum-belt system weight (per unit heat-radiation rate) was conducted to indicate the influence of the major design variables involved. System weight was found to be highly dependent on the value of the belt-drum contact conductance. Means must therefore be provided to obtain good contact conductance. The desirability of high condensing coefficients was also indicated for low system weight.

An illustrative example of the incorporation of a belt radiator into a simple Rankine turbogenerator cycle at a power level of about 5 megawatts was computed. Calculations showed that a belt-radiator-system weight can be substantially less than the weight for a corresponding fin-tube radiator.

Because the belt radiator offers promise of substantial weight savings over a fin-tube radiator because of its reduced susceptability to meteoroid damage and since it offers a compact launch package, the belt-radiator system appears to have a significant advantage for electrically powered space-propulsion systems. However, the mechanical complexity and unique heat-transfer characteristics of the belt radiator required detailed design studies and experimental work before its true potential can be established.

INTRODUCTION

A number of proposed propulsion systems for future space missions utilize electrical energy for production of thrust. To be of practical value, the system, including fuel for producing electricity, must have low weight per unit

power and per unit energy. A nuclear powerplant offers low weight per unit energy and considerable potential for low weight per unit power. To date, most nuclear power-generation systems being considered convert thermal energy from a reactor into electricity and are Carnot limited (e.g., turbogenerators, thermionic converters, thermoelectric converters, and regenerative fuel cells). Therefore, the overall system must reject large amounts of waste heat into space.

In general, the only practical means of heat rejection in space is radiation. This waste heat can be radiated by a fluid-filled tubular radiator (refs. 1 and 2) or a moving-belt-type radiator system (refs. 3 to 5). The purpose herein is to analyze a moving-belt-type radiator system for nuclear electric powerplants. Before proceeding further, some desirable characteristics of a radiator should be pointed out. First, as with any system put into space, it should be as light as possible and reliable. According to reference 1 the fluid-filled tubular radiator can be one of the heavier components of the powerplant and is physically the largest. Second, the radiator must be insensitive to the hostilities of the space environment. Protection of fluid-filled components from meteoroids is essential, and, therefore, the exposed area of such components should be kept small. Third, it is desirable to reduce the radiator to a compact package for launching or atmospheric braking.

The radiator proposed in references 3 to 5 consists of a continuously moving belt, which travels alternately to a heat exchanger where by virtue of its heat capacity it absorbs waste heat and through space where it rejects heat by radiation (see fig. 1). More specifically, the radiator system could be composed of a belt moving continuously across a rotating drum that contains the condensing cycle fluid. If good heat transfer is obtained between the cycle fluid and the belt, the fluid-filled drum will be relatively small; as a consequence, the area vulnerable to meteoroid damage will be smaller than that for a comparable tubular radiator. Hence, the meteoroid protection would be relatively light, which would make the whole radiator system comparatively light. The belt, although large, could probably be rolled into a compact package for launching and atmospheric braking. Thus, the belt radiator system has the potential for satisfying some of the desirable characteristics of a waste-heat-rejection system.

To date, studies of the belt radiator system have not given a detailed, rigorous heat-transfer analysis of transient heat conduction through the drum wall into the belt. No weight optimization has been presented that included a trade-off between the drum and belt weights to minimize the heat-rejection-system weight. Also, parametric studies that show the weight dependence of the drum-belt system on the various system parameters are lacking.

This report presents an analysis of the heat-transfer and weight characteristics of a drum-belt radiator system. A general description of belt radiator systems is given first. This is followed by a detailed discussion of the drum-belt system chosen for the analysis. Special emphasis is placed on conductive heat transfer, and an eigenvalue solution is presented for the transient heat transfer between the drum and the belt. A simple approximation for this heat transfer is also developed for ease of use. A parametric study of drum-belt system weight in terms of Btu per second of heat radiated is given, and the

effect of various parameters on weight is shown. The relative merit of operation off minimum weight for a more favorable belt speed and system is discussed. The weight of the radiator system in terms of kilowatts of electrical output is also presented with the use of typical powerplant cycle assumptions. In addition, an illustrative example of a nuclear, electric power-conversion system incorporating a belt radiator is presented with a simplified weight analysis for a 5-megawatt class powerplant.

SYMBOLS

A $2\nu\bar{\epsilon}/\rho_b b c_b V$

a acceleration causing condensate in drum to flow, ft/hr^2

B belt width = drum length, ft

b belt thickness, ft

C coefficient

c specific heat, Btu/(lb)(^oR)

D drum diameter, ft

E coefficient

$\mathcal{E}$ $\rho_b b/6r\beta\nu\bar{\epsilon}T_e^3$, design parameter

$\mathcal{E}_\sigma$ $\frac{1}{432}\sqrt{\frac{\rho_b}{2g\sigma_a}}\left(\frac{G\pi}{N\nu\bar{\epsilon}}\right)^2\frac{D}{\beta r^3 T_e^6 c_b}$, design parameter

F coefficient

f $F\cos\lambda_b(S - x)$

f $C\sin\lambda_d x$

G contact area/πBD

g 32.2 ft/sec^2 = 4.17×10^8 ft/hr^2

H contact conductance, Btu/(sq ft)(hr)(^oR)

H_h $\left(\frac{1}{h} + \frac{1}{H}\right)^{-1}$, Btu/(sq ft)(hr)($^oR$)

h film condensation heat-transfer coefficient, Btu/(sq ft)(hr)(^oR)

K coefficient

K_{db} $\left(\frac{s}{k_d} + \frac{b}{2k_b}\right)^{-1}$

k thermal conductivity, Btu/(ft)(hr)(^{o}R)

L total belt length, ft

$\mathfrak{L}$ length to give Reynolds number for condensing heat transfer, ft

l latent heat of vaporization, Btu/lb

N number of belt loops

P $\frac{\gamma_d^2}{\gamma_b^2}\frac{k_b}{k_d} = \frac{\rho_b c_b}{\rho_d c_d}$

P_e electrical output, kw

$p(x)$ orthogonal weighting function

p_c contact pressure, lb/sq in.

Q thermal output of heat source, w

q rejected heat, w or Btu/sec

r thermal resistance from condensing vapor to center of belt thickness, $r' + 3600/h$, (sq ft)(sec)(^{o}R)/Btu

r' thermal resistance from inner drum wall surface to center of belt thickness, $\left(\frac{1}{H} + \frac{s}{k_d} + \frac{b}{2k_b}\right)3600$, (sq ft)(sec)(^{o}R)/Btu

S $s + b$, ft

s drum wall thickness, ft

T temperature (T at (x,t) in drum wall and belt), ^{o}R

T_{av} average temperature through belt thickness at any time, ^{o}R

T_e turbine-exit temperature (condensation temperature), ^{o}R

T_i turbine-inlet temperature, ^{o}R

T_w inner wall temperature, ^{o}R

T_1 average temperature through belt thickness after contact $t = t_c$, $^\circ R$

T_2 average temperature through belt thickness before contact $t = 0$, $^\circ R$

t time, sec

u ratio of turbine-exit to maximum belt temperature, T_e/T_1

V belt speed, ft/sec

v_f view factor

w weight, lb

w_t drum plus belt weight, $w_d + w_b$, lb

x coordinate in sketch (c)

x' coordinate in sketch (e)

y coordinate in sketch (d)

z $\lambda_d s$

$\overline{\alpha}$ total powerplant specific weight, lb/kw

α' primary radiator specific weight, lb/kw

β drum weight parameter (drum-system weight/contact area), lb/sq ft

γ $\sqrt{k/c\rho}$

ϵ emissivity

$\overline{\epsilon}$ $\frac{1}{2}(v_f\epsilon)_{out} + \frac{1}{2}(v_f\epsilon)_{in}$

η_F net power output factor, 1 - fraction of power internally consumed

η_R product of component efficiencies, $\eta_B\eta_F\eta_C\eta_A\eta_T$

θ $(\gamma_d/\gamma_b)\left[(S/s) - 1\right]$

Λ F/C

λ constant determined by heat-transfer boundary conditions

μ	viscosity
ν	4.73×10^{-13} Btu/(sec)(sq ft)(^{o}R)^{4}
ρ	density, lb/cu ft
σ	tensile stress in belt, lb/sq in.
σ_a	allowable tensile stress, lb/sq in.
τ	T_2/T_1
φ	k_d/sH
$\psi(\ )$	see eq. (A18)
ω	$(k_d/k_b)(\gamma_b/\gamma_d)$

Subscripts:

A	alternator
B	boiler loop
b	belt
C	power conditioning
c	contact
d	drum
i	turbine inlet
in	inner belt surface
m,n	index numbers
o	condensate
opt	optimum
out	outer belt surface
T	turbine
t	total

GENERAL DESCRIPTION

The belt radiator can be used in principle with any system requiring the rejection of waste heat. Although the primary purpose of this study is to analyze the belt-radiator system, it is necessary to specify a particular power-conversion cycle to define the components and heat-flow paths and to permit minimization of the belt-radiator-system weight (belt and heat exchanger). In so doing, it is also easier to show the full potential of a belt radiator system to reduce the weight per kilowatt of an entire powerplant compared to that of a tubular radiator.

A Rankine thermodynamic cycle that uses a turbogenerator was chosen for the present study. Therefore, waste heat is removed from the cycle fluid in the radiator system by condensation at an essentially constant temperature determined by the overall system optimization. The cycle fluid could be mercury, cesium, rubidium, potassium, or sodium depending on the cycle temperatures and pressures.

The main problem of the belt radiator system is the transfer of heat to the belt. The following methods may be considered (see fig. 2):

(1) Heat can be transferred to the belt through surface contact with the outside of a rotating or stationary drum within which the working fluid is condensed (figs. 2(a) to (c)).

(2) The belt can be passed through an enclosure filled with the working vapor, which then condenses on the belt (fig. 2(d)).

(3) The belt can be passed between a stack of plates or tubes that radiate to the belt (fig. 2(e)). This configuration is lighter in weight than that in which the tubes are arranged in a single plane so that they can radiate to space because less area is exposed to meteoroid damage. Thus, the weight of the meteoroid shielding would be less than that for a single-plane tubular radiator.

(4) A "household flat iron" type of heat exchanger, which could eliminate cyclic flexing of the belt, can be used. The belt can slide over the flat iron on a liquid-metal interface. As an alternate method, the flat iron would move with the belt for a short distance while making contact, then would break contact and move back to its initial location, where it contacts a new segment of the belt and repeats the process.

The heat-rejection system analyzed in detail in this report is the drum-belt system (figs. 2(a) to (c)). In general, whether the drum is rotating or the belt is revolving does not affect the analysis. Sketches of possible belt configurations for this system are presented in figure 3.

For the case of the rotating drum, the need for a rotating seal between the drum and the rest of the powerplant can be eliminated by allowing the entire powerplant to rotate. If the belt revolves around a stationary drum, there is no need for a rotating seal. If the drum alone rotates, the belt can form open loops, as shown in figure 3(a). The open-loop configuration permits heat radiation from both sides of the belt. For the case of the revolving belt, the

loops tend to close and thus result in an unfavorable view factor for the inside of the belt (figs. 3(b) and (c)). Sometimes it may be desirable to combine a revolving belt and a rotating drum.

For the case in which the drum alone rotates, no contact pressure is produced by the tension generated from the centrifugal force, which acts on the belt traveling through the radiation loop. This tension simply cancels the centrifugal force tending to throw the belt off the drum. Basically, the tensile stress generated by a completely flexible belt traveling curved paths depends only on the density and speed of the belt. The tension is independent of the radius of curvature of the belt; however, revolving the belt produces a tension that will give a contact pressure between the drum and the belt. Some contact pressure is always desirable for moving-belt systems.

HEAT-TRANSFER ANALYSIS

The four heat-transfer processes to consider with the drum-belt heat-rejection system are as follows:

(1) The transfer of heat from the condensing fluid to the drum inner wall

(2) Conduction through the drum wall and across the interface into the belt

(3) Mechanical transfer by the moving belt

(4) Rejection of heat into space by radiation from the belt

Sketch (a) shows the heat-transfer path from the vapor to the belt with the associated heat-transfer conductances:

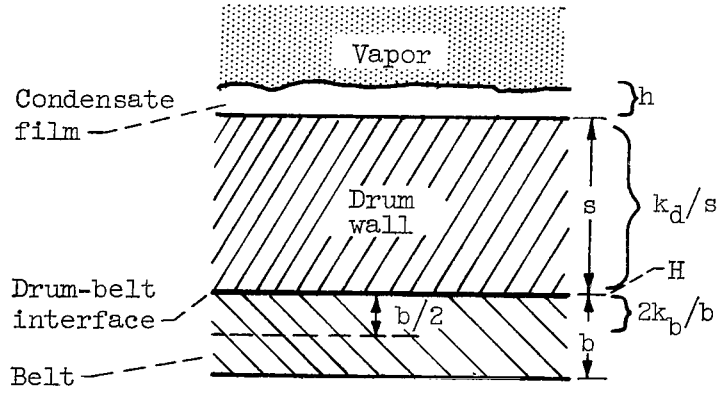

(a)

Adding the reciprocal of the conductances (see sketch (a)) gives the thermal resistance from the condensing vapor to the center of the belt thickness (approximation to the effective distance that the heat flows):

$$r = \left(\frac{1}{h} + \frac{s}{k_d} + \frac{1}{H} + \frac{b}{2k_b}\right)3600 \qquad \text{(sq ft)(sec)(}^{\circ}\text{R)/Btu} \qquad (1)$$

For a steady-state heat-transfer process, the thermal resistance and the temperature drop are all that are necessary to determine the heat flux. For a transient problem, such as for the drum and the belt, the heat capacity along the heat-transfer path is also a factor.

Condensing Heat Transfer

For either a rotating or a stationary drum, vapor from the turbine exhaust could be channeled through tubes or passages bonded to the inside of the drum. Condensing heat-transfer coefficients for metallic vapor flowing in tubes, however, have not been accurately established. Condensation directly on the drum wall is also possible if the drum wall serves as one side of the flow passage. In either case, it is desirable to obtain as high a condensing heat-transfer coefficient as possible.

For the rotating drum, it may be possible for condensation to occur directly on the drum wall without passages on the inside of the drum. An insight into the problem involved in obtaining a high condensing heat-transfer coefficient in this case can be obtained from the classical Nusselt equation for film condensing given by reference 6:

$$h = 0.943\left(\frac{\rho_o^2 k^3 l a}{\mathfrak{L}\mu(\delta T)}\right)^{1/4} \qquad \text{Btu/(sq ft)(hr)(}^{\circ}\text{R)} \qquad (2)$$

where h is the average heat-transfer coefficient over the length of flow $\mathfrak{L}$, a is the acceleration causing the condensate to flow, and δT is the temperature drop across the film thickness. The other terms, ρ_o, k, l, and μ are condensate properties. Centrifugal force will keep the condensate against the wall, and a slight taper in the drum would cause the condensate to flow to the large end. The other terms in the equation that can be controlled in the design of the drum are $\mathfrak{L}$ and a. For example, high values of a and low values of $\mathfrak{L}$ might be obtainable in the peak to trough direction of a grooved structure such as that shown in sketch (b).

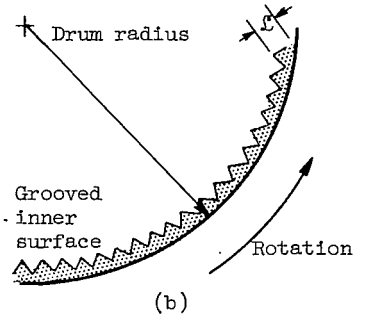

(b)

In the parametric study presented in the section WEIGHT ANALYSIS, the effect of the condensing heat-transfer coefficient on radiator-system weight is included as an input variable. However, the heat transfer between the drum and the belt is, in general, much more critical for the system and, therefore, is discussed next in greater detail.

Drum to Belt Heat Transfer

A solution for the heat transfer through the drum wall into the belt is needed to determine the temperature drop across this part of the heat-transfer path. The solution requires an expression that will give the temperature at any point x throughout the thickness of the drum wall and the belt as a function of the time t, the contact conductance H, the thermal properties of the wall and the belt materials, and their thicknesses. The analysis of the problem was based on the model shown in sketch (c).

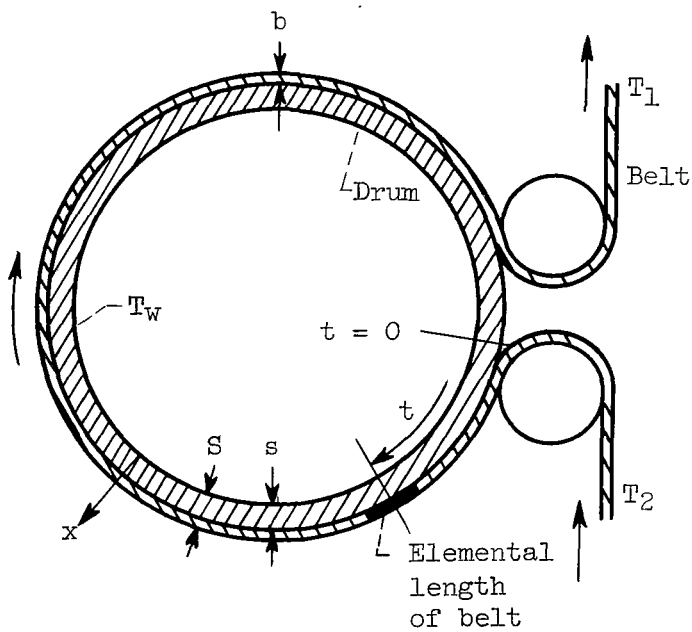

(c)

In the analysis, an elemental length of belt will be followed around the drum. The position of the element along the drum is determined by the time t, the belt speed V, and the drum diameter D. The heat transferred in the longitudinal and circumferential direction is small compared with that in the radial direction. Thus, only heat transferred in the direction perpendicular to the drum and the belt contacting surfaces will be considered. This direction will be called the x-direction. The inner drum-wall surface will be set at $x = 0$. The belt surface opposite the contacting surface will be at $x = S$. The x-coordinate will be considered to be fixed in the drum and rotate with the elemental length of belt (and adjacent drum wall) being studied.

If the radius of the drum is assumed large compared to the combined thick-

ness of the belt and the drum wall, the problem becomes a one-dimensional transient heat-transfer problem. The equation for one-dimensional heat transfer is

$$\frac{\partial^2 T}{\partial x^2} = \frac{1}{\gamma^2}\frac{\partial T}{\partial t} \tag{A1}$$

It will be assumed that the inner drum-wall surface ($x = 0$) will be kept at a constant temperature T_w by the condensing vapor (boundary condition, see appendix A). Actually, T_w at any point would vary about an average value in a periodic manner because, as the temperature of a contacting belt element increases, the driving temperature drop between the vapor and the belt element decreases. Thus the local heat-transfer rate is reduced. When the heated belt element breaks contact with the drum, it is replaced with a cool belt element, which initially gives a large temperature drop. Therefore, successive contacts of cool elemental belt lengths to the same point on the drum causes the local heat flux to undergo periodic variations. (The heat capacity in the drum wall tends to dampen these heat-flux variations to the inner drum wall surface.) Changes in T_w, depending on the magnitude of the condensing heat-transfer coefficient h, will, therefore, occur to accommodate the changes in heat flux. The value assumed for T_w for purposes of this analysis is considered equal to that needed for a steady-state condensing process determined by the required powerplant heat-rejection rate, the condensing heat-transfer coefficient, the condensing area, and the vapor temperature.

The heat radiated from the belt surface at $x = S$ during the time of contact is assumed negligible compared to that absorbed by the belt (boundary condition 2; see appendix A). This simplifying assumption is conservative and a good approximation in view of the generally small ratio of drum surface area to belt area and the radiation-impedance effect of the meteoroid shield. A series solution for this problem is derived in appendix A. The results are obtained in parametric form, referenced to the average incoming belt temperature T_2 and the inner wall temperature T_w. The final equations are the following:

The local temperature through the drum wall in parametric form is

$$\frac{T - T_2}{T_w - T_2} = 1 - \sum_{n=1}^{\infty} e^{-(\lambda_d)_n^2 \gamma_d^2 t} C_n \sin (\lambda_d)_n x \qquad \text{for } 0 \le x \le s^- \tag{3}$$

and through the belt thickness is

$$\frac{T - T_2}{T_w - T_2} = 1 - \sum_{n=1}^{\infty} e^{-(\lambda_b)_n^2 \gamma_b^2 t} F_n \cos (\lambda_b)_n (S - x) \qquad \text{for } s^+ \le x \le S \tag{4}$$

(The conventional notation for left- and right-hand limits is used: s^- denotes the left-hand limit and s^+ denotes the right.)

where

$$\gamma^2 = k/\rho c$$

$$C_n = \frac{\int_0^s T(x,0) \sin (\lambda_d)_n x \, dx + P\Lambda_n \int_s^S T(x,0) \cos (\lambda_b)_n (S - x) \, dx}{\frac{1}{(\lambda_d)_n}\left[\frac{1}{2}(\lambda_d)_n s - \frac{1}{4}\sin 2(\lambda_d)_n s\right] + \frac{P\Lambda_n^2}{(\lambda_b)_n}\left[\frac{1}{2}(\lambda_b)_n (S - s) + \frac{1}{4}\sin 2(\lambda_b)_n (S - s)\right]}$$

where $T(x,0)$ is the initial temperature distribution in parametric form, $1 - (T - T_2)/(T_w - T_2)$

$$F_n = \Lambda_n C_n$$

$$\Lambda_n = \frac{k_d \gamma_b \cos (\lambda_d)_n s}{k_b \gamma_d \sin (\lambda_d)_n \frac{\gamma_d}{\gamma_b} (S - s)}$$

and

$$P = \frac{\rho_b c_b}{\rho_d c_d}$$

The method for determining the λ's is discussed in appendix A. The λ's are dependent on H, and the thermal properties and the thicknesses of the drum wall and the belt.

Contact conductance H is the heat-transfer rate between two surfaces divided by the product of the apparent area of contact and their temperature difference. It is a function of the percent of actual physical contact, the size of the individual contacts, and the conductances of the two contacting materials (ref. 7). If perfect physical contact were made over the entire area of apparent contact, H would equal ∞. Actual physical contact between two metal surfaces without high contact pressure is usually only a very small fraction of 1 percent of the apparent contact.

To compute numerical results from equations (3) and (4), a drum wall of 0.05-inch-thick molybdenum was assumed, which is possibly a good material because of its high heat conductivity and strength at high temperatures and its resistance to corrosion by possible liquid-metal working fluids. The belt was assumed to be 0.01-inch-thick beryllium. Beryllium was chosen because of its high specific heat, which is desirable in a belt radiator. The properties assumed for

molybdenum were $k = 84.5$ Btu/(ft)(hr)($^{\circ}$R), $\rho = 636$ lb/cu ft, and $c = 0.065$ Btu/(lb)($^{\circ}$R). For beryllium, $k = 80$ Btu/(ft)(hr)($^{\circ}$R), $\rho = 112$ lb/cu ft, and $c = 0.5$ Btu/(lb)($^{\circ}$R). These values are for room temperatures.

Local temperature. - The time history of the temperature through the drum wall and the belt thickness in terms of the temperature parameter $(T - T_2)/(T_w - T_2)$ is shown for $H = 10{,}000$ Btu/(sq ft)(hr)($^{\circ}$R) in figure 4. This value of H was chosen because it shows a significant variation in the drum wall temperature with time. (The heat-transfer solution of ref. 5 does not give this variation and hence does not give the belt temperature as accurately.) For lower values of H, the variation of the temperature parameter through the drum wall and the belt is less. An H of ∞ would eliminate the temperature drop across the contact. Even for the relatively high $H = 10{,}000$ Btu/(sq ft)(hr)($^{\circ}$R), the temperature drop across the contact is much larger than the drop in the wall or the belt thickness (see fig. 4).

For calculation of the curves in figure 4, the initial temperature distribution used to obtain the coefficients C_n and F_n was a uniform value of T_2 throughout the belt thickness and a uniform value of T_w throughout the drum wall. The assumption for the temperature through the belt is valid for all cases. The assumption for the temperature through the drum is always good for the first cycle. As an elemental segment of the drum wall is cycled, that is, contacted with a new cool elemental belt length, the wall segment may not have returned to the uniform temperature value of T_w (i.e., $(T - T_2)/(T_w - T_2) = 1$)). (See curve for $t_c = 0.02$ sec (fig. 4).) However, the average belt temperature after contact is not very significantly affected for the range of initial conditions obtained during practical operation.

Temperature after contact. - The average temperature after contact is of interest for determining the optimum contact time. The heat the belt takes away from the drum is a function of the difference between the average temperature after contact T_1 and the average temperature before contact T_2. The average temperature through the belt thickness is defined as $T_{av} = \frac{1}{S - s}\int_s^S T\,dx$. The value of this integral after the total contact time t_c is defined as T_1. An expression for T_1 in parametric form as a function of total contact time is

$$\frac{T_1 - T_2}{T_w - T_2} = 1 - \sum_{n=1}^{\infty} F_n e^{-(\lambda_b)_n^2 \gamma_b^2 t_c} \left[\frac{\sin (\lambda_b)_n (S - s)}{(\lambda_b)_n (S - s)}\right] \tag{5}$$

(See appendix A for derivation.)

In the solution of equation (5), no more than five terms of the series were necessary. The belt high-temperature parameter $(T_1 - T_2)/(T_w - T_2)$ is shown in figure 5 for several values of H as a function of t_c. With increasing values of t_c (obtained by slowing belt speed or increasing the drum circumference) T_1 approaches T_w. For any fixed t_c, T_1 increases as H increases. For example, at $t_c = 0.1$ second, the value of $(T_1 - T_2)/(T_w - T_2)$ ranges from nearly 1.0 for

$H = \infty$ to 0.07 for $H = 125$ Btu/(sq ft)(hr)($^{\circ}$R). The effect of cycling on initial conditions and $(T_1 - T_2)/(T_w - T_2)$ is discussed in appendix B.

Simple Approximation of Drum to Belt Heat Transfer

Obtaining values of $(T_1 - T_2)/(T_w - T_2)$ from the series solution (eq. (5)) is rather involved. A simple approximation can be obtained, however, if it is assumed that the heat flows into the belt through a pure resistance from the inner drum wall surface and the center of the belt thickness r' given by

$$r' = \left(\frac{1}{H} + \frac{s}{k_d} + \frac{b}{2k_b}\right)3600 \qquad \frac{(\text{sq ft})(\text{sec})(^{\circ}\text{R})}{\text{Btu}} \tag{6}$$

The driving temperature difference across this resistance is $T_w - T_{av}$ where T_{av} is the average belt temperature at any time. The heat capacity per square foot of the belt is $\rho_b b c_p$. Thus

$$\int_0^{t_c} \frac{T_w - T_{av}}{r'}\,dt = \int_{T_2}^{T_1} \rho_b b c_b\,dT_{av} \tag{7}$$

Rearranging equation (7) and integrating give

$$\frac{T_w - T_1}{T_w - T_2} = e^{-\frac{t_c}{r'\rho_b b c_b}} \tag{8}$$

Subtracting both sides of equation (8) from unity gives

$$\frac{T_1 - T_2}{T_w - T_2} = 1 - e^{-\frac{t_c}{r'\rho_b b c_b}} \tag{9}$$

This simple approximation (eq. (9)) is shown to compare favorably with the series solution for about $H \leq 10{,}000$ Btu/(sq ft)(hr)($^{\circ}$R) in figure 6. Hence, equation (9) can be used in parametric studies or analyses provided that the value of H is not greater than about 10,000 Btu/(sq ft)(hr)($^{\circ}$R).

Belt Heat-Rate Capacity

The rate at which the belt takes heat away from the drum is the product of c_b, $T_1 - T_2$, and the weight flow of the belt leaving (or arriving at) the drum, which is $NVB\rho_b b$. This must also equal the heat radiated from the belt q. Letting $\tau = T_2/T_1$ gives

$$q = NVBc_b\rho_b T_1(1 - \tau)b \tag{10}$$

where N is the number of loops in the belt (see fig. 3). Multiloop belts lower the belt speed. If all parameters except V and N are held constant in equation (10), then $V \sim 1/N$. However, there is a practical limit to the number of loops due to the view factor and mechanical considerations. The relation between speed and geometry will be discussed in the section Speed and Geometry.

Belt Heat Radiation

In this analysis, a combined emissivity and view factor $\bar{\epsilon}$ will be used, which is defined as

$$\bar{\epsilon} \equiv \frac{1}{2} (v_f \epsilon)_{out} + \frac{1}{2} (v_f \epsilon)_{in}$$

where the subscripts out and in refer to the two sides of the belt. Thus, the heat radiated from the belt is

$$q = 2\nu\bar{\epsilon}\overline{T}^4 LB \tag{11}$$

where

$$\overline{T}^4 = \frac{1}{L} \int_{T_1}^{T_2} T^4 \, dL \tag{12}$$

The derivation of $\overline{T}^4$ from reference 3 is given as follows: For a unit area of the belt in the free-space part of the circuit, the heat radiated equals the loss in stored heat, or

$$2\nu\bar{\epsilon}T^4 \, dt = - \rho_b b c_b \, dT \tag{13}$$

Since $dt = (dL/V)$, then letting $A = 2\nu\bar{\epsilon}/c_b V \rho_b b$ results in

$$\int_0^{L/N} dL = - \frac{dT}{AT^4} \Bigg]_{T_1}^{T_2} \tag{14}$$

Integrating equation (14) yields

$$L = \frac{N}{3A} \left(\frac{1}{T_2^3} - \frac{1}{T_1^3} \right) \tag{15}$$

Substituting equations (14) and (15) into equation (12) and integrating from T_1 to T_2 give

$$\overline{T}^4 = \frac{3T_1^4 \left(1 - \frac{T_2}{T_1} \right)}{\left(\frac{T_2}{T_1} \right)^{-3} - 1} \tag{16}$$

Equation (16) together with equation (11) can be used to determine the belt area required for a given heat rejection.

WEIGHT ANALYSIS

It is desirable to calculate and minimize the drum plus the belt weight per heat-rejection rate w_t/q. Consider the case of a fixed value of r. The transfer of heat from the drum to the belt can be handled by (1) making the drum large to give many square feet of contact area or (2) making the difference between T_1 and the vapor temperature T_e large. Using a large drum results in a high drum weight but a low belt weight. A large temperature difference gives a small, light drum but requires a large area for the radiation process, which makes the belt heavy. A compromise between the two ways of handling this heat transfer gives the lightest heat-rejection system. To minimize the total weight of the belt radiator system mathematically, it is necessary to develop an analytical relation for the total weight of the system.

Weight Relations

Belt weight. - The weight of the belt w_b is

$$w_b = \rho_b b L B \tag{17}$$

Substituting for LB by means of equations (11) and (16) gives

$$\frac{w_b}{q} = \frac{\rho_b b}{\bar{\epsilon}} \frac{\frac{1}{\tau^3} - 1}{6\nu T_1^4 (1 - \tau)} \tag{18}$$

Equation (18) should be used when the belt thickness b is fixed. It can be seen from equation (18) that b should be small to make the value of w_b/q small. If all parameters except τ are fixed in equation (18), $\tau = 1$ gives the lowest possible w_b; however, equation (10) shows that as $\tau \to 1$ with all parameters except NVB fixed $NVB \to \infty$. Thus, some value of $\tau < 1$ must be used.

Another expression can be obtained for w_b by considering NVB fixed and b variable. Substituting for b from equation (10) into equation (18) gives

$$\frac{w_b}{q} = \frac{q}{6\nu\bar{\epsilon} NVB c_b T_1^5} \frac{\frac{1}{\tau^3} - 1}{(1 - \tau)^2} \tag{19}$$

which for constant q, NVB, and T_1 gives $\tau_{opt} = 0.69$ (a result presented in ref. 3). A belt weight minimization based on a fixed belt aspect ratio L/B was derived in reference 4.

Drum weight. - A drum weight parameter β, will be used that is defined as the weight of the drum and its accessories (rollers, drive mechanism, and meteoroid shield) divided by the contact area. For simplicity in the minimization of the drum-belt radiator-system weight, β was assumed to be independent of total contact area. Actually, the drum weight parameter will not be entirely independent of drum size. For example, the meteoroid shield weight varies as the 1.3 power of the drum area to give the same probability of no puncture for different size areas. However, for the range of variation of drum area for a given minimization calculation, it should be acceptable to assume that β is constant. As a result of this assumption in the weight minimization, the precise minimum is not obtained; however, the effect of different values of β on total system weight is analyzed.

The weight of the drum w_d is then the contact area (assumed to be $G\pi BD$) multiplied by β.

$$w_d = \beta G \pi B D \tag{20}$$

where $G \equiv$ contact area/πBD. For simplicity the approximate heat-transfer solution (eq. (8)) will be used to obtain D. To include h in equation (8), r (eq. (1)) will be substituted for r' (eq. (6)), and, correspondingly, the turbine-exit temperature T_e will be substituted for T_w. Then substituting $\pi GD/NV$ for t_c and solving for D give

$$D = \frac{NVr\rho_b b c_b}{\pi G} \ln\left(\frac{T_e - T_2}{T_e - T_1}\right) \tag{21}$$

Except where noted, $G = 1.0$ will be assumed for simplicity.

The use of the approximate heat-transfer solution (eq. (8)) produces results that differ somewhat from the series solution for $H = \infty$; however, for $H = \infty$, the drum weight is a small part of the drum-belt-system weight. For cases of low H, where the drum weight is large relative to the belt weight, the approximate solution is accurate. In general, for a 0.05-inch-thick molybdenum drum wall and 0.01-inch-thick beryllium belt, the simple approximate heat-transfer solution overestimates t_c for $(T_1 - T_2)/(T_w - T_2) < 0.8$ and underestimates t_c for $(T_1 - T_2)/(T_w - T_2) > 0.8$ (fig. 6). The error in drum size (or drum weight) is directly proportional to the error in t_c, which can be determined from figure 6. Substituting B from equation (10) and D from equation (21) into equation (20) and letting $T_e/T_1 = u$ yield

$$\frac{w_d}{q} = \frac{\beta}{(1 - \tau)} \frac{ru}{T_e} \ln\left(\frac{u - \tau}{u - 1}\right) \tag{22}$$

Weight Minimization

The total weight of the heat-rejection system is

$$w_t = w_d + w_b \tag{23}$$

where w_d is obtained from equation (22), and equation (17) or (18) can be used to determine w_b depending on whether b or NVB is considered variable. If b is considered constant, substituting these expressions for w_d and w_b into equation (23) with $T_1 = T_e/u$ and dividing by q give

$$\frac{w_t}{q} = \frac{\beta r}{T_e}\left(\frac{u}{1-\tau}\right)\ln\left(\frac{u-\tau}{u-1}\right) + \frac{1}{6}\left(\frac{\rho_b b}{\bar{\epsilon}}\right)\frac{u^4}{\nu T_e^4}\frac{\left(\frac{1}{\tau^3}-1\right)}{(1-\tau)} \tag{24}$$

where from equation (10) $q/NVB = c_b\rho_b b(1-\tau)\dfrac{T_e}{u}$. When q/NVB is constant,

$$\frac{w_t}{q} = \frac{\beta r}{T_e}\left(\frac{u}{1-\tau}\right)\ln\left(\frac{u-\tau}{u-1}\right) + \frac{1}{6\nu\bar{\epsilon}}\left(\frac{q}{NVB}\right)\frac{u^5}{c_b T_e^5}\frac{\left(\frac{1}{\tau^3}-1\right)}{(1-\tau)^2} \tag{25}$$

where $b = uq/NVBc_bT_e(1-\tau)\rho_b$ from equation (10). The choice of equation (24) or (25) for minimizing the system weight depends on whether a minimum value of b or some value of NVB/q is the limiting parameter.

Both the individual and combined drum and belt weights are dependent on the temperature ratios τ and u as can be seen in equations (24) and (25). For equation (25) the partial derivatives of w_t/q with respect to τ and u can be set equal to zero simultaneously to obtain a minimum value of w_t/q; however, for a fixed value of b (eq. (24)) it is impossible to set the two partial derivatives equal to zero simultaneously.

The case for fixed b (eq. (24)) will be used in the analysis herein. The parameters considered constant are $\rho_b b/\bar{\epsilon}$, β, r, and T_e. Note that the maximum belt temperature, T_1, which was considered a constant in the previous section is now a variable. A minimum w_t/q for the latter case can be obtained for a constant τ by setting $\partial\left(\frac{w_t}{q}\right)\Big/\partial u = 0$ (eq. (24)). Setting this partial derivative equal to zero and rearranging give

$$\mathcal{E} \equiv \frac{\rho_b b}{6r\beta\nu\bar{\epsilon}T_e^3} = \frac{\dfrac{u(1-\tau)}{(u-\tau)(u-1)} - \ln\left(\dfrac{u-\tau}{u-1}\right)}{4u^3\left(\dfrac{1}{\tau^3}-1\right)} \tag{26}$$

Figure 7 shows the relations among $\mathcal{E}$, u, and τ, which give the minimum w_t/q for τ fixed and u variable. If both τ and u are variable, then the lowest value of w_t/q occurs as $\tau \to 1.0$, although the partial derivative of w_t/q with respect to τ as $\tau \to 1.0$ is not zero. As previously indicated, however, $\tau = 1.0$ is a physically impossible value.

Effect of Variables

The effect of different values of the drum-belt-system design parameter on the system weight will now be discussed. The results will be first presented as w_t/q and, in the section APPLICATION TO POWERPLANT, as radiator weight per kilowatt of electrical output for an assumed powerplant cycle. Finally, the effect of the strongest parameters on the weight of illustrative turboelectric space powerplants is shown by using some simple approximations.

In determining the effect of H, h, the belt cycle temperature ratio τ, and T_e on the radiator weight, the following assumptions were made:

(1) $\rho_b b/\bar{\epsilon} = 0.1038$ pound per square foot, which corresponds to a beryllium belt 0.01 inch thick with $\bar{\epsilon} = 0.9$ (or $\bar{\epsilon} = 0.45$ with a 0.005-inch thickness). For materials with densities near that of steel, the thicknesses would be 0.0022 and 0.0011 inch.

(2) $\beta = 16$ lb/sq ft (appendix C).

(3) u = value that gives the minimum weight (fig. 7).

(4) In the determination of r, a belt 0.01-inch-thick beryllium and a drum wall of 0.05-inch-thick molybdenum were assumed. This gives a value of 18,400 Btu/(sq ft)(hr)($^\circ$R) for $\left(\frac{s}{k_d} + \frac{b}{2k_b}\right)^{-1} \equiv K_{db}$. The weight results for a belt of 0.005-inch-thick beryllium or for belts made of different materials would be negligibly different for the same value of $\rho_b b/\bar{\epsilon}$.

Turbine-exit temperature. - The variation of w_t/q with turbine-exit temperature (radiator-inlet vapor temperature) T_e, as seen in figure 8, is strong. This would be expected because of the T^4 radiation-rate relation; however, the total belt-system weight does not vary as T_e^{-4}. This is shown in figure 9, which is a comparison of a T_e^{-4} curve with a few of the $\tau = 0.69$ curves from figure 8. In figure 9, w_t/q is approximately proportional to T_e^{-2} for H = 125 Btu/(sq ft)(hr)($^\circ$R) and to $T_e^{-3.3}$ for $H = \infty$.

Contact conductance. - Figure 8 also shows that H has a large effect on w_t/q. For example, in the higher temperature range in this figure, the weight for H = 125 Btu/(sq ft)(hr)($^\circ$R) is more than 10 times that for $H = \infty$. Thus, from a weight point of view, high values of H are very desirable; however, high values of H are normally associated with high values of contact pressure p_c. For example, in a vacuum of 10^{-4} millimeter of mercury, for one magnesium to magnesium and several aluminum to aluminum contacts with surface finishes ranging from 6 to 45 microinches, conductances were found to range from 15 to 35 Btu/(sq ft)(hr)($^\circ$R) for a contact pressure of $2\frac{1}{2}$ lb/sq in. and 55 to 125 Btu/(sq ft)(hr)($^\circ$R) at 35 lb/sq in. (ref. 8). For an aluminum contact to uranium dioxide contact at 250° C with a 10-microinch finish, conductances of

1600 and 3500 Btu/(sq ft)(hr)($^{\circ}$R) were obtained at contact pressures of 100 and 200 lb/sq in., respectively (ref. 9).

It is doubtful, however, that high contact pressures could be used in a belt radiator system without excessive weight penalties. To obtain good contact conductance without extremely high contact pressure, a thin film of liquid metal could be used between the surfaces. (Ref. 7 reports the use of liquid metal between surfaces to increase contact conductance.) This method could be applied to the belt radiator system by using liquid metals that have a very low evaporation rate at operating belt temperatures. The low evaporation rate is necessary to minimize evaporation losses in the vacuum of space. Possible metals, which might be used in this respect over a wide range of temperatures, are melted tin and gallium. The liquid film must be at least as thick as the sum of the roughness of the two contacting surfaces. The liquid metal used must also have the ability to wet the surfaces but not amalgamate with them or have other harmful effects.

If a wetting film of liquid tin 0.0002 inch thick (to cover a combined roughness of 200 microinches) were maintained on both contacting surfaces (the drum surface and one side of the belt), H would be about 2,000,000 Btu/(sq ft)(hr)($^{\circ}$R). A conductivity of 33.9 Btu/(ft)(hr)($^{\circ}$R) was used for tin. The evaporation loss of tin, which melts at 910° R, would be 4×10^{-6} inch per year at 1480° R, 4×10^{-4} inch per year at 1680° R, and 0.04 inch per year at 1920° R (ref. 10). A loss of 0.04 inch per year (corresponding to more than 10 times the weight of a 0.01-inch-thick beryllium belt) would be prohibitive, but a loss of 4×10^{-4} inch per year or less would probably be tolerable. For an open-loop system, such as in figure 3, there is a penalty for coating one side of the belt with tin. Ordinarily, radiation would be expected from both sides of an open loop of the belt, but if one side of the belt were tinned, that side would radiate very little. Thus, the average emissivity ϵ of the belt would be cut nearly in half. The weight penalty of this will be discussed in the section Effect of Design Variables. If a liquid metal coating is used on the belt, it is important that it be kept on the inside of the belt loops for a closed-loop system (figs. 3(b) and (c)). This would not be possible with the configuration of reference 5 (fig. 2(b)) since the outside surface of the loops contact the drum; however, the alternate method of figure 2(c) could be used.

The contact conductance also exerts a large effect on the ratio of drum weight to belt weight. This is shown in figure 10 for the minimum weight value of u. The weight of the drum relative to the belt decreases with increasing H and increases with increasing T_e.

Belt cycle temperature ratio. - The effect of the belt cycle temperature ratio τ on radiator weight is minor compared to the effect of H, as also shown in figure 8. For values of τ from the physically impossible value of 1.0 (infinite belt speed) down to a value of 0.69, its largest effect on w_t/q occurs at low temperatures for high values of H.

Condensing coefficient. - The effect of h on radiator-system weight is shown in figure 11 for h = 10,000, 100,000, and 1,000,000 Btu/(sq ft)(hr)($^{\circ}$R). In this figure, the difference between curves for $h = \infty$ and h = 1,000,000 Btu/(sq ft)(hr)($^{\circ}$R) are imperceptible. Notice the effect of h on the value

of w_t/q depends on the value of H. For values of h less than 100,000 Btu/(sq ft)(hr)($^{\circ}$R), the effect of h on w_t/q becomes very large for high values of H.

Although some data with mercury and sodium vapors indicate that condensing heat-transfer coefficients of the order of 100,000 Btu/(sq ft)(hr)($^{\circ}$R) or better can be obtained with static systems (ref. 11), experimentation with drum configurations will be necessary to establish the h levels for these systems. In any event, it is clear from figure 10 that high values of both H and h are required for low weight.

To avoid restricting future figures to a particular condensing coefficient, a coefficient called H_h, which includes h, will be used instead of H where

$$\frac{1}{H_h} = \frac{1}{H} + \frac{1}{h} \tag{27}$$

Temperature ratio (u). - In the previous calculations, values of u were used that corresponded to minimum weight for fixed values of τ and the design parameter $\mathcal{E}$ (eq. (26)). For practical reasons, however, it may be desirable to use other than the minimum weight value of u. For example, in some cases, it may be desirable to design for very small belt size, or the drum size corresponding to minimum weight may be impractically small. Since, in general, belt size increases with u and drum size decreases with u, adjustment of component size can be obtained by varying u.

Plots of the variation of w_t/q with u are shown in figure 12 for an inlet vapor temperature of 1210° R and $\tau = 0.9$. The effect is similar for other temperatures as indicated in figure 13, although the minimum range is flatter for higher temperatures. There is, therefore, an appreciable range in u for which drum size can be traded for belt size without excessive weight penalty.

SYSTEM GEOMETRY AND OPERATION

This section contains a discussion of belt system geometry, belt speed, contact time, revolving stress, belt temperature ratio, and the relations that exist between these parameters.

Speed and Geometry

The belt speed is independent of the drum area but depends on the drum length, as can be seen from a rearrangement of equation (10) where $T_e/u = T_1$

$$V = \frac{qu}{NBc_b\rho_b T_e b(1 - \tau)}$$

Belt speed can be set according to the system mechanical considerations such as belt stress, flexing cycles, and drive limitations. The setting of the belt

speed determines the geometry of the system; however, there are practical limits of geometry, which in turn may limit the possible speed range.

Relations for the belt and drum geometry as related to belt speed and heat-rejection rate can be obtained from equations (10), (11), and (21). From equations (10) and (21) and by substituting $T_e/u = T_1$ and $\tau = T_2/T_1$

$$\frac{D}{B} = \frac{V^2N^2(\rho_b bc_b)^2 r T_e(1 - \tau)}{q\pi G u} \ln\left(\frac{u - \tau}{u - 1}\right) \tag{28}$$

and from equations (10) and (11)

$$\frac{L}{B} = \frac{V^2N^2}{q} \frac{1}{2\nu\epsilon\bar{T}^4}\left[\frac{\rho_b bc_b T_e(1 - \tau)}{u}\right]^2 \tag{29}$$

and, expanding $\bar{T}^4$ according to equation (16)

$$\frac{L}{B} = \frac{V^2N^2}{q} \frac{(\rho_b bc_b)^2(1 - \tau)(\tau^{-3} - 1)u^2}{6\nu\epsilon T_e^2} \tag{30}$$

It can be seen, therefore, that for a given set of design parameters. The belt and drum geometry will be determined principally by the belt speed and the number of belt loops, or in some cases where geometry is of prime importance, it will set the speed. Calculated variations of the ratios L/B and D/B with V^2/q are shown in figure 14 for two values of H_h and T_e. The calculations were made for $N = 2$ and $\tau = 0.69$. The D/B ratio is very sensitive to the value of H_h, but the value of L/B is more dependent on turbine-exit temperature.

For a fixed speed, the D/B and L/B ratios decrease as q increases. This may give impractically small D/B ratios for a large q, but several drums could be used to make the D/B ratio of each individual drum more practical.

Speed and Revolving Stress

Tensile stress. - For a revolving belt, the approximate tensile stress at a roller due to centrifugal acceleration can be derived as follows: The angular velocity of the revolving belt is 2V/D, which makes the centrifugal acceleration at a distance y from the drum approximately $(2V/D)^2$ y (see sketch (d)).

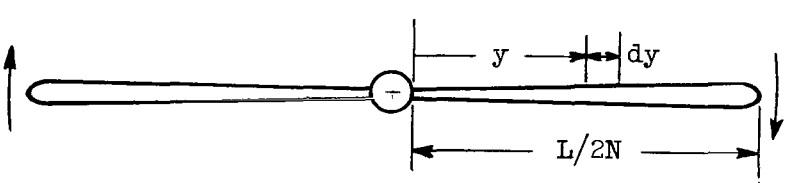

(d)

Thus, the tensile stress contribution of an elemental length of belt dy in lb/sq in. is approximately

$$d\sigma = \frac{1}{144}\left(\frac{1}{Bb}\right)\left(\frac{\rho_b Bb}{g}\right)\left(\frac{2V}{D}\right)^2 y\, dy$$

Integration of this expression from $y = 0$ to $y = L/2N$ gives

$$\sigma = \frac{1}{144}\left(\frac{\rho_b}{2g}\right)\left(\frac{VL}{ND}\right)^2 \tag{31}$$

or substituting for L and D from equations (28) and (30), respectively,

$$\sigma = \frac{1}{144}\left(\frac{\rho_b}{2g}\right)\left(\frac{V}{N}\right)^2 \left[\frac{\pi G(\tau^{-3} - 1)u^3}{r6\nu\bar{\epsilon}T_e^3 \ln\left(\frac{u - \tau}{u - 1}\right)}\right]^2 \tag{32}$$

Variations of belt stress with belt speed are shown in figure 15. The conditions are necessarily different from those of figure 14, which used an $\bar{\epsilon} = 0.9$ (implied from $\rho_b b/\bar{\epsilon} = 0.1038$ lb/sq ft with $b = 0.01$-inch-thick beryllium), since for a revolving system with closed loops, the view factor for the inside of the loop would be nearly zero. Consequently, a value of $\bar{\epsilon} = 0.45$ was used in figure 15.

The stresses shown in figure 15 are prohibitively high for high values of V and H_h. (High values of H_h correspond to low values of r in eq. (32)). At a given V, high values of H_h produce a high stress because the low resistance r results in a small drum diameter D (eq. (21)), which in turn gives a high angular velocity 2V/D and, hence, a high centrifugal force. For a given belt thickness, the use of very low belt speeds to reduce stresses, however, will result in very small ratios of D/B (eq. (28)). Thus, physically impossible or impractical drum geometries (with very small diameters and very long lengths) may result. Belt speed can be reduced without large changes in D/B if b is increased with B fixed; however, this will result in a larger minimum weight.

For a fixed V, the σ could be reduced by increasing N (eq. (32)). If B is held constant as N is increased, the required velocity will also drop (eq. (10)). Thus, for a fixed B, a four-loop system should have 1/16 the stress of the two-loop system if the values of $\bar{\epsilon}$ and G are the same.

According to equation (32), σ is also a very sensitive function of u as shown in figure 16. Thus, reduced stress for a given belt speed can be obtained by designing for values of u less than the minimum weight value of u as given by figure 7. Attendant variations in system weight (figs. 12 and 13) and geometry, however, will occur. In general, for a given allowable percentage increase in weight, the margin for stress reduction decreases as H_h increases. In this respect, higher belt temperatures will allow a larger margin for u and stress reduction without weight penalties (fig. 13) but will also decrease the belt material strength.

Equation (32) can also be used to provide an insight into a desirable material for the revolving belt. First, assume r remains constant despite changes in b_b and k_b. This is essentially true for low values of H_h, and, with a drum wall resistance equivalent to 0.05-inch molybdenum, the contribution of the belt to the overall resistance is small even for high values of H_h. With the assumption of constant r, belts of different materials but the same weight per square foot $\rho_b b$ will have the same $\mathcal{E}$, u, and w_t/q for fixed τ and other design conditions. Thus from equation (32) σ for the different materials would vary as $\rho_b V^2$. From equation (10) with $\rho_b b$ constant and with c_b and V the only variables, $V \sim c_b^{-1}$, which makes $\sigma \sim \rho_b / c_b^2$. Thus a figure of merit for a belt material can be expressed as

$$M = \frac{\sigma_a}{\sigma} \sim \sigma_a \frac{c_b^2}{\rho_b} \tag{33}$$

The material with the highest figure of merit would have the highest σ_a/σ for a given value of $\rho_b b$. In an actual design setting $\sigma_a/\sigma = 1.0$ and determining $\rho_b b$, the material with the highest figure of merit would result in the lowest value of $\rho_b b$ and hence the lightest belt system.

Examination of possible belt materials for use under 1700° R, such as beryllium, Waspalloy, niobium- 1-percent zirconium, stainless steel, and molybdenum - TZM, reveals beryllium to be best according to the criterion of equation (33) based on 10,000-hour creep rupture strength. A composite belt composed of a thin molybdenum outer layer on a beryllium interior layer produces a substantially higher figure of merit than a belt of beryllium alone. Other considerations, however, such as thermal fatigue, ductility, bending stress, and so forth, will certainly influence the choice of belt material for revolving-belt systems.

Stress determined minimum weight. - It is possible to design a minimum weight system for a given allowable tensile stress value σ_a if either drum B or D is fixed with b variable. Considering first the fixed value of B, substituting for V in equation (32) from equation (10) with $T_1 = T_e/u$, and then solving for b with σ_a substituted for σ result in

$$b = \frac{1}{72\sqrt{2g\rho_b\sigma_a}} \frac{q\pi G}{rBc_b\nu\bar{\epsilon}T_e^4} \frac{u^4(\tau^{-3} - 1)}{N^2(1 - \tau)\ln\left(\frac{u - \tau}{u - 1}\right)} \tag{34}$$

Still considering B constant and substituting for b in equation (24) give

$$\frac{w_t}{q} = \frac{\beta r}{T_e}\left(\frac{u}{1 - \tau}\right)\ln\left(\frac{u - \tau}{u - 1}\right) + \frac{1}{432}\sqrt{\frac{\rho_b}{2g\sigma_a}} \frac{q\pi G}{N^2 rB(\nu\bar{\epsilon})^2 T_e^8 c_b} \frac{u^8}{\ln\left(\frac{u - \tau}{u - 1}\right)} \left(\frac{\tau^{-3} - 1}{1 - \tau}\right)^2 \tag{35}$$

Substituting w_d from equation (20) into equation (22), then solving for B, and finally substituting for B in equation (35) give the following equation for the fixed value of D:

$$\frac{w_t}{q} = \frac{\beta r}{T_e} \frac{u}{(1 - \tau)} \ln\left(\frac{u - \tau}{u - 1}\right) + \frac{1}{432} \sqrt{\frac{\rho_b}{2g\sigma_a}} \left(\frac{G\pi}{rN\nu\epsilon}\right)^2 \frac{Du^7(\tau^{-3} - 1)^2}{c_b T_e^7 (1 - \tau)\left[\ln\left(\frac{u - \tau}{u - 1}\right)\right]^2} \tag{36}$$

and for this case

$$b = \frac{1}{72} \frac{1}{\sqrt{2g\rho_b\sigma_a}} \left(\frac{G\pi}{rN}\right)^2 \frac{Du^3}{c_b \nu\epsilon T_e^3} \frac{(\tau^{-3} - 1)}{\left[\ln\left(\frac{u - \tau}{u - 1}\right)\right]^2} \tag{37}$$

The partials with respect to τ and u of the right-hand sides of equations (35) and (36) can be set equal to zero simultaneously giving minimum weight values of u and τ. Equation (36) will be used later to obtain examples of revolving-belt systems.

Contact pressure. - For revolving-belt systems, the belt tension will also produce a contact pressure on the drum given by

$$p_c = \frac{2b}{D} \sigma$$

or from equations (21) and (32)

$$p_c = \frac{V}{144 g c_b} \left[\frac{G\pi}{Nr \ln\left(\frac{u - \tau}{u - 1}\right)}\right]^3 \left[\frac{u^3\left(\tau^{-3} - 1\right)}{6\nu\epsilon T_e^3}\right]^2 \tag{38}$$

Plots of contact pressure are shown in figure 17. These contact pressures were computed for the same conditions as for figure 15. Revolving-belt systems are therefore seen to be inherently capable of generating a contact pressure, which should aid in the achievement of higher contact conductances. In general, however, for allowable belt tensile stresses, the contact pressure is quite low.

Speed and Contact Time

Figure 18(a) presents a plot of the belt speed parameter NVB/q obtained from equation (10) as a function of τ for the same values of H_h and T_e used in figures 14, 15, and 17. The speed parameter is governed primarily by τ and approaches ∞ as τ approaches 1. At any value of τ, the greatest variation in NVB/q is about a factor of two for the range of T_e and H_h shown.

The variation of t_c with τ presented in figure 18(b) was obtained from equation (18) with T_e substituted for T_w and r for r'. The belt contact time approaches zero as τ approaches 1.0 and, as would be expected, is highly dependent on the magnitude of the combined coefficient H_h. For the values of H_h shown, t_c varies by more than a factor of 10. High heat-transfer coefficient systems required for light weight will, therefore, have very short belt contact times.

APPLICATION TO POWERPLANT

Radiator-System Weight Based on Electrical Output

In previous presentations, radiator-system weight was expressed in terms of the required waste heat rejection q. For application to electric powerplant systems, however, it is generally more convenient to express weight in terms of powerplant electrical output in kilowatts. This section will, therefore, discuss radiator-system weight on a power output basis. For the total powerplant, specific weight in pounds per kilowatt will be designated by α, and the primary radiator-system specific weight will be designated by α'.

Powerplant cycle assumptions. - To base the radiator-system weight on electric output, it is necessary to make assumptions concerning the powerplant cycle. Figure 19 shows a block diagram of a Rankine vapor powerplant cycle. The assumptions made about this cycle pertinent to the present study are the following:

(1) All the heat entering the turbine and not converted to turbine output power is rejected by the primary radiator system. Hence, the rejected heat is

$$q = \left[1 - \eta_T\left(1 - \frac{T_e}{T_i}\right)\right] \frac{\eta_B Q}{1060} \qquad \frac{\text{Btu}}{\text{sec}} \tag{39}$$

where Q is the reactor power in watts.

(2) The useful electrical power output is a constant fraction η_R of the Carnot efficiency times the reactor power. Thus, the useful power is

$$P_e = \eta_R\left(1 - \frac{T_e}{T_i}\right)\frac{Q}{1000} \qquad \text{kw} \tag{40a}$$

where η_R is the product of the system component efficiencies

$$\eta_R = \eta_B\eta_F\eta_C\eta_A\eta_T \tag{40b}$$

Dividing equation (40a) by equation (39) and substituting the product of the component efficiencies for η_R give the output power per unit of heat rejected by the radiator:

$$\frac{P_e}{q} = \frac{1.06\ \eta_F \eta_C \eta_A \eta_T \left(1 - \frac{T_e}{T_i}\right)}{1 - \eta_T \left(1 - \frac{T_e}{T_i}\right)} \tag{41}$$

The primary radiator-system specific weight α' is then obtained from equation (36) or (24) and equation (41):

$$\alpha' \equiv \frac{W_t}{P_e} = \left(\frac{W_t}{q}\right) \Big/ \left(\frac{P_e}{q}\right) \qquad \frac{lb}{kw} \tag{42}$$

The values for the turbine-inlet temperature and the component efficiencies used in equation (41) are those given in reference 1 for the so-called conventional system:

Turbine-inlet temperature, T_i, ^oR	2310
Turbine efficiency, η_T	0.77
Alternator efficiency, η_A	0.90
Power-conditioning efficiency, η_C	0.97
Net power output factor, η_F	0.86
Boiler loop efficiency, η_B	0.97

In this report the aforementioned values are referred to as the "reference conditions", and they are used in the "reference" systems.

Effect of design variables. - Figure 20 presents for a rotating-drum system the variation of α' with T_e for several values of H_h for the reference conditions given previously. Both the range of T_e for low weight and the specific value of T_e at which α' minimizes decrease with decreasing H_h. A radiator for which specific weight varied directly with T_e^{-4} would minimize at about 1800° R for the same powerplant assumptions. A shift of the minimum a' toward this temperature is evident for high values of H_h. For the inputs and assumptions used, it is also seen that relatively low values of α' are possible if high contact and condensing coefficients can be obtained.

The parameter $\rho_b b/\bar{\epsilon}$ is the weight of the belt per square foot of area (one side) divided by the combined view factor and emissivity of both sides of the belt. The belt weight per square foot of effective blackbody radiating area is $(1/2)(\rho_b b/\bar{\epsilon})$. The value of 0.1038 lb/sq ft used for this parameter on previous figures corresponds to a beryllium belt 0.01-inch thick with $\bar{\epsilon} = 0.9$ or 0.005-inch thick with $\bar{\epsilon} = 0.45$. For materials with densities near that of steel, the thicknesses would be 0.0022 and 0.0011 inch. Figure 21 shows that even tripling this value of $\rho_b b/\bar{\epsilon}$ will still permit small values of α' at high values of H_h. The effect of variation of $\rho_b b/\bar{\epsilon}$ on the magnitude of α' is most pronounced for low values of H_h and at low values of T_e. There is also a tendency for the minimum α' to shift slightly to higher temperatures as $\rho_b b/\bar{\epsilon}$ is increased.

Figure 22 shows that the variation of α' with the drum weight parameter β (weight of the drum and its accessories per sq ft of contact area) is highly

dependent on the value of H_h. The value of β is dependent on drum design, drum size (which is a function of both power level and H_h), and the amount of meteoroid shielding that is needed. The value of β = 16 lb/sq ft used in previous figures is discussed in appendix C. Changing β from 16 to 32 lb/sq ft changes α' less than 0.1 pound per kilowatt for H_h = 1,000,000 Btu/(sq ft)(hr)($^\circ$R). However, the effect of β on radiator-system weight becomes more pronounced as H_h is reduced, since w_d becomes a larger fraction of the total weight as H_h is reduced. The effect of β is fairly independent of the value of T_e.

If the change in β is brought about by a change in the drum wall thickness s, there is an additional effect on weight that should be considered, since a change in s also changes the thermal resistance r. Variations in s are most noticeable at H_h = 1,000,000 Btu/(sq ft)(hr)($^\circ$R) where r is determined mainly by s. For example, doubling s for H_h = 1,000,000 Btu/(sq ft)(hr)($^\circ$R) has nearly the same effect as doubling β in figure 22. In general, the effect of doubling s on α' is not very significant at any value of H_h.

Effect of powerplant cycle assumptions. - Figure 23 shows the effect of the powerplant cycle assumptions on the radiator-specific weight α' for several values of H_h. The solid curves are for the reference system previously discussed in figures 20 to 22. The dashed curve shows the effect of increasing the component efficiencies: η_T from 0.77 to 0.85, η_A from 0.90 to 0.95, and η_F from 0.86 to 0.90. The increased component efficiencies reduce the radiator specific weight at all turbine-exit temperatures but with a more pronounced effect at the lower turbine-exit temperatures. The temperature for minimum α' is slightly reduced.

The dash-dot curves show the additional effect of increasing the turbine-inlet temperature from 2310° to 2560° R. The efficiencies and temperatures for this curve correspond to the advanced system of reference 1. The increase in turbine-inlet temperature also reduces the α', particularly, at the higher operating temperatures. There is also a shift of the temperature for minimum α' to a higher turbine-exit temperature.

The effects noted previously are most pronounced at the lower values of contact conductances in terms of both absolute changes and percentage changes.

Comparison of Tubular and Belt Radiators

For the 5-megawatt powerplant of reference 1 with "conventional" component efficiencies and turbine-inlet temperatures, the fluid-filled fin-tube radiator has an α' of 4.6 pounds per kilowatt. Figures 20 to 22 indicate that if high contact and condensing coefficients can be obtained, belt radiator systems with an α' of about 1 pound per kilowatt may be attainable. Thus, the potential for a considerable reduction in weight exists for powerplants using a belt radiator system. However, much of the weight of a fin-tube radiator is armor for meteoroid protection. The fin-tube radiator of reference 1 has a probability of no puncture by meteoroids of 0.9. A reduction in the protection requirement for the fin-tube radiator, by a reduction in the severity of the meteoroid environ-

ment for example, will tend to reduce the weight difference between the two radiator types.

Incorporation of Belt Radiator System into Powerplant

Up until now, the discussion has considered the weight variation of the radiator system only. As an illustrative example, the radiator system will now be incorporated in a powerplant, and the effect of the belt radiator system on the powerplant weight will be investigated over a range of turbine-exit temperatures.

Powerplant specific weight. - The powerplant component weights are based on the 5-megawatt Rankine cycle powerplant of reference 1, which has a fluid-filled tubular radiator. The component weights are listed in table I and grouped according to how they are treated in the present study. The first grouping is called fixed weights. In the present example, the reactor thermal power is held constant at 30 megawatts; correspondingly, the weight of the reactor and associated components is held constant. Because varying T_e will cause the electrical power output to vary, the specific weight of these components will also vary. The second grouping is called variable weights. These weights are assumed to be directly proportional to the electrical power output; hence, although their actual weight varies, their specific weight is constant at 4.04 pounds per kilowatt. The third grouping consists of the items that are replaced by the drum-belt radiator system, that is, the condensers and the primary fluid-filled radiators. The fourth group is composed of items that have been omitted from consideration. Much of the structural weight of the fluid-filled tubular radiator is required to support the radiator during boost from the Earth's surface. Because the belt radiator can be conveniently "rolled up", the structural weight may be considerably less. A powerplant using a belt for the primary radiator may still need a secondary radiator system. No analysis has been made of the advantage of using a belt to replace the secondary fluid-filled radiator. The weight of the secondary radiator, however, is comparable to that of the primary radiator in the example given, and a secondary belt system should yield substantial savings in weight.

The specific powerplant weight $\bar{\alpha}$ considered in the following discussion is the sum of the specific weights of the reactor and associated components, the turboalternators and power conditioning equipment, and the radiator system, divided by the net electrical power output.

Figure 24 shows the variation of $\bar{\alpha}$ with T_e for several values of H_h and β for a reference and an advanced powerplant using the same 30-megawatt thermal output reactor. The absolute component weights are assumed the same for both systems. There is, however, a decrease in specific weight in the components of the advanced system because of the power increase caused by the increase in turbine-inlet temperature and component efficiencies. A complete listing of the turbine-inlet temperatures and component efficiencies for both systems is given in figure 23. If an H_h of the order of 1250 Btu/(sq ft)(hr)($^{\circ}$R) or better can

be obtained, the weight of the belt radiator system for the inputs used becomes a small part of the total weight at or above the turbine-exit temperature that gives minimum $\bar{\alpha}$ for both examples. Minimum powerplant specific weight occurs at a T_e of 1000° to 1200° R; this T_e is substantially lower than 1700° R, which is normally associated with minimum powerplant weight for a direct condensing radiator with T_i = 2500° R. The lower values of T_e for minimum $\bar{\alpha}$ for the belt radiator system are a result of the lower minimum α' for the radiator-system weight and the relatively low ratio of radiator-system weight to total powerplant weight. The effect of β on total powerplant weight also shown in the figure, is similar to its effect on α' shown in figure 21. Similarly, the effect of $\rho_b b/\bar{\epsilon}$ may be deduced from figure 22.

The relatively low T_e at which $\bar{\alpha}$ minimizes could raise a problem in the choice of a working fluid in the design of a powerplant for minimum weight. For example, at 1250° R, turbine-exhaust vapor pressures would be about 0.012 lb/sq in. for sodium, 0.14 lb/sq in. for potassium, 0.37 lb/sq in. for rubidium, 0.46 lb/sq in. for cesium, and 7.5 lb/sq in. for mercury. At 2500° R, however, mercury has a vapor pressure of 5800 lb/sq in., while the others have reasonable pressures. In addition to the pressure problems involved, considerable moisture content (of the order of 25 percent) would result in the turbine expansion over this temperature range. Associated specific-volume and turbine-blade-erosion problems might be considerable. In practical designs, therefore, it may not be desirable to design for the minimum weight powerplant with these radiation systems. An indication of the weight penalties involved in going to higher than minimum weight T_e can be obtained from figure 24.

The specific powerplant weight $\bar{\alpha}$ for the reference system with a belt radiator for β = 16 lb/sq ft, H_h = 1250 Btu/(sq ft)(hr)(°R), and T_e = 1500 °R is 7.9 pounds per kilowatt (fig. 24(a)). The corresponding value for a fluid-filled radiator based on the estimations in reference 1 (see table I) is 12.1 pounds per kilowatt. In this case, the belt radiator offers a 35-percent reduction in weight. Using the belt radiator in a system with advanced component performances and for the aforementioned values of β, H_h, and T_e results in an $\bar{\alpha}$ of 4.9 pounds per kilowatt, a 38-percent reduction from the belt radiator system using reference component performances. Recall that not all of the powerplant weights are included in $\bar{\alpha}$ (see table I), and hence all are not included in the previous comparisons.

Radiator weight and dimensions. - To obtain an indication of absolute values of radiator-system weight and dimensions, a potassium vapor cycle with the reference conditions and a turbine-exit temperature corresponding to the conventional 5-megawatt system of reference 1 was assumed. Values of h = 10,000 Btu/(sq ft)(hr)(°R) and H = 1430 Btu/(sq ft)(hr)(°R) were assumed. To obtain high values of H, the belt is assumed to be tin-coated on the side contacting the drum. Therefore, with only one side of the belt radiating, $\bar{\epsilon}$ = 0.45, and for a belt of 0.005-inch-thick beryllium, $\rho_b b/\bar{\epsilon}$ = 0.1038 lb/sq ft. A β of 16 lb/sq ft is believed to allow for adequate meteoroid protection.

Calculations of weight and dimensions were made according to equations (10), (21), and (24), where it was assumed that G = 0.85, and the minimum weight value of u was obtained from figure 7. Results of the calculations for a rotating-

drum system are shown in table II(a).

If it is presumed that the belt can be rolled up around the drum for launching and later deployed in space, the belt system could be contained in a cylinder 25 feet long and 5 feet in diameter. Thus, a relatively compact single package can be obtained for a belt radiator system.

For rotating-drum systems, the belt dynamic stresses ($\rho V^2/144$ g lb/sq in.) are small. The largest stresses, which are developed in flexing around the rollers, can be controlled by proper sizing of the rollers. However, the inputs for the rotating-drum system cannot be applied to a revolving-belt system because the tensile stresses would be prohibitively high (5,260,000 lb/sq in.) if the belt was revolved about a static drum.

To obtain an example of a revolving-belt system, equation (36) (the fixed-drum-diameter case) was used. Figure 25 presents the minimum weight values of u and τ as functions of the design parameter

$$\mathcal{E}_\sigma \equiv \frac{1}{432}\sqrt{\frac{\rho_b}{2g\sigma_a}}\left(\frac{G\pi}{N\nu\epsilon}\right)^2 \frac{D}{\beta r^3 T_e^6 c_b}$$

The minimum weight value of τ increases with increasing $\mathcal{E}_\sigma$, but the minimum weight value of u decreases. For the example systems considered, the minimum weight values of τ and u were used. The assumptions and results for a revolving-belt system are presented in table II(b).

The revolving-belt system is 27 percent heavier than the rotating-drum system, and the revolving-belt system has a lower probability of no puncture by meteoroids, 0.998 compared with 0.999. To achieve the same probability as the rotating-drum system, the weight of the revolving-belt system would increase about 7 percent. A two-loop ($N = 2$) revolving-belt system would weight about $1\frac{1}{2}$ times the four-loop system.

SUMMARY OF RESULTS

The following principal results were obtained from the analysis of heat-transfer and weight characteristics of moving-belt radiator systems:

1. An eigenvalue solution for the transient heat conduction between the drum and the belt of a moving-belt radiator system, which rejects waste heat for a Rankine power cycle, has been developed. This solution permits the calculation of the local temperature variation through the drum wall and belt thickness as a function of their thicknesses, their thermal properties, the contact conductance between them, and the contact time. The average temperature through the belt thickness after contact is also obtained, and a simple approximation to this is shown to be sufficiently accurate for parametric studies.

2. Among the many design parameters affecting the drum-belt system (drum weight per square foot of contact area, belt weight per unit radiating area,

etc.), the contact conductance and the heat-rejection temperature (condensing temperature) were shown to have the largest effect in determining the weight of the system. For example, using illustrative system inputs at 1700° R, the specific weight is estimated to vary from 0.05 to 1.6 lb/(Btu/sec) for contact conductances ranging from ∞ to 50 Btu/(sq ft)(hr)(°R). At 1400° R, the range is from 0.09 to 2.25 lb/(Btu/sec). It may be necessary to use a liquid-metal interface (e.g., tin or gallium) between the drum and the belt to obtain the high conductances needed for low system weight.

3. High condensing heat-transfer coefficients on the inner drum wall in addition to high values of contact conductance are also important for obtaining low specific weight.

4. The variation of the drum-belt-system specific weight with heat-rejection temperature T_e, for the inputs considered, was approximately proportional to $T_e^{-3.3}$ and T_e^{-2} for contact conductances of ∞ and 125 Btu/(sq ft)(hr)(°R), respectively.

5. The ratio of drum weight to belt weight for a weight minimized system decreases as contact conductance increases, but this ratio increases as the heat-rejection temperature increases.

6. For the inputs considered, variation of the ratio of belt outlet temperature to belt inlet temperature from 0.69 to the physically impossible value of 1.0 (infinite belt speed) had little effect on the weight of the system, although the required belt speed was greatly affected.

7. A revolving-belt system, especially for cases of high contact conductance, may require a much larger drum than is necessary for heat-transfer considerations or a thicker belt than that necessary for a nonrevolving system to keep the belt tensile stresses developed within allowable limits. In general, it may not be possible to design for minimum system weight based on heat-transfer requirements with a revolving belt. For a rotating-drum system, the drum can be more readily sized to give minimum system weight.

8. Illustrative calculations of Rankine cycle powerplant systems at about 5-megawatts power showed that the specific weight of a belt-radiator powerplant minimizes at a lower turbine-exit temperature than that of a fin-tube radiator powerplant for the same turbine-inlet temperature. This minimum is quite flat over a wide range of turbine-exit temperatures for high values of contact conductance.

9. The weight of a belt-radiator system is estimated to be considerably less than the weight of a comparable fin-tube radiator. A total specific weight for a belt radiator system of less than 1 pound per kilowatt may be possible for a Rankine cycle with a turbine-inlet temperature of 2500° R if contact conductances of several thousand Btu/(sq ft)(hr)(°R) or better can be obtained.

CONCLUSIONS

Because the belt radiator offers promise of substantial weight savings over a tubular radiator (due to its reduced susceptibility to damage) and also offers a compact launch package, it appears to have a significant advantage for large electrically powered space-propulsion systems. However, its mechanical complexity and unique heat-transfer characteristics require more analytical and experimental work plus detailed design studies before its true potential can be established.

Lewis Research Center
National Aeronautics and Space Administration
Cleveland, Ohio, July 5, 1963

APPENDIX A

CONDUCTIVE HEAT-TRANSFER ANALYSIS AND ORTHOGONALITY PROOF

Conductive Heat-Transfer Analysis

The equation for one-dimensional transient conductive heat transfer is

$$\frac{\partial^2 T}{\partial x^2} = \frac{1}{\gamma^2}\frac{\partial T}{\partial t} \tag{A1}$$

where $\gamma^2 = k/\rho c$. The problem at hand is really a simultaneous solution of two such equations, one for the drum wall and one for the belt. A solution of the aforementioned partial differential equation (A1) is $T = Ce^{-\lambda^2\gamma^2 t} \sin \lambda x$ and/or $Ke^{-\lambda^2\gamma^2 t} \cos \lambda x$ plus some constant. Thus, it will be assumed that the solution for the drum is of the form

$$T = T_w - e^{-\lambda_d^2\gamma_d^2 t}\,(C^* \sin \lambda_d x + K^* \cos \lambda_d x) \qquad \text{for } 0 \le x \le s \tag{A2a}$$

while that for the belt is of a similar form

$$T = T_w - e^{-\lambda_b^2\gamma_b^2 t}\,(E^* \sin \lambda_b x' + F^* \cos \lambda_b x') \qquad \text{for } 0 \le x' \le b \tag{A2b}$$

The coordinate systems are shown in sketch (e).

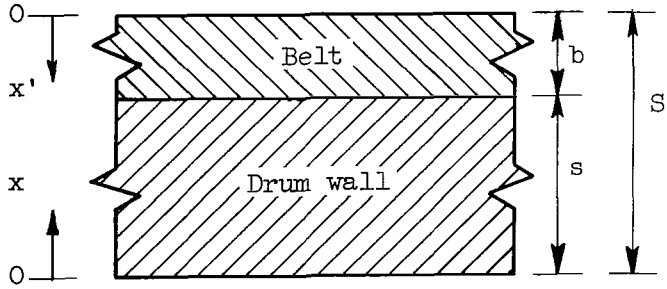

(e)

These coordinate systems are fixed relative to the drum and rotate with it. Boundary condition 1, which is $\partial T/\partial t = 0$ at $x = 0$, implies $K^* = 0$. Boundary condition 2, which is $\partial T/\partial x' = 0$ at $x' = 0$, implies $E^* = 0$.

Subtracting T_2 from both sides of equations (A2a) and (A2b), substituting $S - x = x'$, and rearranging the equations give

$$\frac{T - T_2}{T_w - T_2} = 1 - e^{-\lambda_d^2 \gamma_d^2 t} \; C \sin \lambda_d x \qquad \text{for} \quad 0 \leq x \leq s^- \tag{A3a}$$

$$\frac{T - T_2}{T_w - T_2} = 1 - e^{-\lambda_b^2 \gamma_b^2 t} \; F \cos \lambda_b (S - x) \qquad \text{for} \quad s^+ \leq x \leq S \tag{A3b}$$

where

$$C = \frac{C^*}{T_w - T_2}$$

and

$$F = \frac{F^*}{T_w - T_2}$$

From the continuity of the heat flow across the drum-belt contact,

$$k_d \left(\frac{\partial T_d}{\partial x}\right)_{x=s} = k_b \left(\frac{\partial T_b}{\partial x}\right)_{x=s} \tag{A4}$$

Substituting the derivatives of equations (A3) into equation (A4) gives

$$k_d e^{-\lambda_d^2 \gamma_d^2 t} \; C\lambda_d \cos \lambda_d s = k_b e^{-\lambda_b^2 \gamma_b^2 t} \; F\lambda_b \sin \lambda_b (S - s) \tag{A5}$$

Since equation (A5) must hold for any value of t, then

$$\lambda_b = \lambda_d \frac{\gamma_d}{\gamma_b} \tag{A6}$$

Therefore,

$$\frac{F}{C} = \frac{k_d \lambda_d \cos \lambda_d s}{k_b \lambda_b \sin \lambda_b (S - s)} \tag{A7}$$

or using equation (A6) results in

$$\frac{F}{C} = \frac{k_d}{k_b} \frac{\gamma_b}{\gamma_d} \frac{\cos \lambda_d s}{\sin \lambda_d \frac{\gamma_d}{\gamma_b} (S - s)}$$

If the conductance across the contact is H, then $H \Delta T = k \left(\frac{\partial T}{\partial x}\right)_{x=s}$

or

$$H\left[(T_b)_{x=s} - (T_d)_{x=s}\right] = -k_d\lambda_d\left(\cos\lambda_d s\right)C^* e^{-\lambda_d^2\gamma_d^2 t} \qquad (A8)$$

Substituting from equations (A3) into (A8) using (A6) gives

$$H\left[\sin\lambda_d s - \frac{F}{C}\cos\lambda_d\frac{\gamma_d}{\gamma_b}(S - s)\right] = -k_d\lambda_d\cos\lambda_d s \qquad (A9)$$

which reduces to

$$\tan z - \omega\cot\theta z = -\varphi z \qquad (A10)$$

by means of equation (A7) and the following identities:

$$z \equiv \lambda_d s \qquad \varphi \equiv \frac{k_d}{Hs}$$

$$\omega \equiv \frac{k_d}{k_b}\frac{\gamma_b}{\gamma_d} \qquad \theta \equiv \frac{\gamma_d}{\gamma_b}\left(\frac{S}{s} - 1\right)$$

Sketch (f) is a graphical solution to equation (A10).

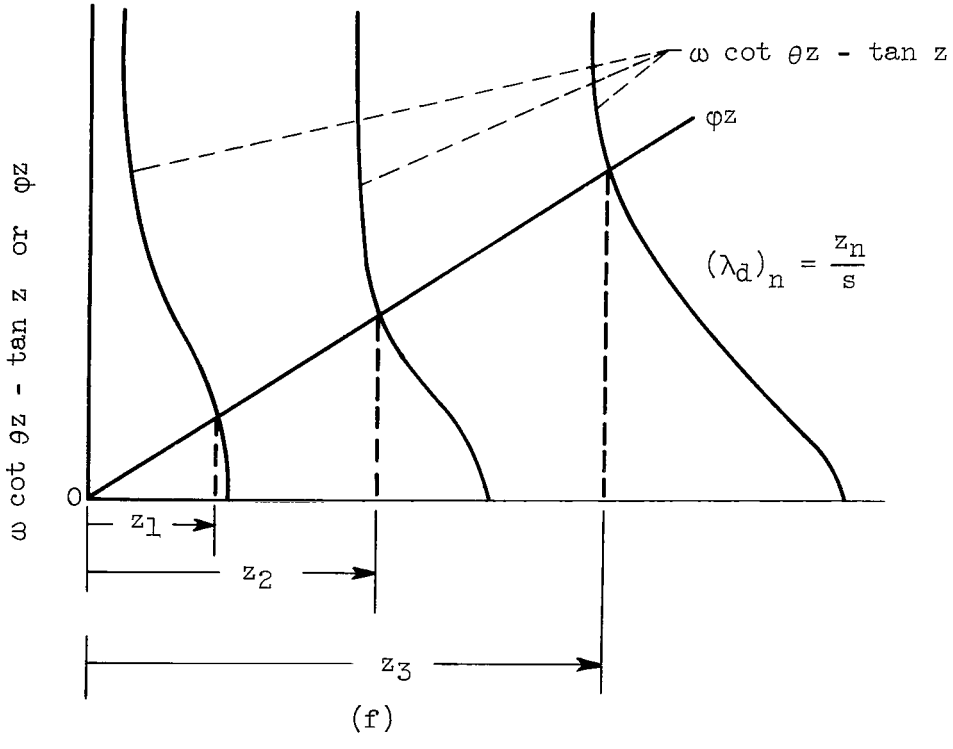

(f)

Each λ_d and corresponding λ_b gives a particular simultaneous solution to the partial differential equations. The proper combination of these particular solutions gives the solution to the problem at hand. The proper combination is determined by the coefficients $F_1, F_2, F_3, \ldots$ and $C_1, C_2, C_3, \ldots$. These coefficients can be determined from the initial temperature distribution through the drum wall and belt thickness if the particular solutions are orthogonal either with or without some weighting function over the interval covered by the solution $(0 \leq x \leq S)$.

Only when $\theta = 1$ and $\varphi = 0$ are the λ's uniformly spaced and will they lead to a Fourier series; $\varphi = 0$ if and only if $H = \infty$ and $\theta = 1$ if and only if $\gamma_b/\gamma_d = (S/s) - 1$. For any case, however, the λ's lead to a set of functions that are orthogonal with respect to a weighting function over the interval $0 \leq x \leq S$. It will be shown in the section Orthogonality Proof that

$$\int_0^S \sin (\lambda_d)_n x \sin (\lambda_d)_m x \, dx + P \frac{F_n}{C_n} \frac{F_m}{C_m} \int_s^S \cos (\lambda_d)_n \frac{\gamma_d}{\gamma_b} (S - x) \cos (\lambda_d)_n \frac{\gamma_d}{\gamma_b} (S - x) \, dx = 0 \qquad \text{(A11)}$$

for $n \neq m$ and

$$P \equiv \frac{\gamma_d^2}{\gamma_b^2} \frac{k_b}{k_d} = \frac{\rho_b c_b}{\rho_d c_d}$$

The ratio F/C is known from equation (A7).

If the initial temperature distribution is known, the coefficients F_n and C_n can be determined in the following manner: Rearranging equations (A3) and indicating the summation give

$$\frac{T_w - T}{T_w - T_2} = \sum_{n=1}^{\infty} e^{-(\lambda_d)_n^2 \gamma_d^2 t} C_n \sin (\lambda_d)_n x \qquad \text{for } 0 \leq x \leq s^- \qquad \text{(A12a)}$$

$$\frac{T_w - T}{T_w - T_2} = \sum_{n=1}^{\infty} e^{-(\lambda_b)_n^2 \gamma_b^2 t} F_n \cos (\lambda_b)_n (S - x) \qquad \text{for } s^+ < x < S \qquad \text{(A12b)}$$

Letting $t = 0$ with $\frac{T_w - T}{T_w - T_2} = T(x,0)$, then multiplying both sides of equation (A12a) by $\sin (\lambda_d)_m x \, dx$ and integrating from 0 to s, multiplying both sides of equation (A12b) by $P \frac{F_m}{C_m} \cos (\lambda_b)_m (S - x) \, dx$ and integrating from s to S, and finally adding the two resulting equations yield

$$\int_0^s T(x,0) \sin (\lambda_d)_m x \, dx + P \frac{F_m}{C_m} \int_s^S T(x,0) \cos (\lambda_b)_m (S - x) \, dx$$

$$= \int_0^s \left[\sum_{n=1}^{\infty} C_n \sin (\lambda_d)_n \right] x \sin (\lambda_d)_m x \, dx$$

$$+ \int_s^S \left[\sum_{n=1}^{\infty} F_n \cos (\lambda_b)_n (S - x) \right] P \frac{F_m}{C_m} \cos (\lambda_b)_m (S - x) \, dx \qquad (A13)$$

Making use of equation (A11) gives

$$\int_0^s T(x,0) \sin (\lambda_d)_n x \, dx + P \frac{F_n}{C_n} \int_s^S T(x,0) \cos (\lambda_b)_n (S - x) \, dx$$

$$= C_n \int_0^s \sin^2 (\lambda_d)_n x \, dx + F_n \frac{F_n}{C_n} P \int_s^S \cos^2 (\lambda_b)_n (S - x) \, dx \qquad (A14)$$

Performing the integration on the right, substituting $(F_n/C_n) = \Lambda_n$ and $\Lambda_n C_n = F_n$, and rearranging result in

$$C_n = \frac{\int_0^s T(x,0) \sin (\lambda_d)_n x \, dx + P\Lambda_n \int_s^S T(x,0) \cos (\lambda_b)_n (S - x) \, dx}{\frac{1}{(\lambda_d)_n}\left[\frac{1}{2}(\lambda_d)_n s - \frac{1}{4} \sin 2(\lambda_d)_n s\right] + P\Lambda_n^2 \left[\frac{1}{2}(\lambda_b)_n (S - s) + \frac{1}{4} \sin 2(\lambda_b)_n (S - s)\right] \frac{1}{(\lambda_b)_n}} \tag{A15}$$

or

$$F_n = \frac{\frac{1}{P\Lambda_n} \int_0^s T(x,0) \sin (\lambda_d)_n x \, dx + \int_s^S T(x,0) \cos (\lambda_b)_n (S - x) \, dx}{\frac{1}{(\lambda_d)_n} \frac{1}{P\Lambda_n^2}\left[\frac{(\lambda_d)_n}{2} s - \frac{1}{4} \sin 2(\lambda_d)_n s\right] + \frac{1}{(\lambda_b)_n}\left[\frac{1}{2} (\lambda_b)_n (S - s) + \frac{1}{4} \sin 2(\lambda_b)_n (S - s)\right]} \tag{A16}$$

In most cases the temperatures of interest are for times when only the first term of the series is significant. Also, the higher the contact resistance is, the lower H is and the more insignificant the other terms become. The average belt temperature across its thickness T_{av} can be determined from

$$\frac{T_{av} - T_2}{T_w - T_2} = \frac{1}{S - s} \int_s^S \left[1 - \sum_{n=1}^{\infty} F_n e^{-(\lambda_b)_n^2 r_b^2 t} \cos (\lambda_b)_n (S - x)\right] dx$$

$$= 1 - \sum_{n=1}^{\infty} F_n e^{-(\lambda_b)_n^2 r_b^2 t} \frac{\sin (\lambda_b)_n (S - s)}{(\lambda_b)_n (S - s)} \tag{A17}$$

Orthogonality Proof

For the proof of the orthogonality of the eigenfunctions of the heat-transfer solution over the interval $x = 0$ to $x = S$, the following notation

will be used:

$$\psi(n) = f(n) \equiv C_n \sin (\lambda_d)_n x \qquad \text{for} \quad 0 \leq x \leq s^-$$

$$\psi(n) = f(n) \equiv F_n \cos (\lambda_b)_n (S - x) \qquad \text{for} \quad s^+ \leq x \leq S \tag{A18}$$

The eigenfunctions are orthogonal with respect to a weighting function $p(x)$ if

$$\int_0^S \psi(n)\psi(m)p(x)\, dx = 0$$

$$\text{for} \quad m \neq n \qquad \text{(Sturm-Liouville problem)}$$

It will be shown that

$$\left.\begin{aligned} p(x) &= 1 \qquad \text{for} \quad 0 \leq x \leq s^- \\ \text{and} \\ p(x) &= \frac{k_b}{k_d} \qquad \text{for} \quad s^+ \leq x \leq S \end{aligned}\right\} \tag{A19}$$

is a satisfactory weighting function. From (A18) it is obvious that

$$\frac{\partial^2 \psi(n)}{\partial x^2} = - \lambda_n^2 \psi(n) \tag{A20}$$

and

$$\frac{\partial^2 \psi(m)}{\partial x^2} = - \lambda_m^2 \psi(m) \tag{A21}$$

Multiplying (A20) by $\psi(m)p(x)\, dx$, (A21) by $\psi(n)p(x)\, dx$, then subtracting one from the other, and finally integrating give

$$\int_0^S -\left[\psi(n) \frac{\partial^2 \psi(m)}{\partial x^2} - \psi(m) \frac{\partial^2 \psi(n)}{\partial x^2}\right] p(x)\, dx = \int_0^S \left(\lambda_n^2 - \lambda_m^2\right) \psi(m)\psi(n)p(x)\, dx \tag{A22}$$

By using equations (A18), (A19), and (A6), equation (A22) becomes

$$\int_0^s \left[f(n) \frac{\partial^2 f(m)}{\partial x^2} - f(m) \frac{\partial^2 f(n)}{\partial x^2} \right] dx + \frac{k_b}{k_d} \int_s^S \left[f(n) \frac{\partial^2 f(m)}{\partial x^2} - f(m) \frac{\partial^2 f(n)}{\partial x^2} \right] dx$$

$$= \left[(\lambda_d)_n^2 - (\lambda_d)_m^2 \right] \left[\int_0^s f(n) f(m)\, dx + \frac{k_b}{k_d} \frac{\gamma_d^2}{\gamma_b^2} \int_s^S f(n) f(m)\, dx \right] \qquad \text{(A23)}$$

Working with the first term of the first integral on the left of equation (A23) and making use of $\int u\, dv = uv - \int v\, du$ twice in succession give

$$\int_0^s f(n) \frac{\partial^2 f(m)}{\partial x^2} dx = - \left[f(m) \frac{\partial f(n)}{\partial x} - \frac{\partial f(m)}{\partial x} f(n) \right]_0^s + \int_0^s f(m) \frac{\partial^2 f(n)}{\partial x^2} dx$$

As a result, the left side of equation (A23) becomes

$$- \left[f(m) \frac{\partial f(n)}{\partial x} - \frac{\partial f(m)}{\partial x} f(n) \right]_0^s - \frac{k_b}{k_d} \left[f(m) \frac{\partial f(n)}{\partial x} - \frac{\partial f(m)}{\partial x} f(n) \right]_s^S$$

Since $f = 0$ at $x = 0$ and $(\partial f/\partial x) = 0$ at $x = S$ (boundary conditions 1 and 2), the left side of (A23) becomes

$$- \left\{ f(m) \frac{\partial f(n)}{\partial x} - \frac{\partial f(m)}{\partial x} f(n) - \frac{k_b}{k_d} \left[f(m) \frac{\partial f(n)}{\partial x} - \frac{\partial f(m)}{\partial x} f(n) \right] \right\}_s$$

From equations (A3)

$$\frac{k_b}{k_d} \left(\frac{\partial f}{\partial x} \right)_s = \left(\frac{\partial f}{\partial x} \right)_s$$

The left side of (A23) is then

$$- \left\{ \frac{\partial f(m)}{\partial x} \left[f(n) - f(n) \right] - \frac{\partial f(n)}{\partial x} \left[f(m) - f(m) \right] \right\}_s$$

From equation (A9) at $x = s$

$$f = \frac{k_d}{H} \frac{\partial \mathit{f}}{\partial x} + \mathit{f}$$

With this substitution for f the left-hand side of equation (A23) becomes zero. Since on the right-hand side of equation (A23)

$$(\lambda_d)_n^2 - (\lambda_d)_m^2 \neq 0 \qquad \text{for} \quad n \neq m$$

then

$$\int_0^s \mathit{f}(n)\mathit{f}(m)\, dx + P \int_s^S f(n)f(m)\, dx = 0 \qquad \text{for } n \neq m \qquad \text{(A24)}$$

where

$$P = \frac{r_d^2}{r_b^2} \frac{k_b}{k_d}$$

Substituting for f and f from equation (A18) and dividing by $C_n C_m$ result in equation (A11).

APPENDIX B

EFFECT OF CYCLING

For the calculations of figures 4 and 5, the initial temperature distribution assumed for the drum wall was a uniform value of T_w across its thickness. This is always a good assumption for the first cycle. If the contact time is short (e.g., the curve for $t_c = 0.02$ sec in fig. 4), the assumption may not be valid for later cycles. In this appendix the effect of cycling on the belt average temperature after contact T_1 is discussed.

Cycling results in a change of the initial drum wall temperature distribution, which affects the average value of the belt temperature after contact. The most rigorous method of determining the effect of cycling would be iteration of the series solution for a given contact time. A constant temperature through the drum wall can be assumed, and a first value of the belt high-temperature parameter $(T_1 - T_2)/(T_w - T_2)$ and the local temperature parameter $(T - T_2)/(T_w - T_2)$ could be calculated. For the second calculation, $T(x,0)$ of the drum wall is taken as the values obtained at the end of the first cycle. (The initial belt assumption of a uniform temperature through its thickness is still valid.) The process can be repeated until the decreasing value of $(T_1 - T_2)/(T_w - T_2)$ reaches an asymptote when plotted as a function of the number of cycles.

The method described in the preceding paragraph is rather involved; however, it is possible to obtain some limiting values without iterating by using, for the initial drum wall temperature variation $T(x,0)$, that variation obtained by cycling at a contact time approaching zero with zero time between contacts. (For these cases, $(T_1 - T_2)/(T_w - T_2)$ also approaches zero.) For the illustrative case of $H = \infty$, the temperature profile in the drum wall would approach a straight line constant in time, as shown in sketch (g) where $T(x,0) = 1 - (T - T_2)/(T_w - T_2)$. If $t_c > 0$, the drum wall temperatures would be

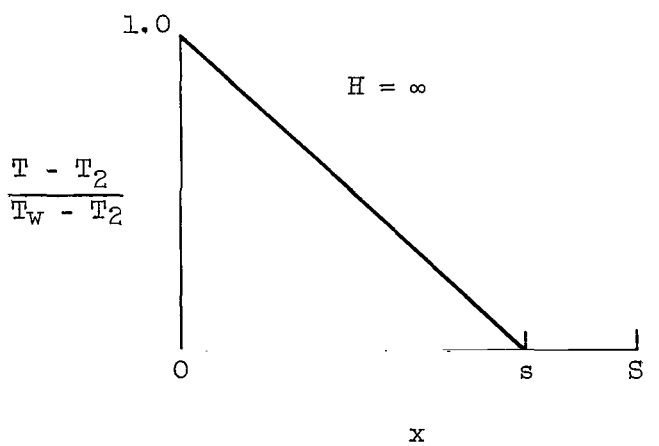

(g)

higher at the end of a contact period than that given by the variation in sketch (g). Thus, using the $T(x,0)$ obtained from a cycle time approaching zero produces a lower value of $(T_1 - T_2)/(T_w - T_2)$ than the true value. In another example where $H = 10{,}000$ Btu/(sq ft)(hr)($^\circ$R), the drum temperature distribution approaches the value shown in sketch (h) for cycled contact time approaching zero. In this example, only one-third of the ΔT drop occurs in the drum wall (the conductance of the drum wall for the assumed thickness of 0.05-in.-thick molybdenum is about 20,000 Btu/(sq ft)(hr)($^\circ$R)).

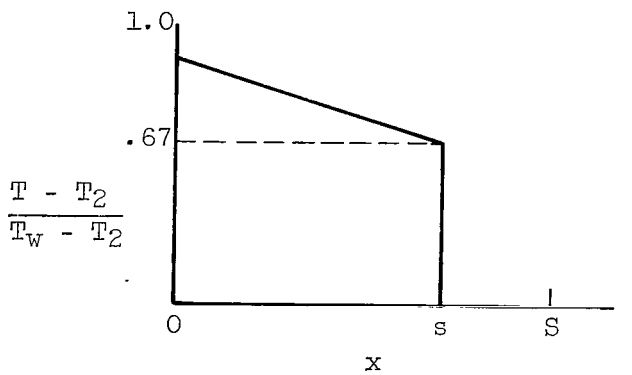

(h)

From the results of these and similar cases, limiting values of $(T_1 - T_2)/(T_w - T_2)$ for several values of H were computed and plotted in figure 26. The upper limit of each shaded area was obtained by assuming the initial temperature distribution to be constant at T_w throughout the drum wall. The lower limit line was obtained by assuming for $T(x,0)$ the temperature variation obtained by cycling the belt at $t_c \to 0$ as indicated in the two aforementioned examples. An iteration for $(T_1 - T_2)/(T_w - T_2)$ at a particular value of H for any t_c would fall in the corresponding shaded area. In the region of low values of $(T_1 - T_2)/(T_w - T_2)$, the iterative value would be near the bottom of the shaded area. In the region of high values of $(T_1 - T_2)/(T_w - T_2)$ the iterative value would be near the top of the shaded area. The spread in $(T_1 - T_2)/(T_w - T_2)$ is seen to increase as H increases. However, since, in general, the spread is not large and for belt-radiation-system operation $(T_1 - T_2)/(T_w - T_2)$ is high, the effect of cycling on the drum to belt heat ransfer is not considered very significant.

APPENDIX C

DRUM WEIGHT ESTIMATE

In this appendix an estimate of drum weight is obtained by considering an illustrative structure composed of a four-loop stationary drum (revolving belt) 20 feet long and 3 feet in diameter. A sketch of the drum cross section is shown in figure 27. The drum is assumed to be composed of an inner and an outer cylinder with separators (which also serve as support structures) to provide for longitudinal flow channels. All parts of the basic drum were assumed to be molybdenum. The outer cylinder was 36 inches in diameter and 0.05 inch thick. The inner cylinder was 34 inches in diameter and 0.02 inch thick. The separators are 0.05 inch thick and spaced 4 inches apart. This geometry may require the introduction of vapor at several positions along the length of the drum. The turbine housing is assumed to form one end of the drum. The drum will not need to support any compressive loads if the turbine-exhaust pressure is higher than the belt contact pressure and if the entire drum is pressurized by the exhaust. Annular passages could also be used for condensation with presumably no difference in weight.

To determine the weight of the meteoroid shield, the probability of no puncture through the shield in 500 days was assumed to be 0.999. The calculations were based on reference 12. Beryllium was used for shield material, since it gives the lightest weight at the assumed shield temperature of 1000° R (ref. 13). The shield also provided the support structure for the rollers.

The rollers for this example were assumed to be made of stainless steel and 5 inches in diameter. (This diameter would actually be determined by the thickness of the belt material and the mechanical properties at the operating temperatures.) The rollers consisted of hollow cylinders with 0.030-inch-thick walls and suitable internal support structure. They were supported at 4-foot intervals by bearings attached to the shield. The weight breakdown of the 3- by 20-foot drum and accessories is presented in the following table:

Component	Weight, lb
Drum outer cylinder	500
Inner cylinder	90
Separators and stiffening members	120
Drum end	20
Rollers	460
Bearings and drive mechanism	150
Internal piping	100
Meteoroid shield	910
Total	2350

The total weight is 2350 pounds, and the actual contact area is 153 square feet, which gives a drum weight parameter β of 16 lb/sq ft.

REFERENCES

1. Denington, Robert J., LeGray, William J., Shattuck, Russell D.: Electric Propulsion for Manned Missions. Proc. of AIAA-NASA Conf. on Engineering Problems of Manned Interplanetary Exploration, Palo Alto (Calif.), Sept. 30 - Oct. 1, 1963, pp. 145-159.

2. Krebs, Richard P., Winch, David M., and Lieblein, Seymour: Analysis of a Megawatt Level Direct Condenser-Radiator. Paper 2545-62, Am. Rocket Soc., Inc., 1962.

3. Weatherston, Roger C., and Smith, William E.: A Method of Heat Rejection from Space Powerplants. ARS Jour., vol. 30, no. 3, Mar. 1960, pp. 268-269.

4. Weatherston, Roger C., and Smith, William E: A New Type of Thermal Radiator for Space Vehicles. Paper 60-78, Inst. Aero. Sci., Inc., 1960.

5. Burge, H. L.: Revolving Belt Space Radiator. ARS Jour., vol. 32, no. 8, Aug. 1962, pp. 1243-1248.

6. McAdams, William H.: Heat Transmission. Third ed., McGraw-Hill Book Co., Inc., 1954, p. 329.

7. Fenech, H., and Rohsenow, W. M.: Thermal Conductance of Metallic Surfaces in Contact. Rep. NYO-2136, AEC, May 1959.

8. Fried, Erwin, and Costello, Frederick A.: The Interface Thermal Contact Resistance Problem in Space Vehicles. Paper 1690-61, Am. Rocket Soc., Inc., 1961.

9. Wheeler, R. G.: Thermal Conductance of Fuel Element Materials. Rep. HW 60343, Hanford Atomic Products Operation, AEC, 1959.

10. Jaffe, L. D., and Rittenhouse, J. B.: Behavior of Materials in Space Environments. Tech. Rep. 32-150, Jet Prop. Lab., C.I.T., Nov. 1, 1961.

11. Misra, B., and Bonilla, C. F.: Heat Transfer in the Condensation of Metal Vapors: Mercury and Sodium Up to Atmospheric Pressure. Preprint 11, AIChE, 1955.

12. Loeffler, I. J., Lieblein, Seymour, and Clough, Nestor: Meteoroid Protection for Space Radiators. Paper 2543-62, Am. Rocket Soc., Inc., 1962.

13. Diedrich, James H., and Lieblein, Seymour: Materials Problems Associated with the Design of Radiators for Space Powerplants. Paper 2535-62, Am. Rocket Soc., Inc., 1962.

TABLE I. - WEIGHT BREAKDOWN OF RANKINE CYCLE POWERPLANT

WITH FLUID-FILLED RADIATORS

[Electric output, 5 Mw; total reactor thermal power, 30 Mw; turbine-inlet temperature, 2310° R; turbine-exit temperature, 1610° R; turbine efficiency, 0.77; alternator efficiency, 0.90; net power output factor, 0.85.]

Group	Component	Component weight, lb	Group weight, lb	Specific weight, lb/kw
Fixed weights	Reactor	3,000	17,800	
	Shield	1,500		
	Boilers	6,500		
	Primary loop and pumps	5,400		
	Startup loops	1,400		
Variable weights	Turboalternators	7,500	20,200	4.04
	Power conditioning	12,700		
Weights replaced by drum-belt system	Condensers	7,700		
	Primary radiators	15,000		
	Subtotal	22,700	60,700	12.1
Weights not considered	Structure	17,000		
	Secondary radiator	13,500		
	Secondary piping	1,800		
	Miscellaneous and contingencies	7,000		
	Total	39,300	100,000	20

TABLE II. - EXAMPLES OF 5-MEGAWATT POWERPLANT SYSTEMS

(a) Rotating drum

Assumed inputs	
$\rho_b b/\overline{\epsilon}$, lb/sq ft	0.1038
Drum weight parameter, β, lb/sq ft	16
Belt thickness, b, in.	0.005 (beryllium)
Drum wall thickness, s, in.	0.05 (molybdenum)
Drum length, B, ft	20
Number of belt loops, N	2
Belt cycle temperature ratio, τ	0.69
Results	
Belt weight, w_b, lb	1620
Drum weight, w_d, lb	2270
Radiator-system weight, lb	3890
Radiator specific weight, α', lb/kw	0.78
Drum diameter, D, ft	2.26
Length of belt in one loop, L/N, ft	865
Belt speed, V, ft/sec	54.5
u (minimum weight value)	1.21
Contact time, t_c, sec	0.0652

(b) Revolving belt

Assumed inputs	
Drum weight parameter, β, lb/sq ft	16
Drum diameter, D, ft	2.26
Number of belt loops, N	4
Allowable tensile stress, σ_a, lb/sq in.	5000
$\overline{\epsilon}$	0.45
G	0.85
$\mathscr{E}_\sigma$	0.24
Results	
Drum weight, w_d, lb	3990
Belt weight, w_b, lb	1057
Radiator-system weight, lb	5047
Radiator specific weight, α', lb/kw	1.01
Drum length, B, ft	41.4
u (minimum weight value)	1.075
Belt cycle temperature ratio, τ	0.720
Belt thickness, b, in.	0.00576
Length of belt in one loop, L/N, ft	118.5
Belt speed, V, ft/sec	11.25

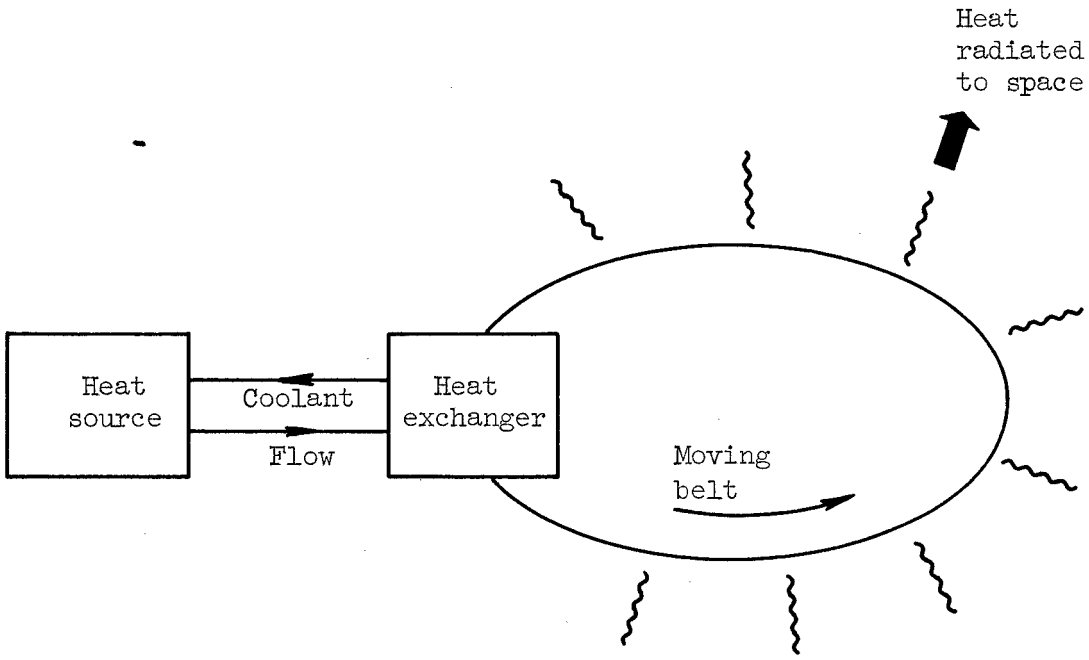

Figure 1. - Basic concept of moving-belt-radiator system.

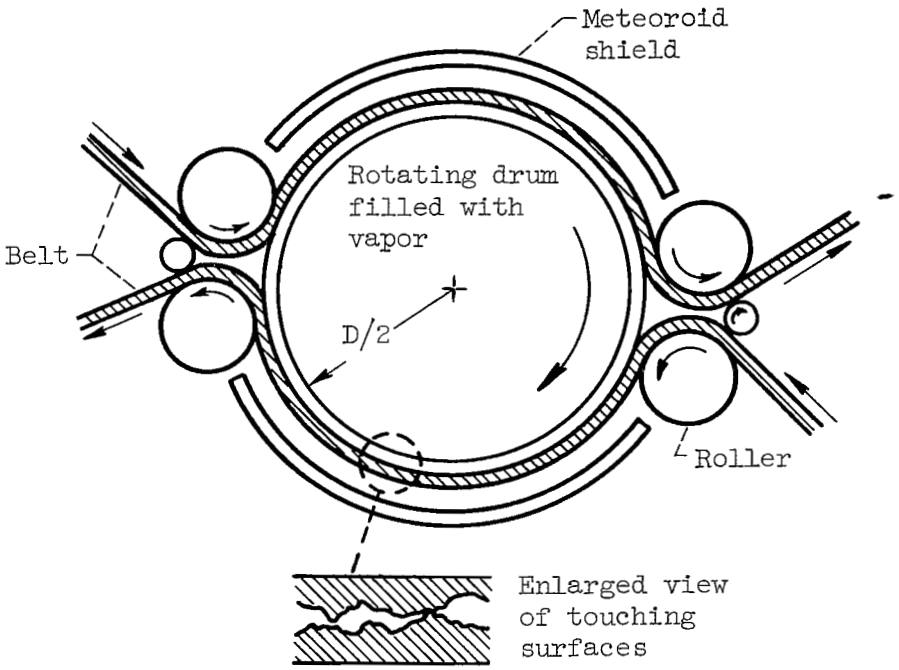

(a) Rotating-drum system.

Figure 2. - Mechanisms of heat transfer for moving-belt radiators.

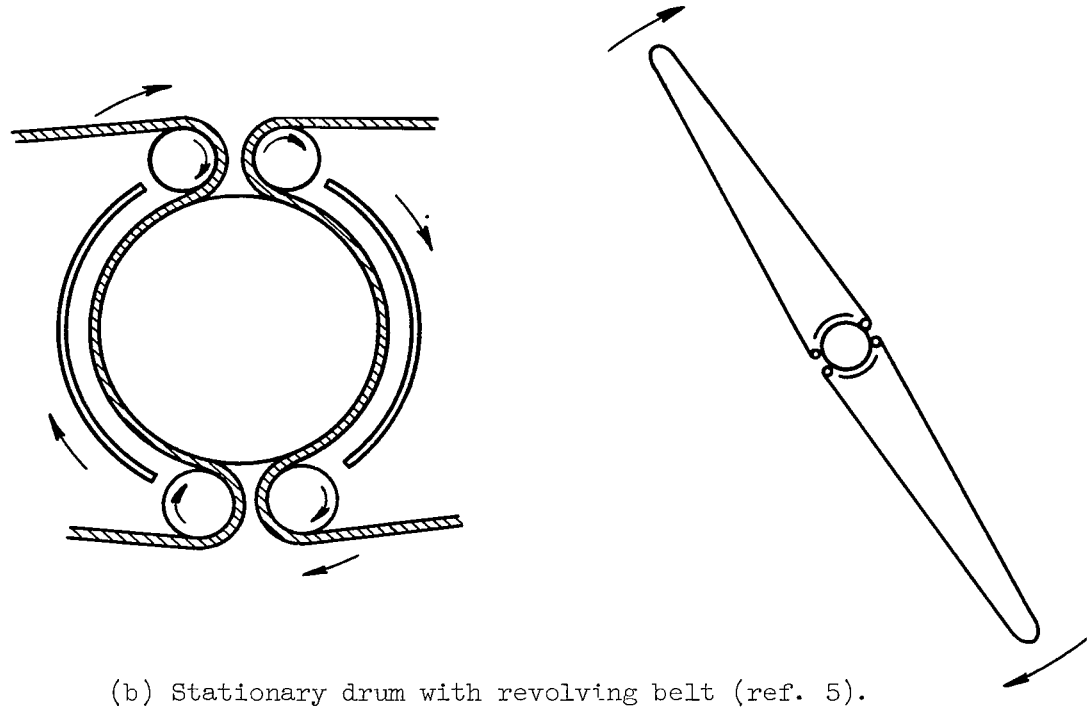

(b) Stationary drum with revolving belt (ref. 5).

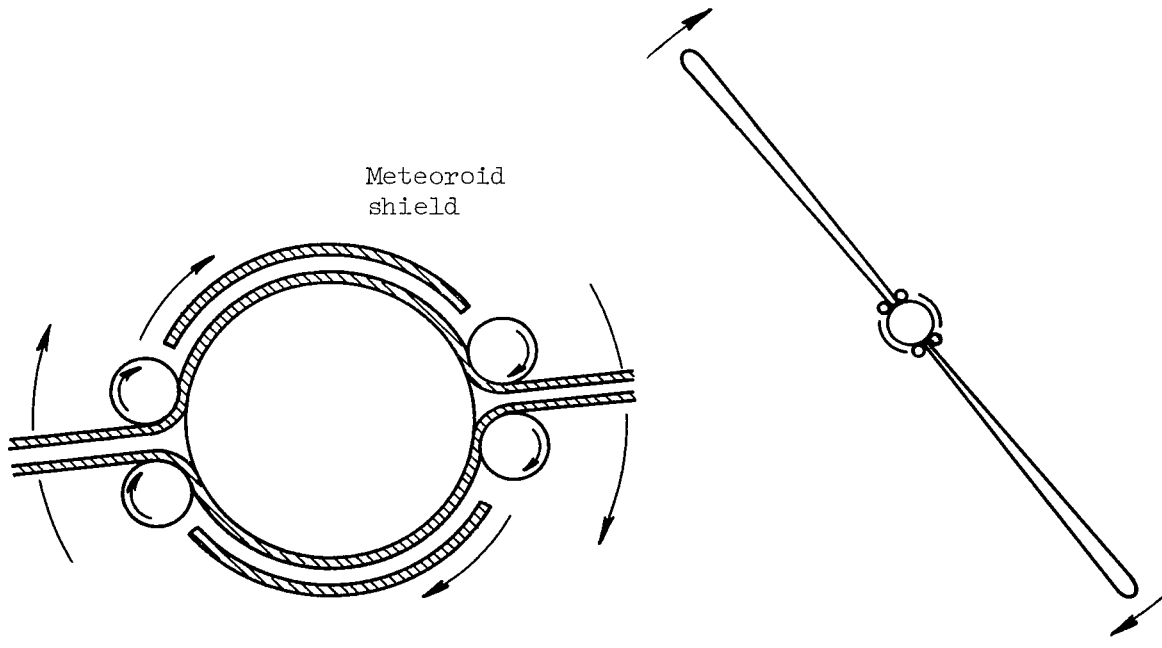

(c) Stationary drum with revolving belt (alternate method).

Figure 2. - Continued. Mechanisms of heat transfer for moving-belt radiators.

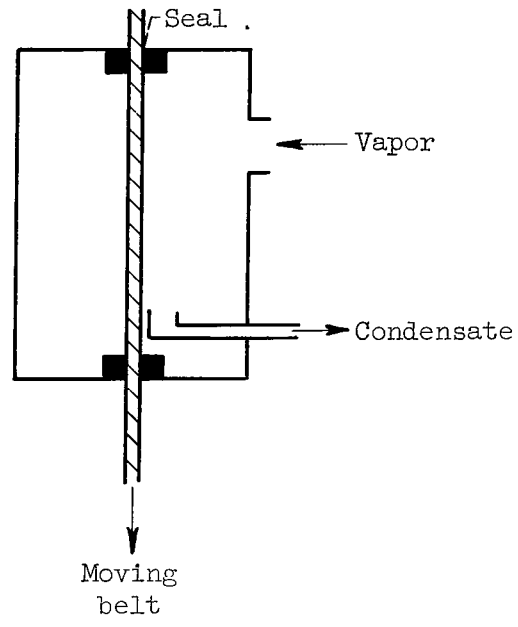

(d) Direct condensation.

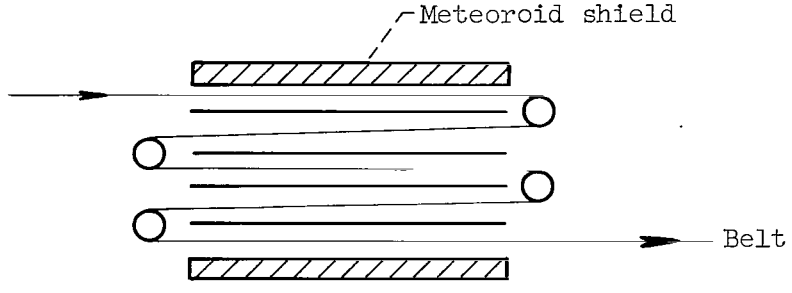

(e) Radiation.

Figure 2. - Concluded. Mechanisms of heat transfer for moving-belt radiators.

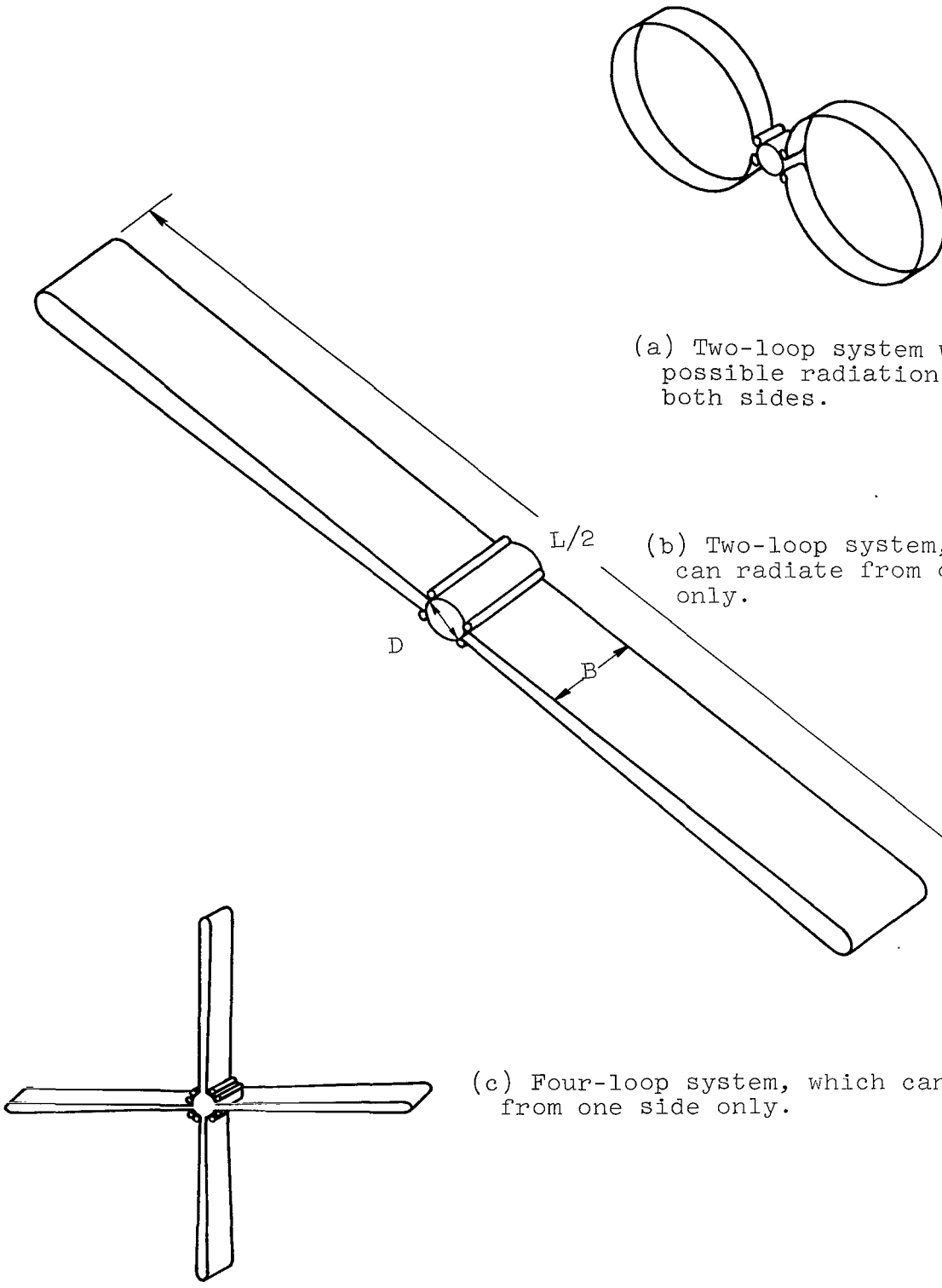

(a) Two-loop system with possible radiation from both sides.

(b) Two-loop system, which can radiate from one side only.

(c) Four-loop system, which can radiate from one side only.

Figure 3. - Belt configurations for system analyzed.

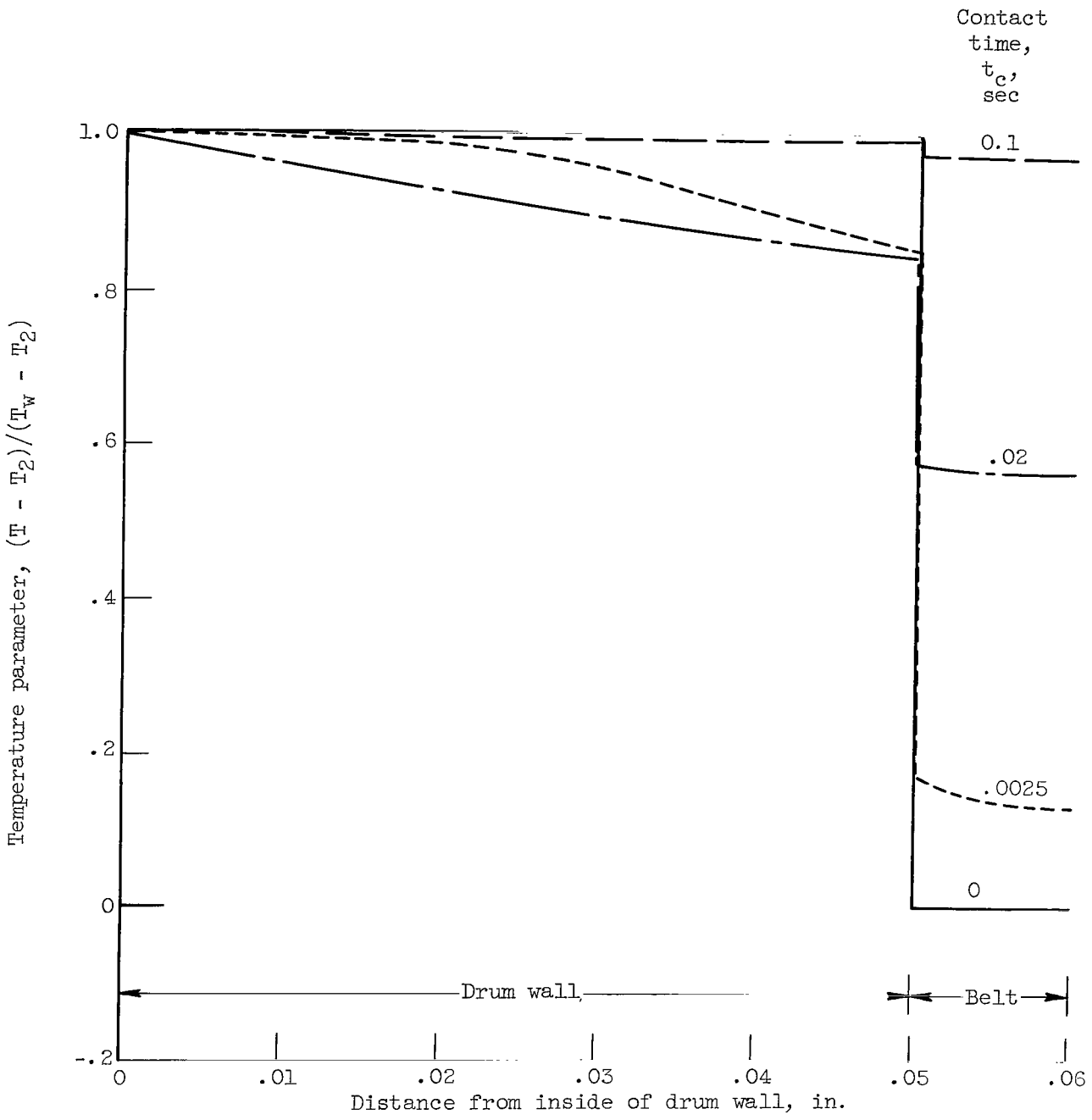

Figure 4. - Time history of temperature through drum wall and belt thickness. Contact conductance, 10,000 Btu/(sq ft)(hr)($^{\circ}$R); drum wall, 0.05-inch-thick molybdenum; belt, 0.01-inch-thick beryllium.

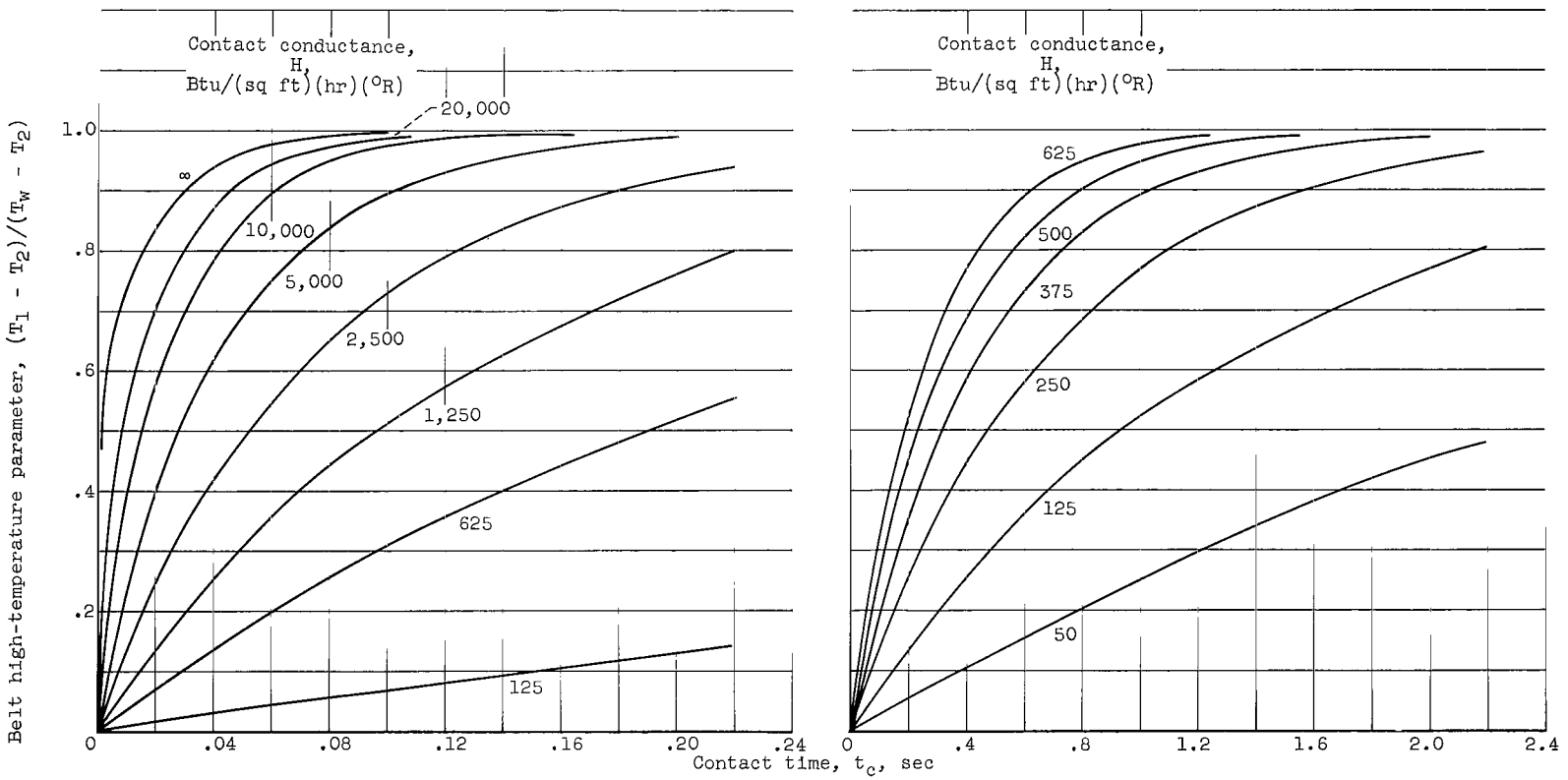

Figure 5. - Belt high-temperature parameter as a function of contact time.

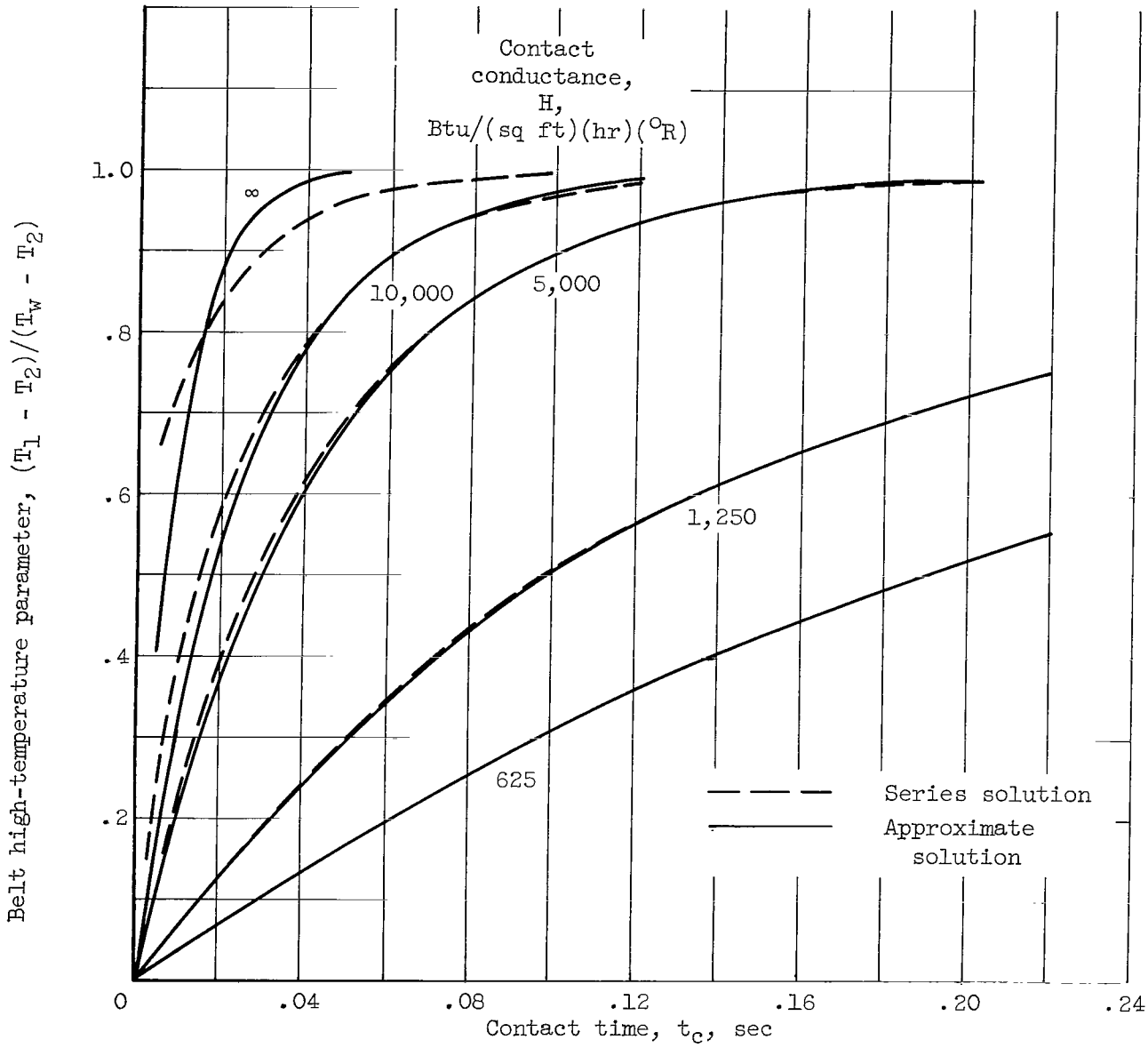

Figure 6. - Comparison of approximate solution with series solution of belt high temperature. Drum wall, 0.05-inch-thick molybdenum; belt, 0.01-inch-thick beryllium.

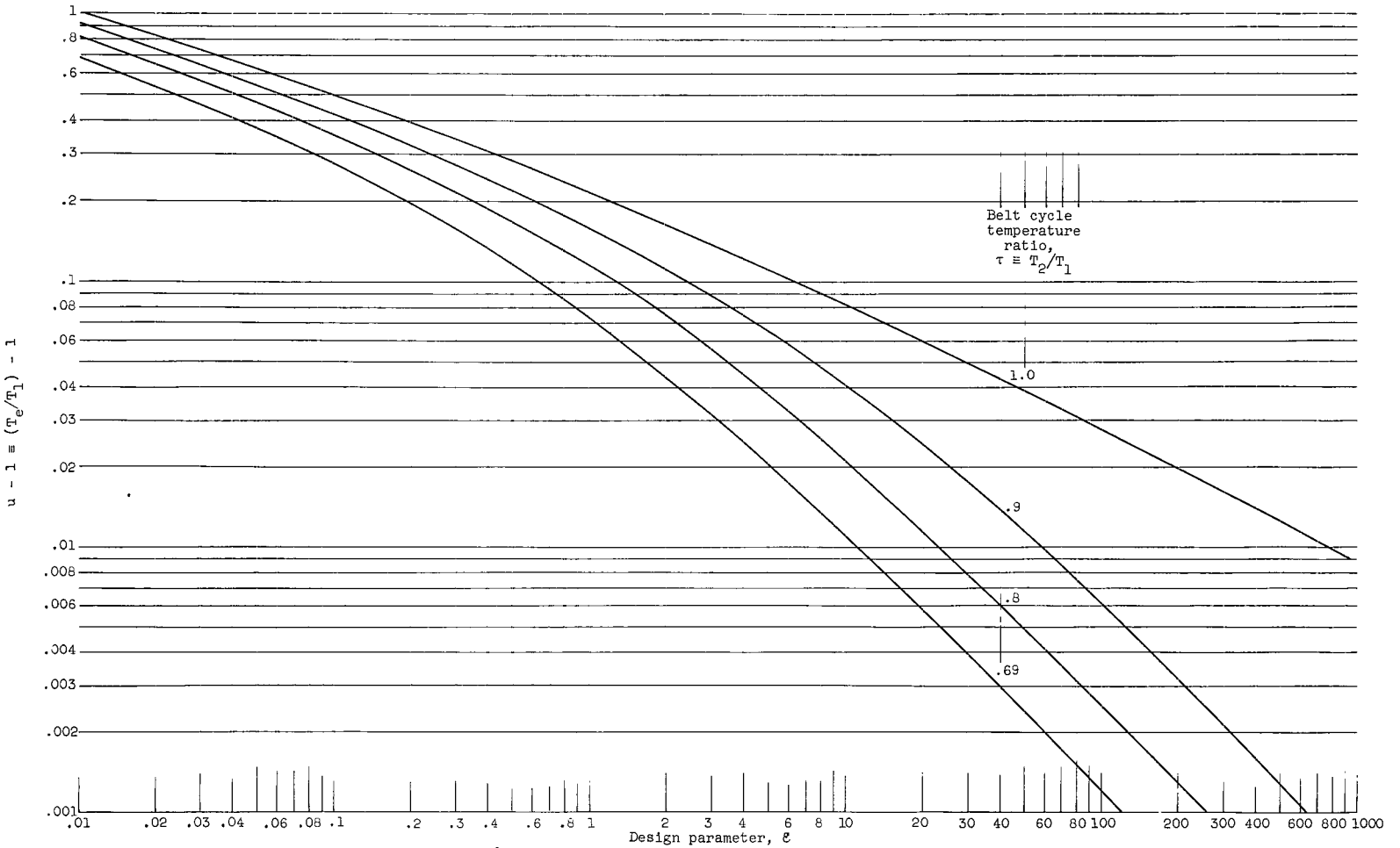

Figure 7. - Value of $u - 1$ that gives minimum total weight as a function of $\varepsilon \equiv \rho_b b/6r\beta v\bar{e}T_e^3$ for constant belt cycle temperature ratios.

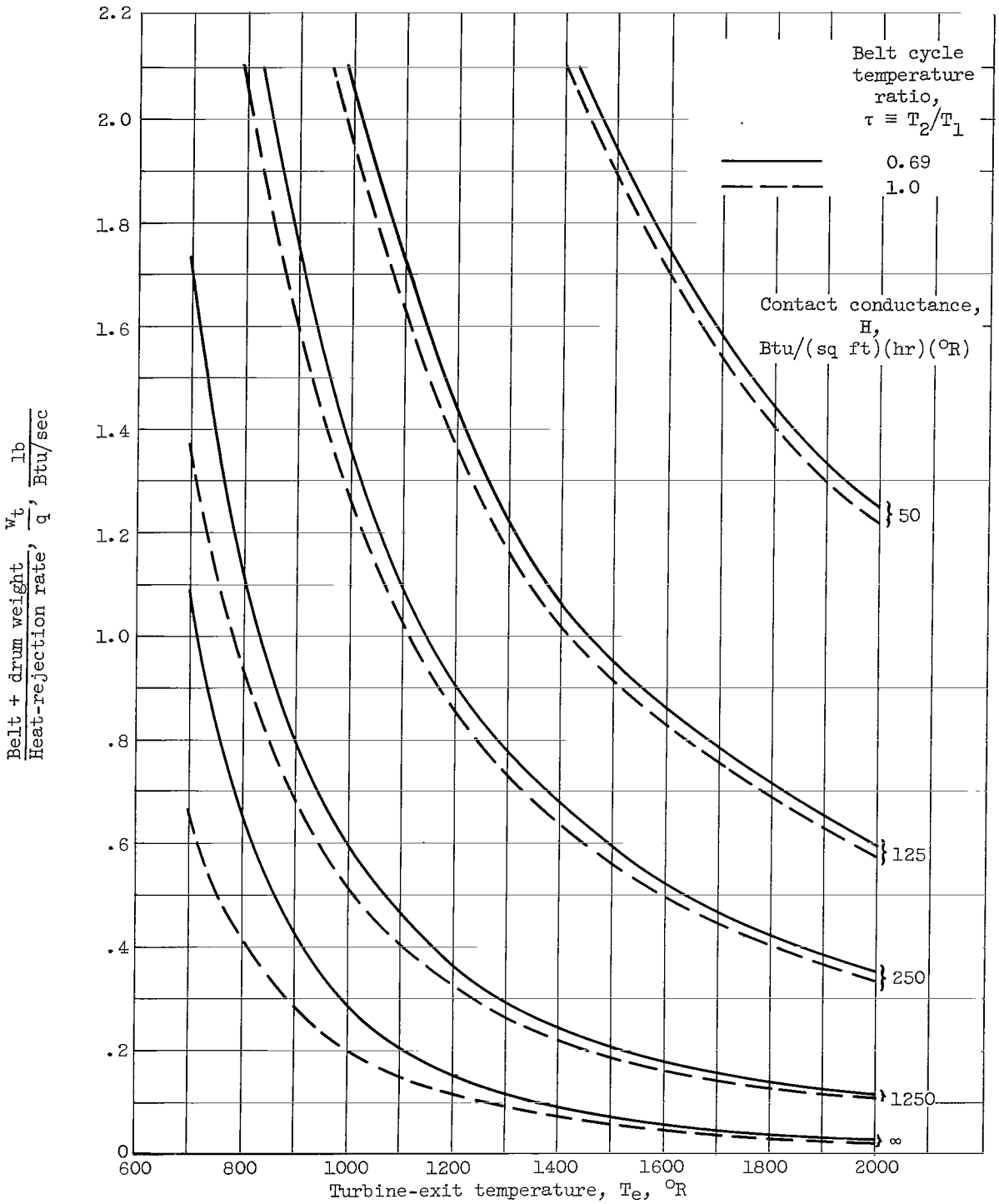

Figure 8. - Variation of drum plus belt weight per heat-rejection rate with turbine-exit temperature for several contact conductances and belt cycle temperature ratios. Drum weight parameter, 16 lb/sq ft; $\rho_b b/\bar{\epsilon}$, 0.1038 lb/sq ft; condensation heat-transfer coefficient, 1,000,000 Btu/(sq ft)(hr)(°R); K_{db}, 18,400 Btu/(sq ft)(hr)(°R); u (minimum weight value).

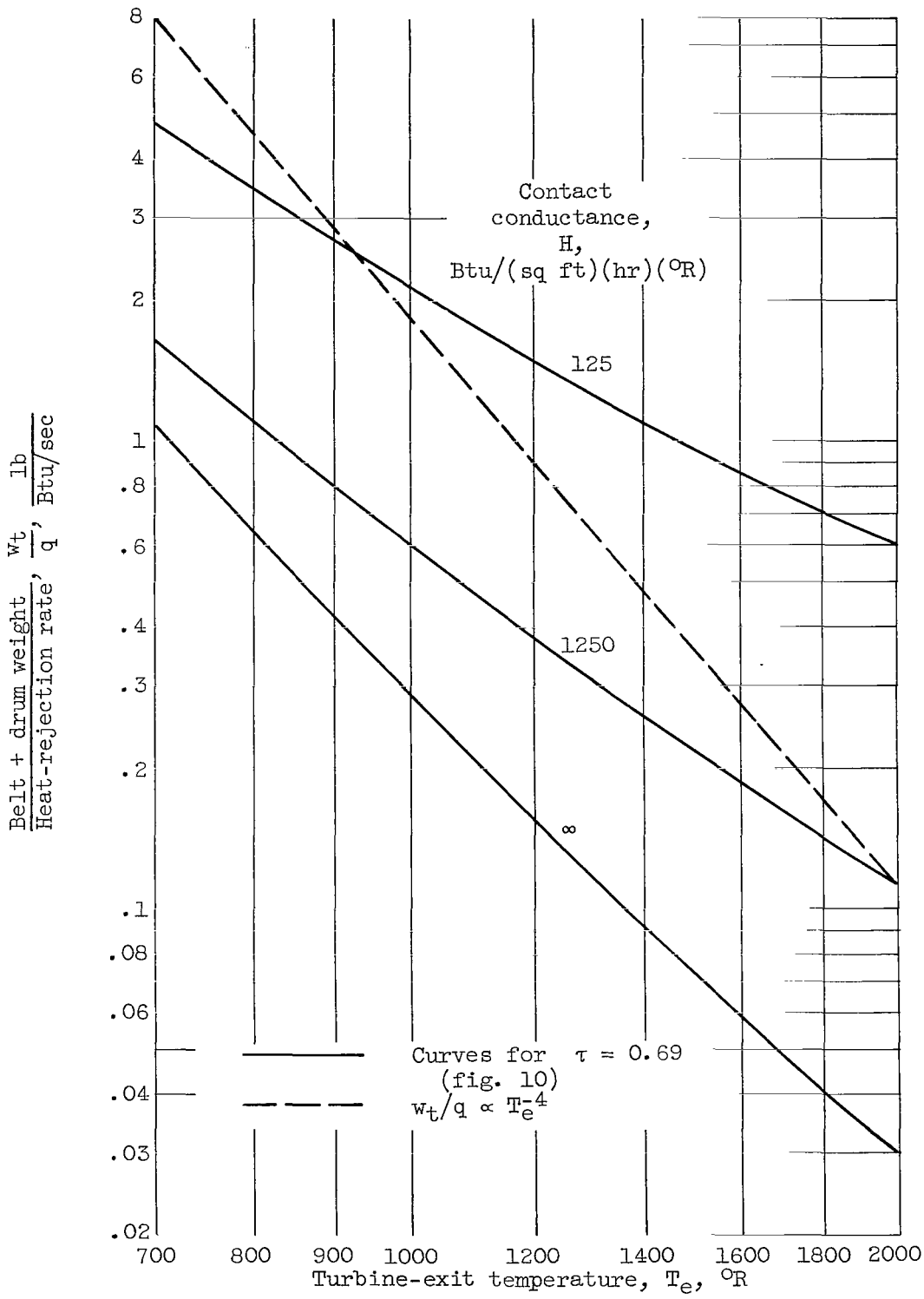

Figure 9. - Variation of radiator-system weight with temperature.

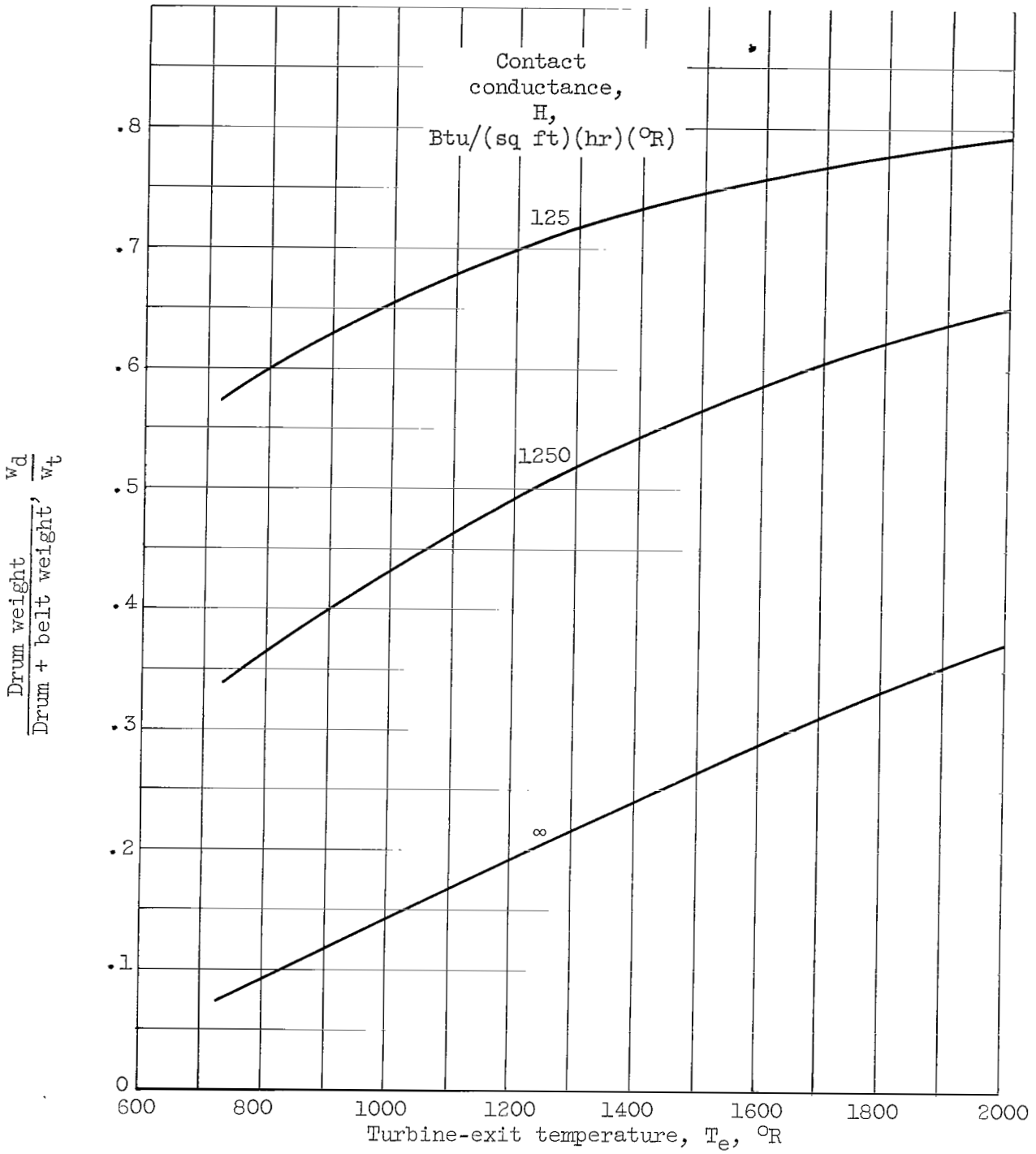

Figure 10. - Relative weight of drum and belt in a weight minimized system. Drum weight parameter, 16 lb/sq ft; $\rho_b b/\overline{\epsilon}$, 0.1038 lb/sq ft; condensation heat-transfer coefficient, 1,000,000 Btu/(sq ft)(hr)(°R); K_{db}, 18,400 Btu/(sq ft)(hr)(°R); belt cycle temperature ratio, 0.69; u (minimum weight value).

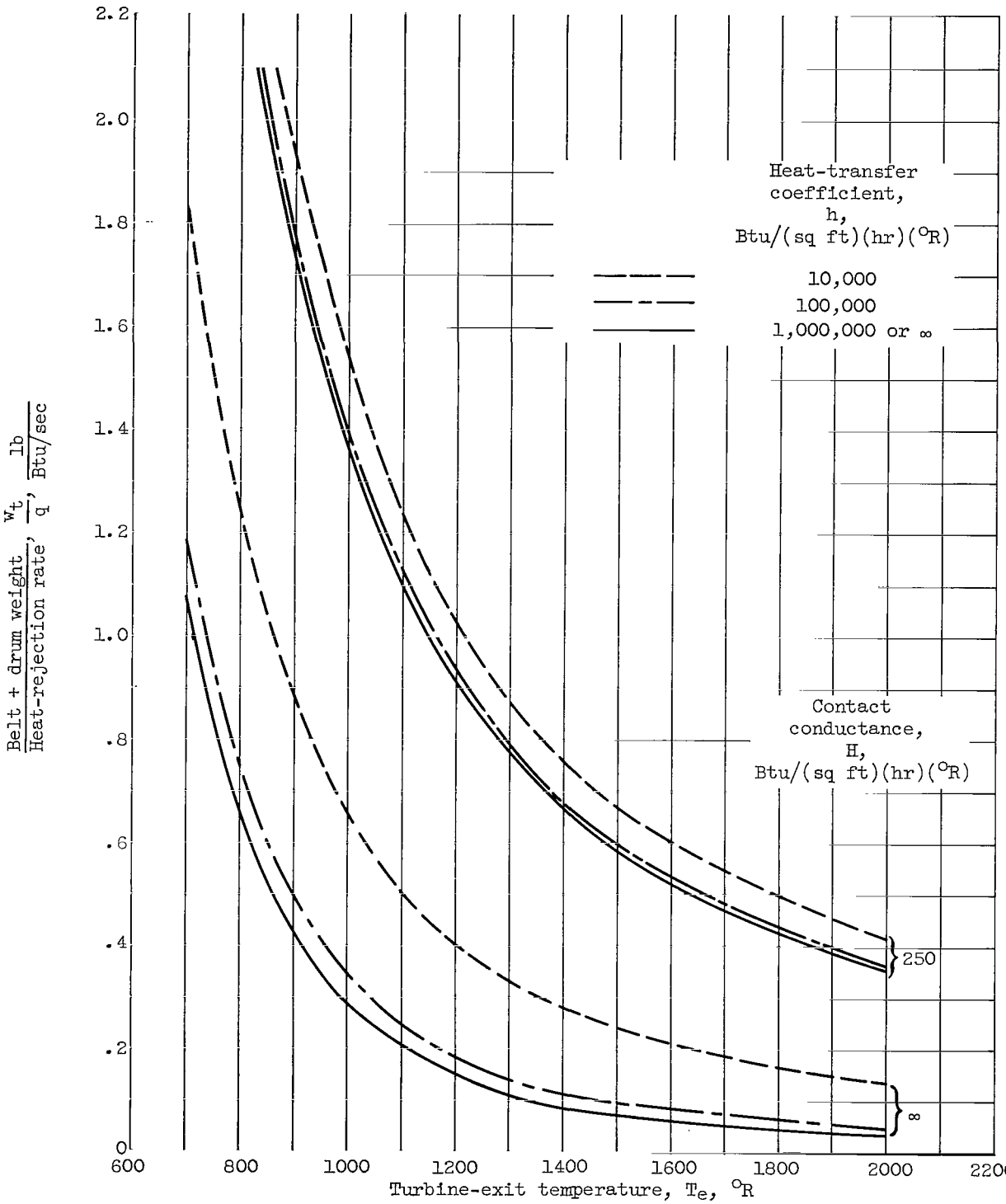

Figure 11. - Effect of condensing heat-transfer coefficient on drum plus belt specific weight. Drum weight parameter, 16 lb/sq ft; $\rho_b b/\bar{\epsilon}$, 0.1038 lb/sq ft; K_{db}, 18,400 Btu/(sq ft)(hr)(°R); belt cycle temperature ratio, 0.69; u (minimum weight value).

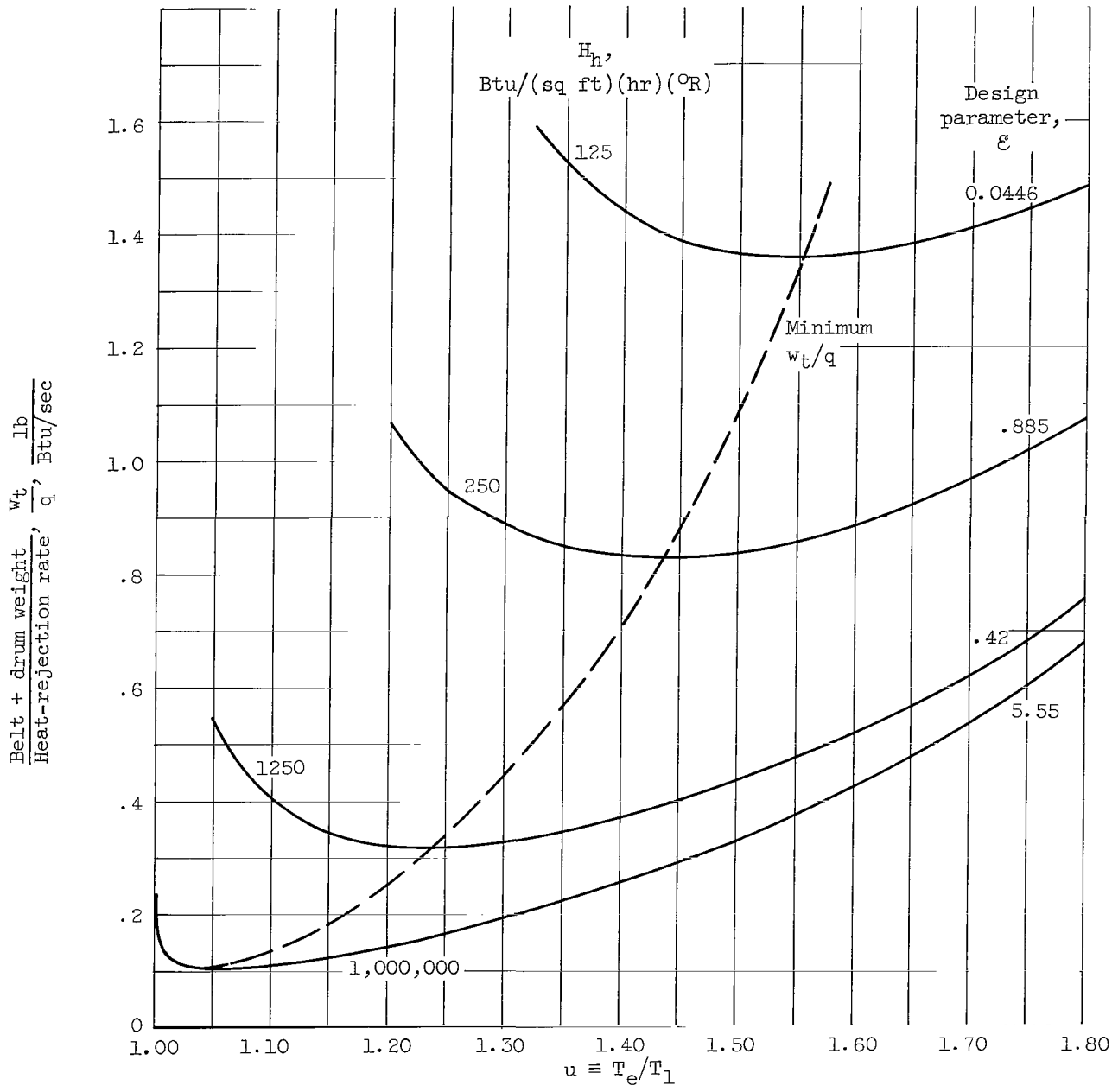

Figure 12. - Variation of drum plus belt weight per heat-rejection rate with u for various design parameters $\mathcal{E}$ and values of H_h. Drum weight parameter, 16 lb/sq ft; $\rho_b b/\bar{\epsilon}$, 0.1038 lb/sq ft; K_{db}, 18,400 Btu/(sq ft)(hr)(°R); belt cycle temperature ratio, 0.9; turbine-exit temperature, 1210° R.

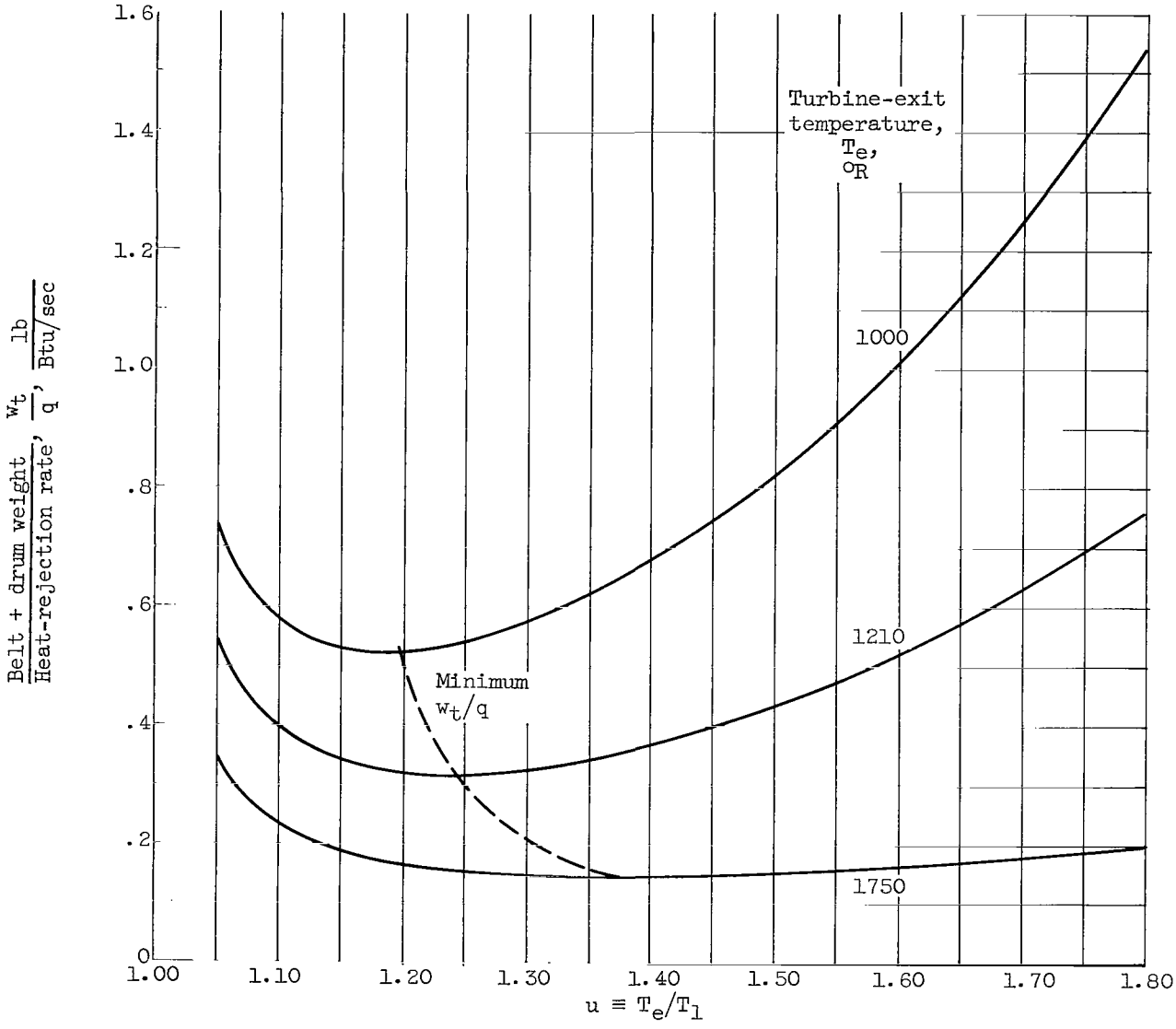

Figure 13. - Variation of drum plus belt weight per heat-rejection rate with u for various turbine-exit temperatures. Drum-weight parameter, 16 lb/sq ft; $\rho_b b/\bar{\epsilon}$, 0.1038 lb/sq ft; K_{db}, 18,400 Btu/(sq ft)(hr)(°R); belt cycle temperature ratio, 0.9; H_h, 1250 Btu/(sq ft)(hr)(°R).

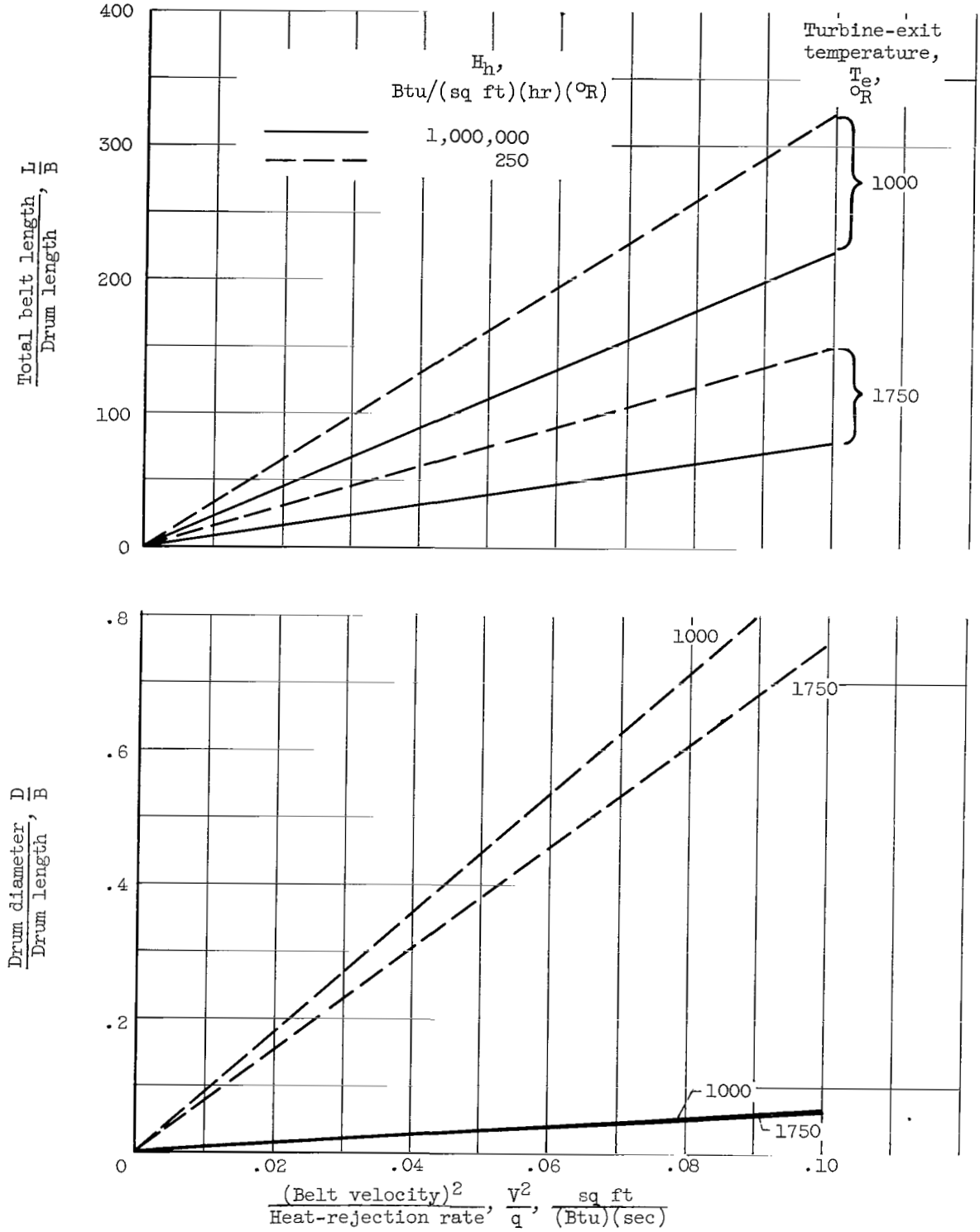

Figure 14. - Dependence between belt-system geometry and speed. Drum weight parameter, 16 lb/sq ft; $\rho_b b/\bar{\epsilon}$, 0.1038 lb/sq ft; belt, 0.01-inch-thick beryllium; K_{db}, 18,400 Btu/(sq ft)(hr)(°R); belt cycle temperature ratio, 0.69; u (minimum weight value); number of belt loops, 2.

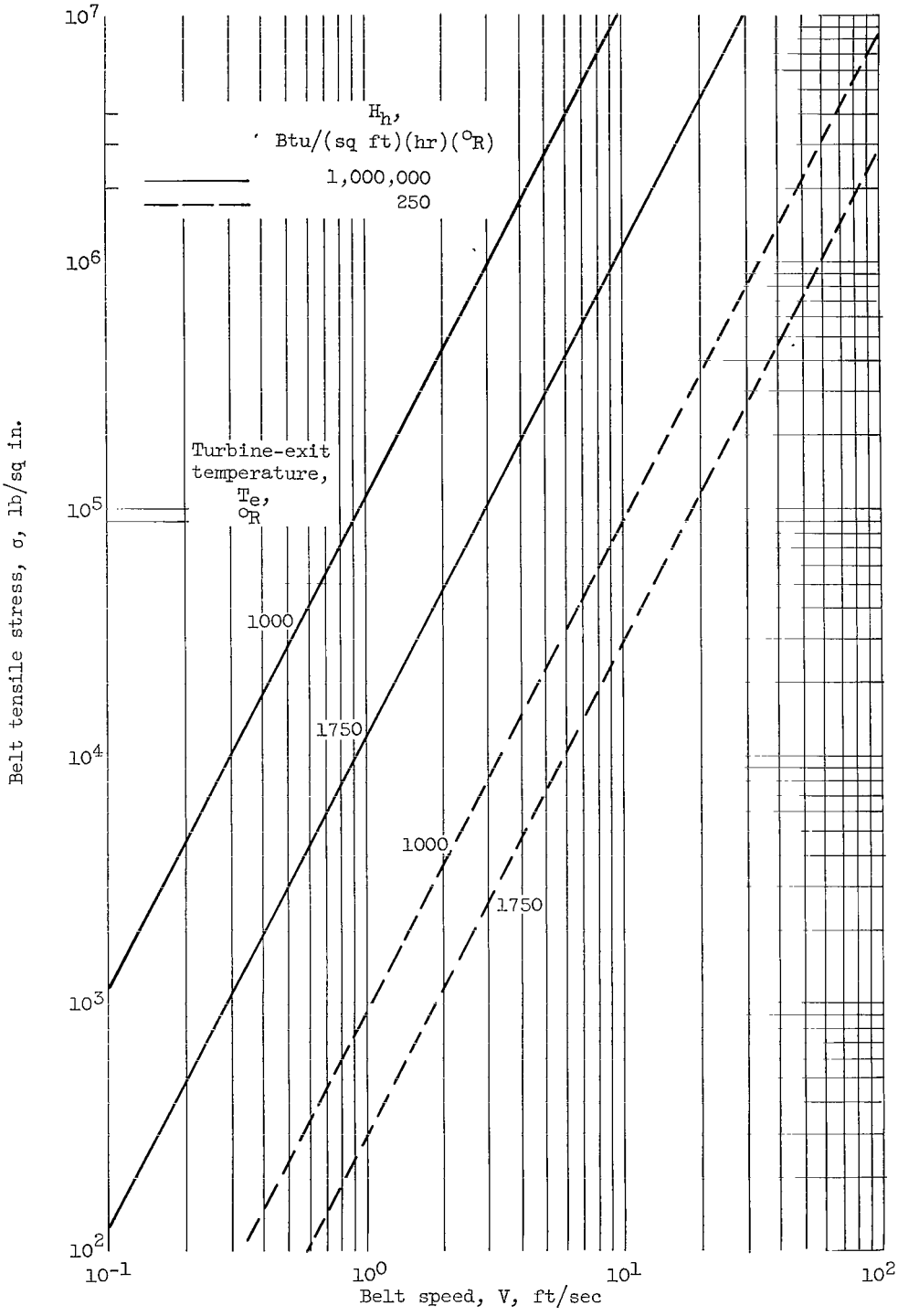

Figure 15. - Variation of belt stress for stationary drum with revolving belt. Drum weight parameter, 16 lb/sq ft; $\rho_b b/\bar{\epsilon}$, 0.2076 lb/sq ft; belt, 0.01-inch-thick beryllium; K_{db}, 18,400 Btu/(sq ft)(hr)(^oR); belt cycle temperature ratio, 0.69; u (minimum weight value); number of belt loops, 2.

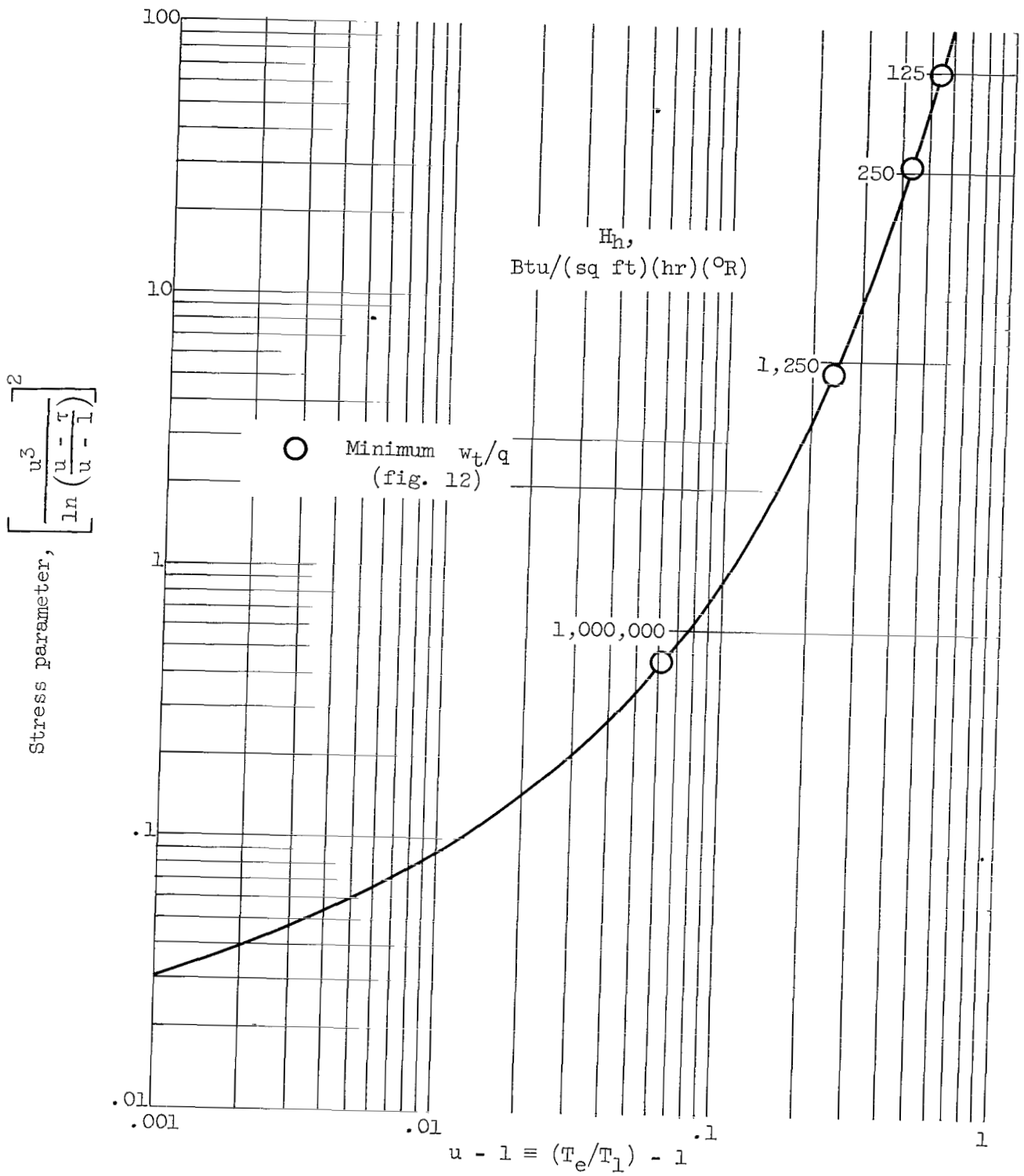

Figure 16. - Relation between stress parameter and $u - 1$ for belt cycle temperature ratio of 0.69.

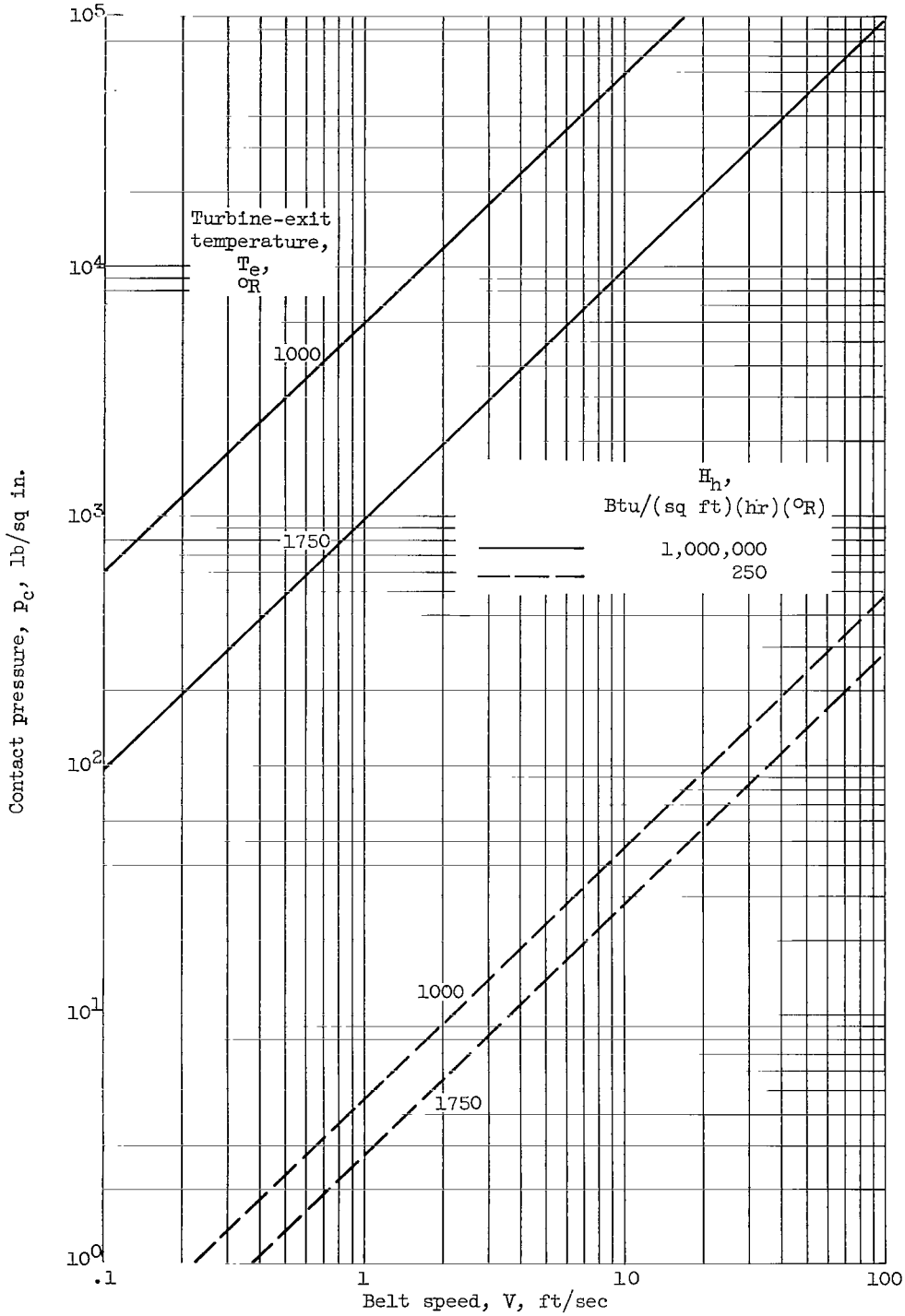

Figure 17. - Variation of contact pressure for stationary drum with revolving belt. Drum weight parameter, 16 lb/sq ft; $\rho_b b/\bar{\epsilon}$, 0.2076 lb/sq ft; belt, 0.01-inch-thick beryllium; K_{db}, 18,400 Btu/(sq ft)(hr)(°R); belt cycle temperature ratio, 0.69; u (minimum weight value); number of belt loops, 2.

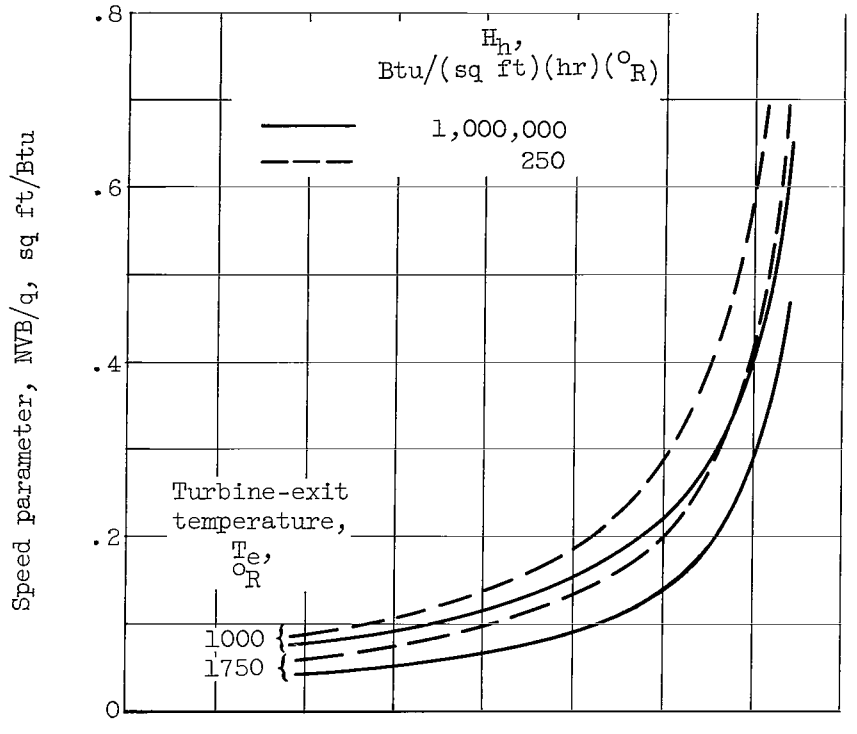

(a) Speed parameter.

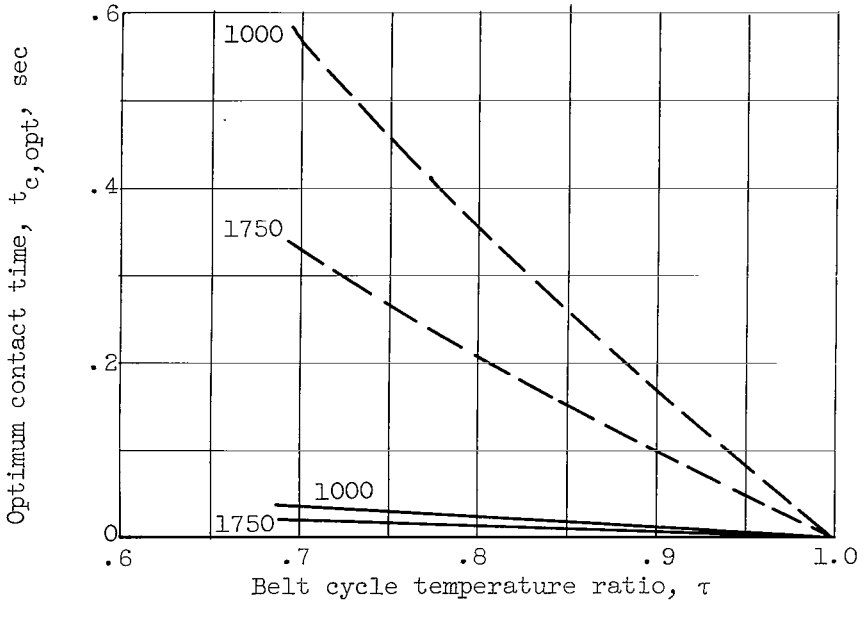

(b) Contact time.

Figure 18. - Variation of belt speed and contact time with belt cycle temperature ratio. Drum weight parameter, 16 lb/sq ft; $\rho_b b/\bar{\epsilon}$, 0.1038 lb/sq ft; belt, 0.01-inch-thick beryllium; K_{db}, 18,400 Btu/(sq ft)(hr)(^oR).

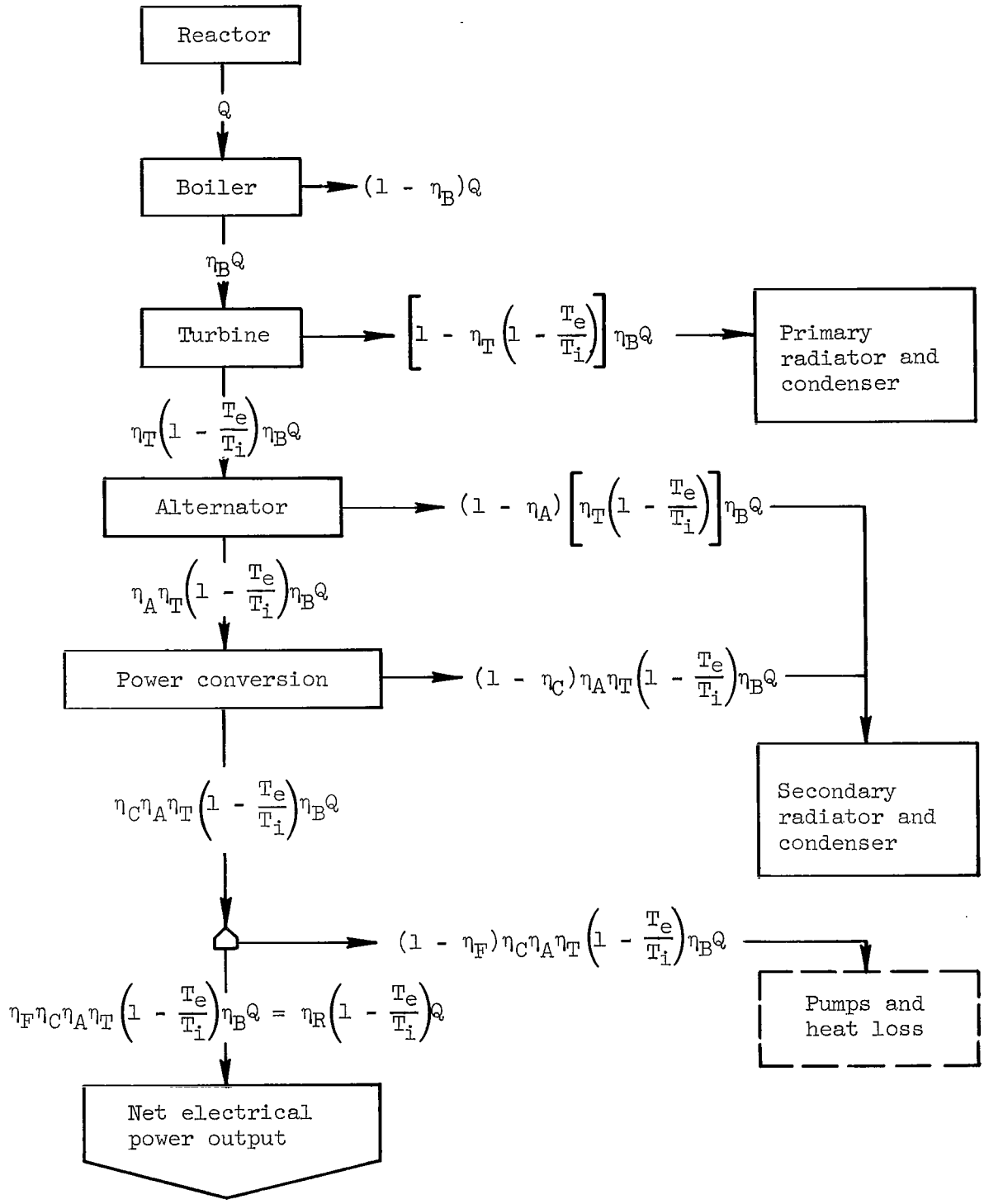

Figure 19. - Block diagram of Rankine vapor powerplant cycle.

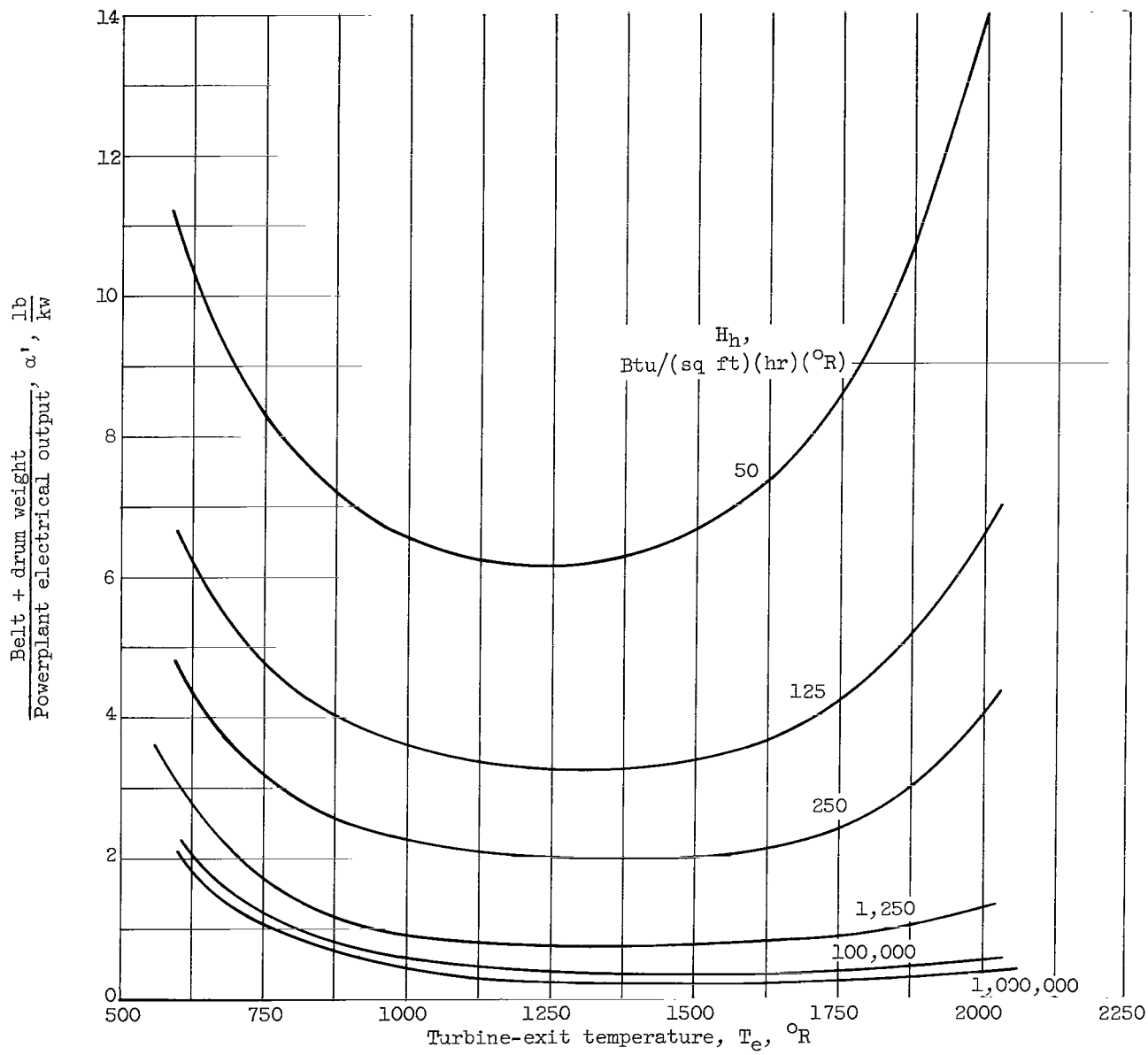

Figure 20. - Radiator specific weight as a function of H_h and turbine-exit temperature. Drum weight parameter, 16 lb/sq ft; $\rho_b b/\bar{\epsilon}$, 0.1038 lb/sq ft; K_{db}, 18,400 Btu/(sq ft)(hr)(°R); belt cycle temperature ratio, 0.69; u (minimum weight value); turbine-inlet temperature, 2310° R; $\eta_C \eta_P \eta_T \eta_A$, 0.578; η_T, 0.77.

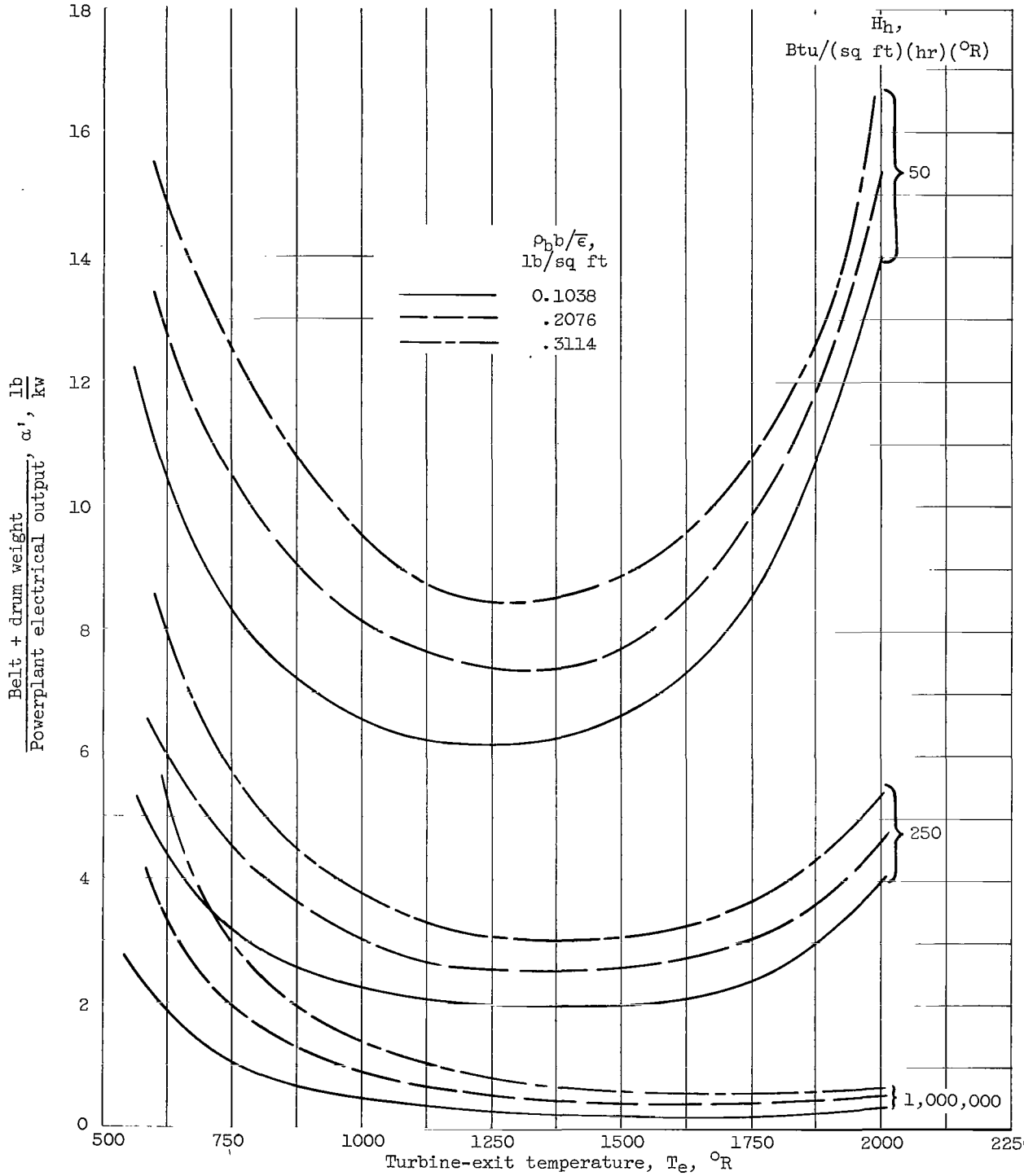

Figure 21. - Variation of radiator specific weight with $\rho_b b/\epsilon$ for various values of H_h. Drum weight parameter, 16 lb/sq ft; K_{db}, 18,400 Btu/sq ft)(hr)(°R); belt cycle temperature ratio, 0.69; u (minimum weight value); turbine-inlet temperature, 2310° R; $\eta_F\eta_C\eta_A\eta_T$, 0.578; η_T, 0.77.

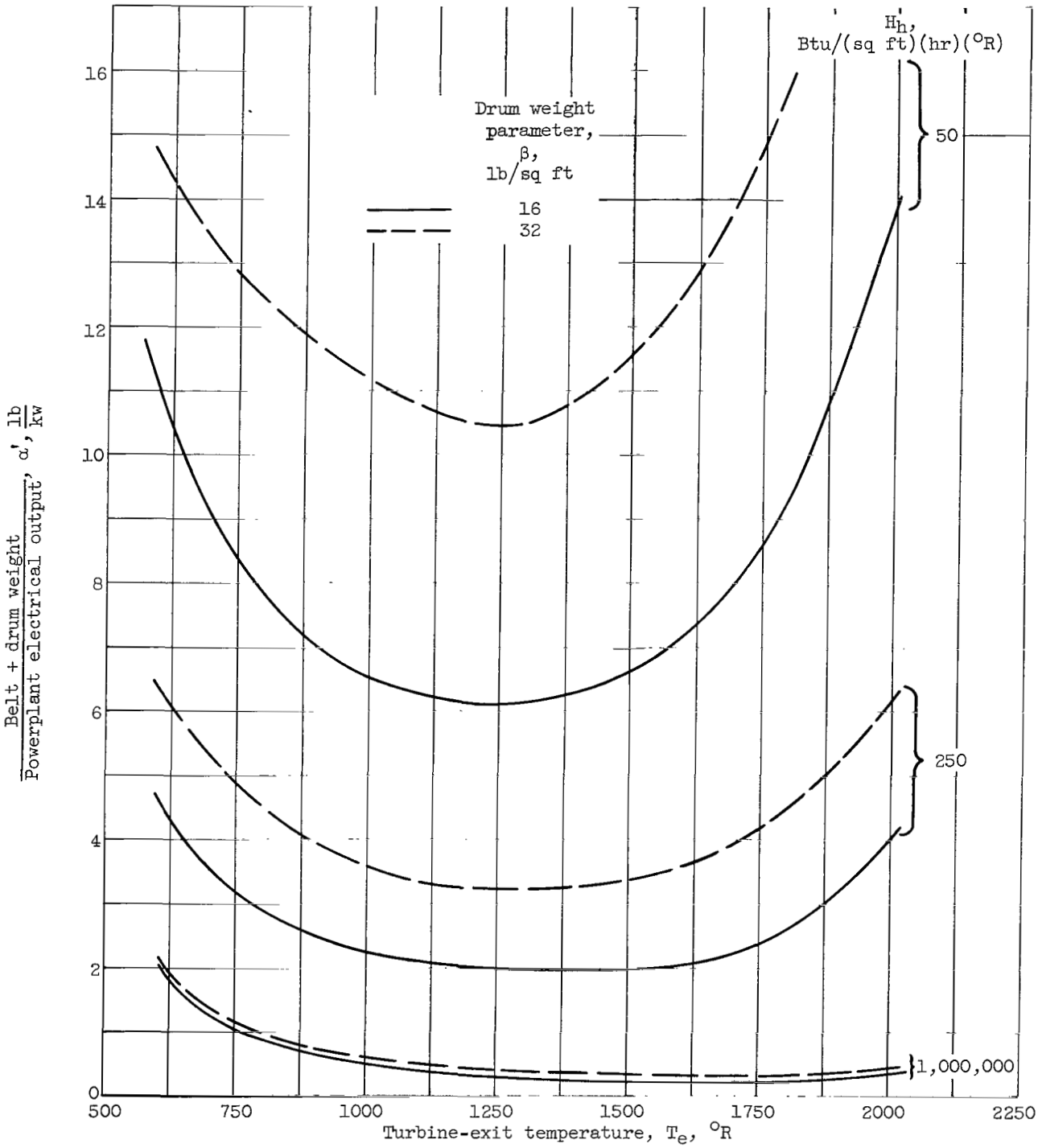

Figure 22. - Variation of radiator specific weight with drum weight parameter for various values of H_h. $\rho_b b/\bar{\epsilon}$, 0.1038 lb/sq ft; K_{db}, 18,400 Btu/(sq ft)(hr)($^\circ$R); belt cycle temperature ratio, 0.69; u (minimum weight value); turbine-inlet temperature, 2310° R; $\eta_F\eta_C\eta_A\eta_T$, 0.578; η_T, 0.77.

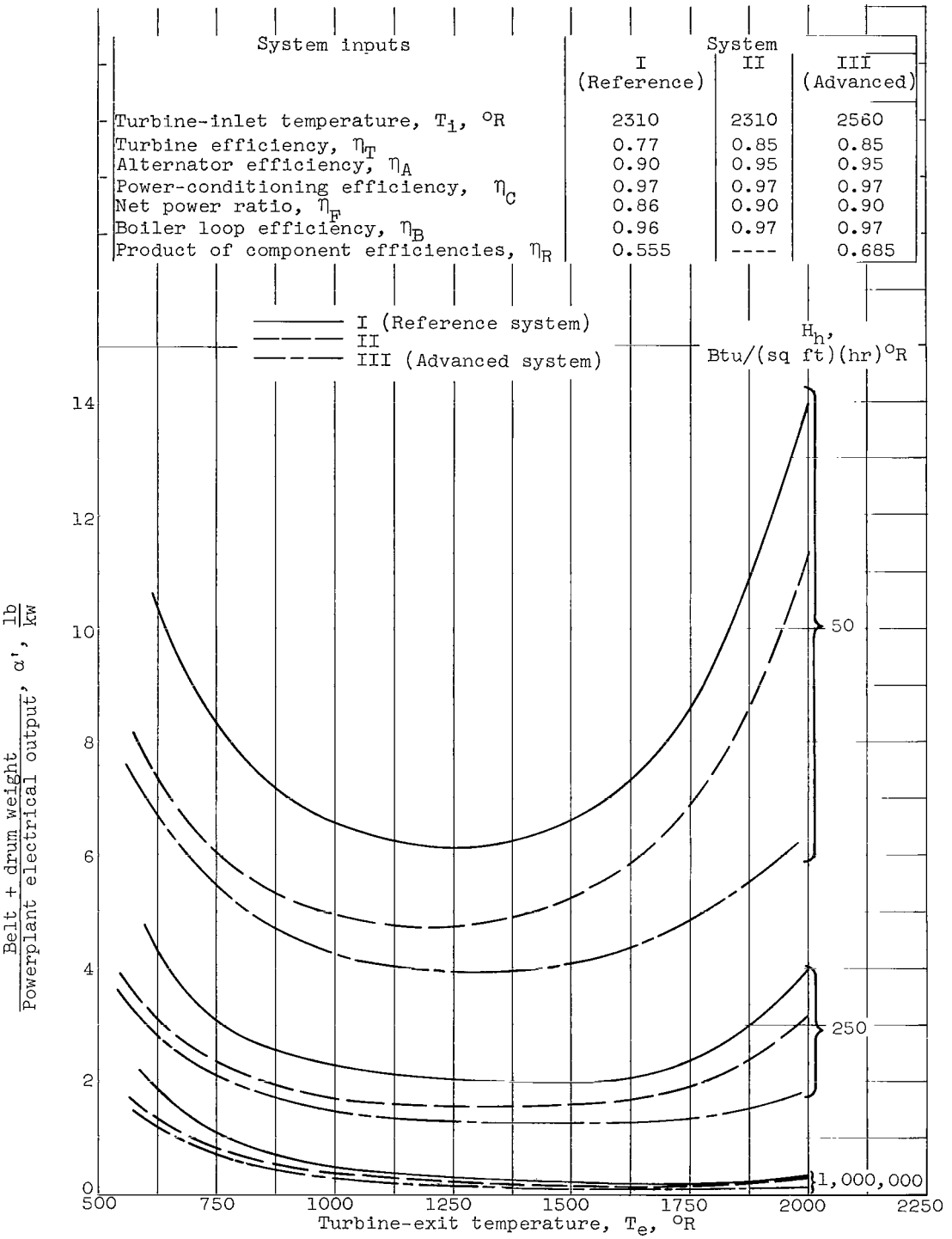

Figure 23. - Variation of radiator specific weight with component efficiency and turbine-inlet temperature for various values of H_h. $\rho_b b/\epsilon$, 0.1038 lb/sq ft; drum weight parameter, 16 lb/sq ft; K_{db}, 18,400 Btu/(sq ft)(hr)(°R); belt cycle temperature ratio, 0.69; u (minimum weight value).

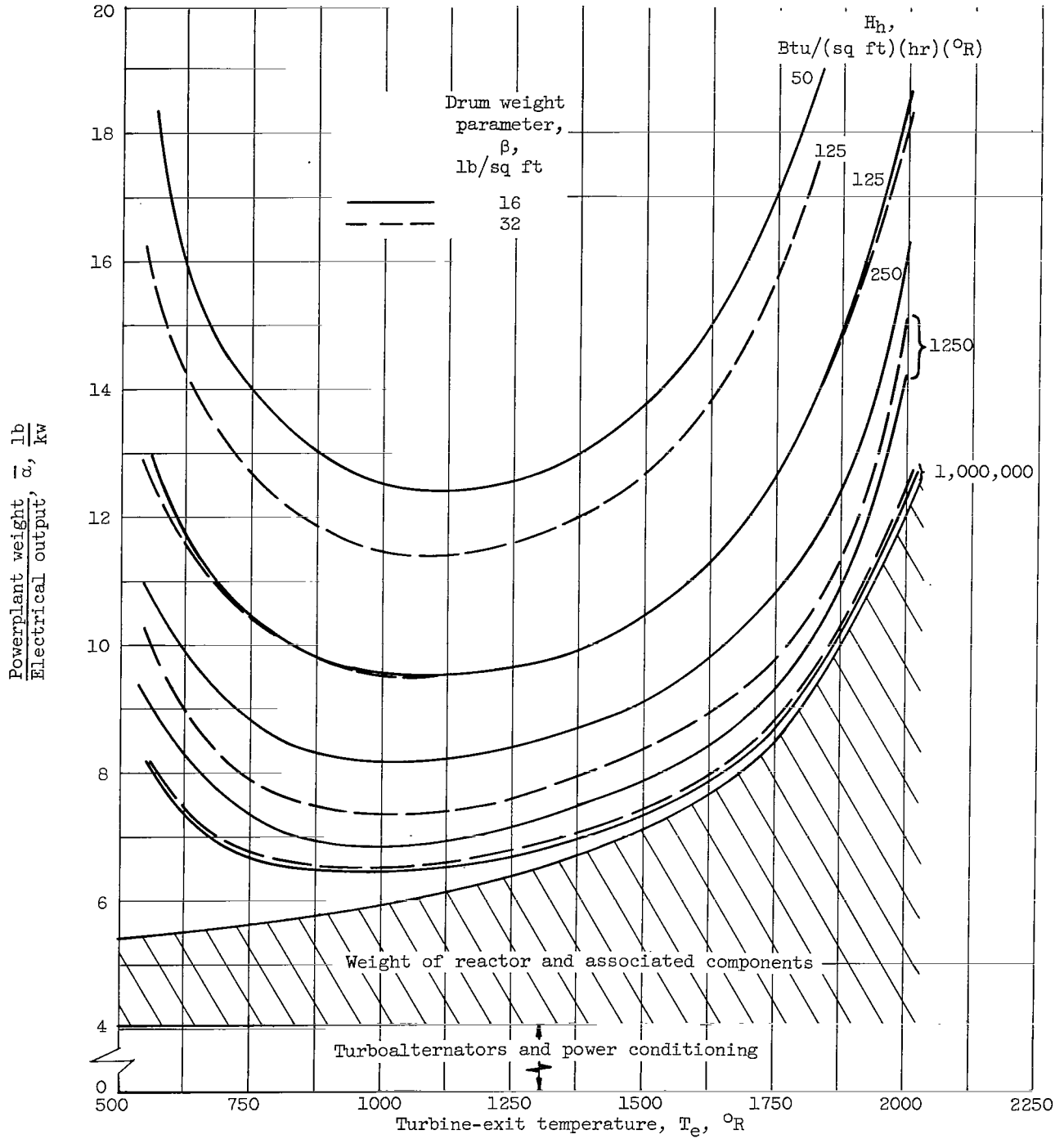

(a) Reference system; electrical output, 5 megawatts; η_R, 0.555; turbine-inlet temperature, 2310° R.

Figure 24. - Variation of total powerplant specific weight with H_h and turbine-exit temperature for conventional and advanced systems. $\rho_b b/\bar{\epsilon}$, 0.1038 lb/sq ft; K_{db}, 18,400 Btu/(sq ft)(hr)(°R); belt cycle temperature ratio, 0.69; u (minimum weight value).

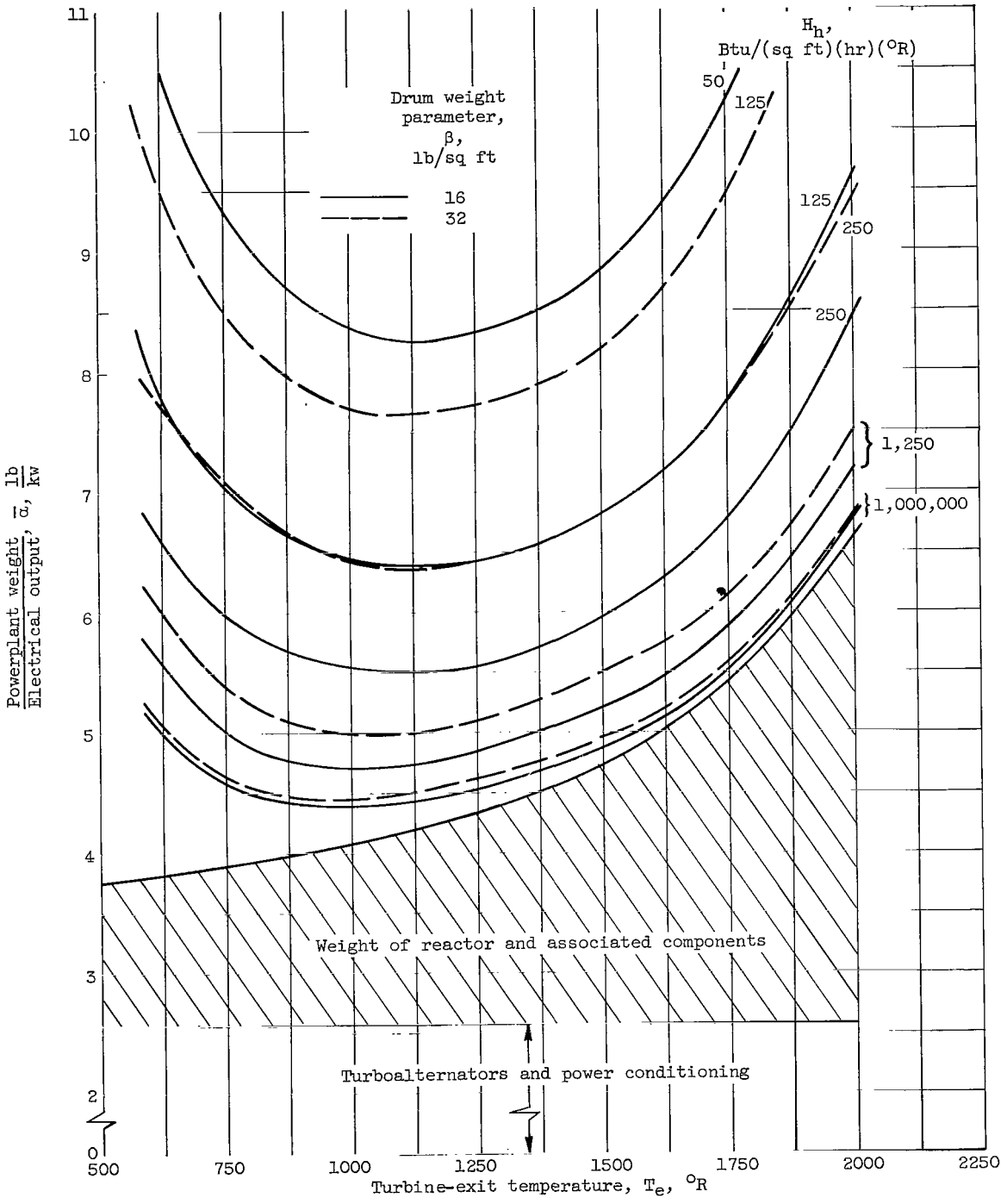

(b) Advanced system; electrical output, 5.7 megawatts; η_R, 0.685; turbine-inlet temperature, 2560° R.

Figure 24. - Concluded. Variation of total powerplant specific weight with H_h and turbine-exit temperature for conventional and advanced systems. $\rho_b b/\bar{\epsilon}$, 0.1038 lb/sq ft; K_{db}, 18,400 Btu/(sq ft)(hr)(°R); belt cycle temperature ratio, 0.69; u (minimum weight value).

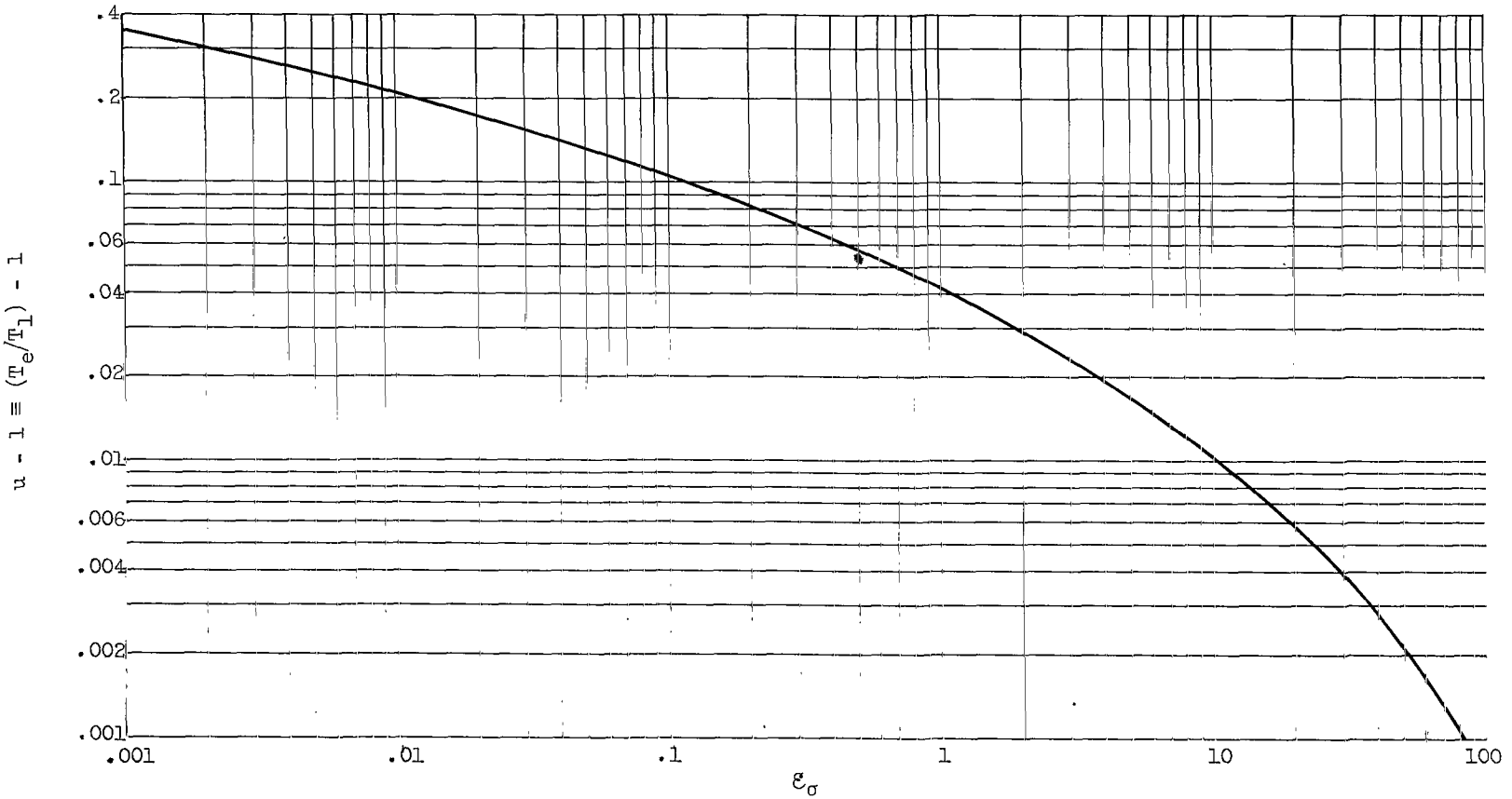

(a) Minimum weight value of $u - 1$.

Figure 25. - Minimum weight values of τ and $u - 1$ for revolving-belt radiators as a function of design parameter $\varepsilon_\sigma \equiv \frac{1}{432}\sqrt{\frac{\rho_b}{2g\sigma_a}}\left(\frac{G\pi}{N\nu\epsilon}\right)^2 \frac{D}{\beta r^3 T_e^6 c_b}$.

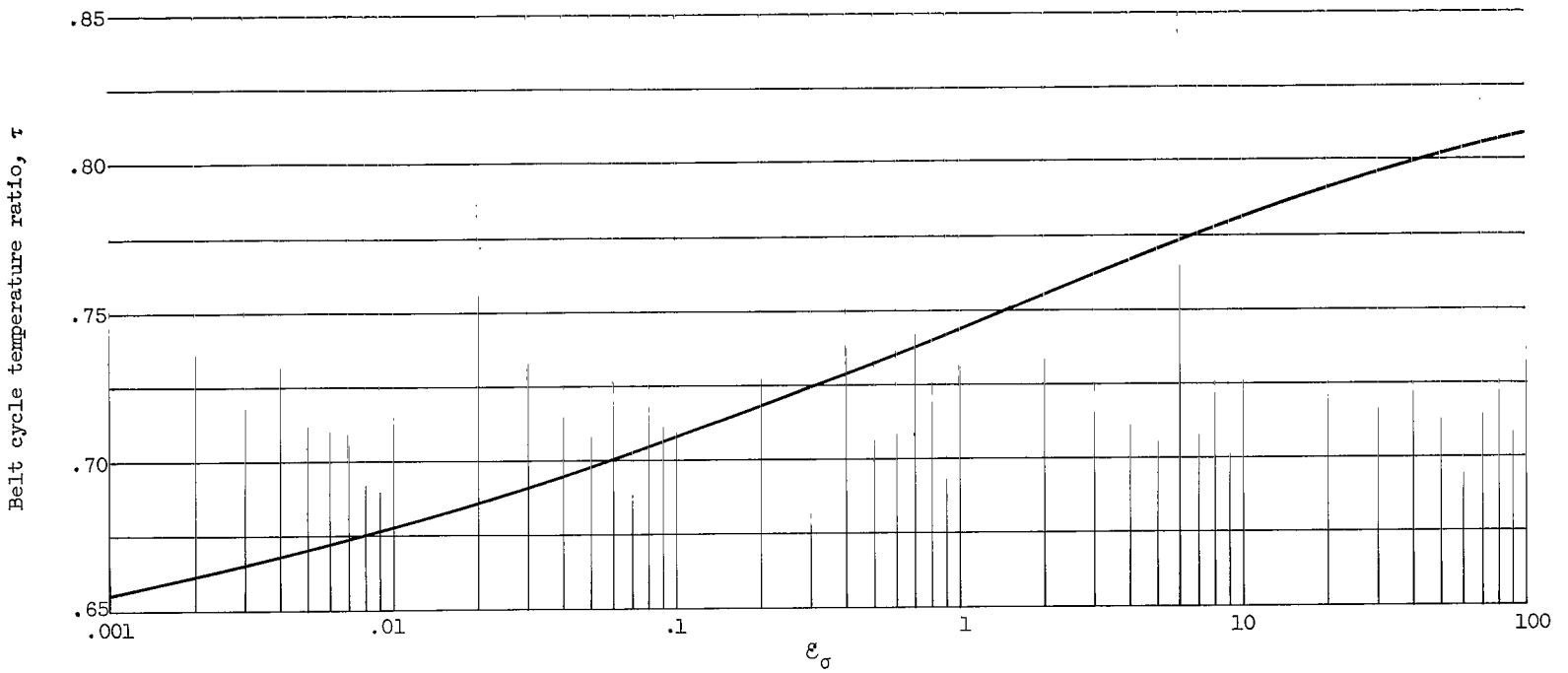

(b) Minimum weight value of τ.

Figure 25. - Concluded. Minimum weight values of τ and $u - 1$ for revolving-belt radiators as a function of design parameter $\mathcal{E}_\sigma \equiv \frac{1}{432}\sqrt{\frac{\rho_b}{2g\sigma_a}}\left(\frac{G\pi}{N\nu\epsilon}\right)^2 \frac{D}{\beta r^3 T_e^6 c_b}$.

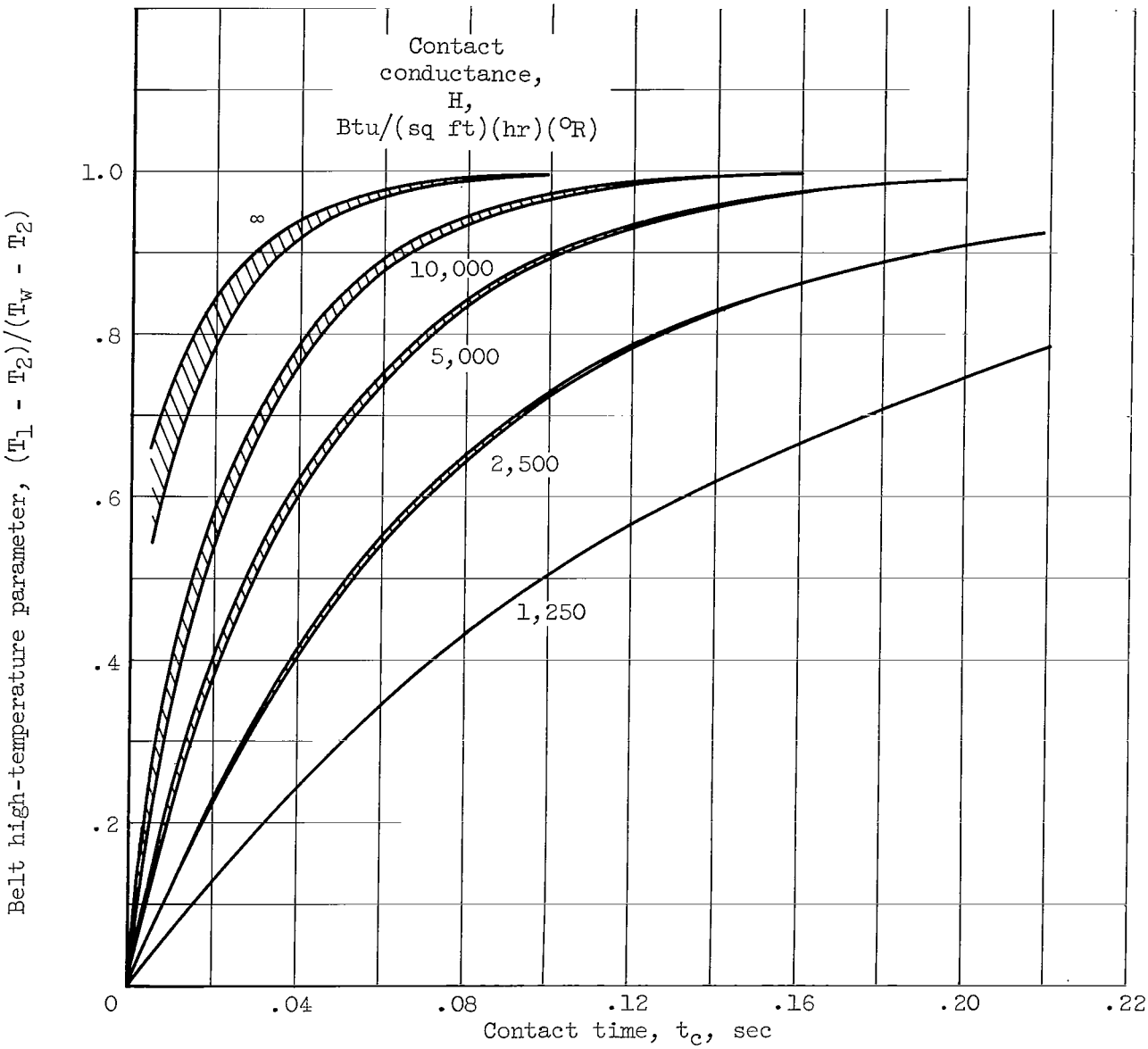

Figure 26. - Effect of cycling on belt temperature. Belt, 0.01-inch-thick beryllium; drum wall, 0.05-inch-thick molybdenum.

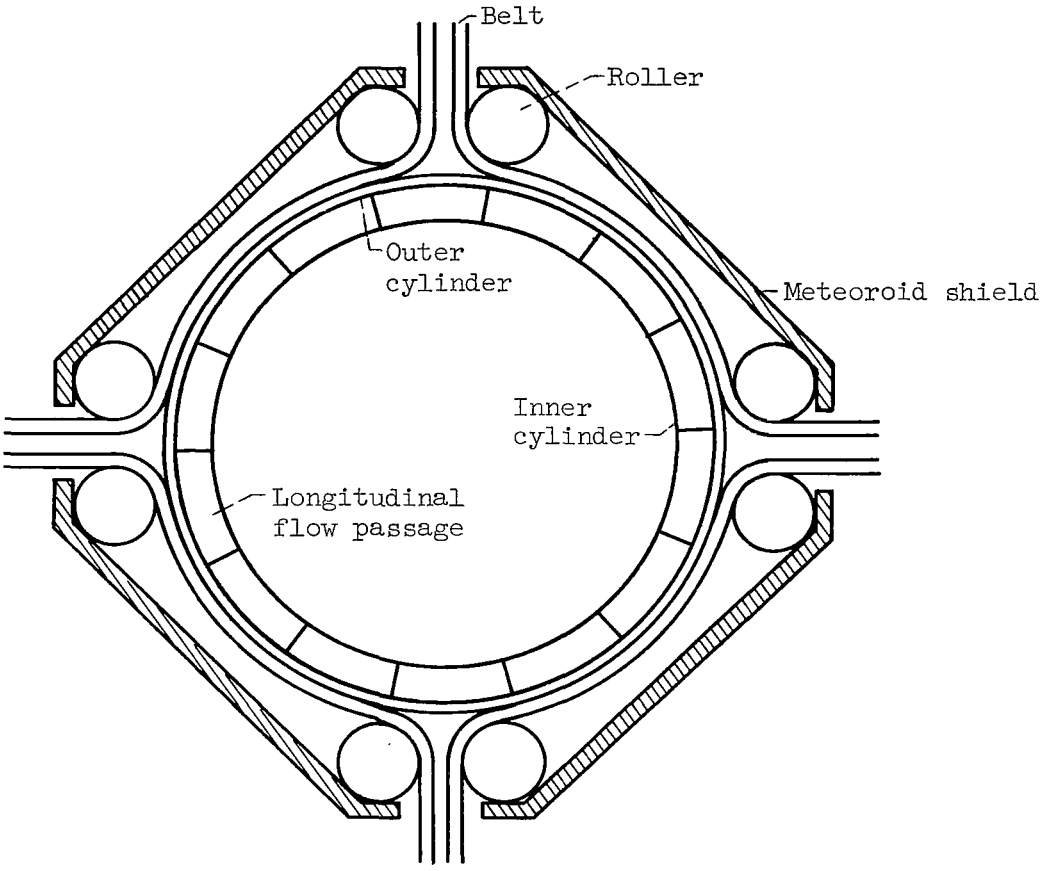

Figure 27. - Cross section of drum configuration for weight estimation.

"The aeronautical and space activities of the United States shall be conducted so as to contribute . . . to the expansion of human knowledge of phenomena in the atmosphere and space. The Administration shall provide for the widest practicable and appropriate dissemination of information concerning its activities and the results thereof."

—NATIONAL AERONAUTICS AND SPACE ACT OF 1958

NASA SCIENTIFIC AND TECHNICAL PUBLICATIONS

TECHNICAL REPORTS: Scientific and technical information considered important, complete, and a lasting contribution to existing knowledge.

TECHNICAL NOTES: Information less broad in scope but nevertheless of importance as a contribution to existing knowledge.

TECHNICAL MEMORANDUMS: Information receiving limited distribution because of preliminary data, security classification, or other reasons.

CONTRACTOR REPORTS: Technical information generated in connection with a NASA contract or grant and released under NASA auspices.

TECHNICAL TRANSLATIONS: Information published in a foreign language considered to merit NASA distribution in English.

TECHNICAL REPRINTS: Information derived from NASA activities and initially published in the form of journal articles.

SPECIAL PUBLICATIONS: Information derived from or of value to NASA activities but not necessarily reporting the results of individual NASA-programmed scientific efforts. Publications include conference proceedings, monographs, data compilations, handbooks, sourcebooks, and special bibliographies.

Details on the availability of these publications may be obtained from:

SCIENTIFIC AND TECHNICAL INFORMATION DIVISION

NATIONAL AERONAUTICS AND SPACE ADMINISTRATION

Washington, D.C. 20546